INSTITUTE OF BIOORGANIC CHEMISTRY OF POLISH ACADEMY OF SCIENCES

Anna Radomiła Stasińska

Doctoral thesis

CYSTAMINE-MODIFIED RNA OLIGONUCLEOTIDES: SYNTHESIS AND APPLICATION IN CROSS-LINKING AND CONJUGATION VIA DISULFIDE BOND

This research project was carried out at
Department of Biopolymer Chemistry
under supervision of
Dr hab. Marcin K. Chmielewski, prof. IBCH

Poznań, 2022

I would like to thank

professor Marcin Chmielewski

for giving me an opportunity to conduct my research under his supervision,

sharing his knowledge and experience,

and introducing me to fascinating world of oligonucleotide chemistry.

I would like to thank each and every person that accompanied me on my doctoral journey, I could not have done it without you. Special thanks go to:

Professor dr hab. Jacek Stawiński and Professor dr hab. Adam Kraszewski for sharing eagerly their broad knowledge and experience during lectures and scientific discussions.

Current and former members of the Department of Biopolymer Chemistry: dr Jolanta, Dominika, Magdalena and dr Agnieszka for being the best support group ever and creating a great working environment.

Wonderful colleagues at FutureSynthesis: Natalia, Kasia, Piotr, Ola, Samanta, Krzysztof, Kamil and of course Mrs Joanna for making work a fun place to be, regardless how busy it was.

Members of the Department of Molecular Probes and Prodrugs for their amazing companionship during my time at IBCH. Dr Jacek Kolanowski for time, support and a good advice whenever I asked for it, dr Michał Gładysz for being low-key mean to me whenever I did not ask for it, Mrs Katarzyna for being the sweetest part of the team, dr Ola M. for every early morning coffee, drs Dorotas for being the best ciotkas, Anna and Francesca for sharing the unique PhD student experience hand-in-hand, Adam- Ryju.

My former fellow PhD buddies and now serious scientists: dr Tomek Cz., dr Marta R., dr Justyna G. and dr Witek A. (although only as a serious scientist) for being a great support and even greater company throughout my time at the Institute, also outside of work.

Each of the wonderful people that I have ever come across at the Institute.

DNARepairMan consortium, especially professor Joyce Lebbink. Being part of this project was a truly amazing adventure.

All of my dear friends for their sheer existence. Your collective effort kept me sane during the past 4 years.

Aleksander. For everything.

Last but not the least, I would like to thank my family for believing in me till the very end. Honestly, I would not make it here if it was not for you.

Pracę dedykuję mojej najbliższej rodzinie: rodzicom oraz dziadkom.

Pośrednio jest ona Waszym dziełem. :)

Streszczenie

OLIGONUKLEOTYDY RNA MODYFIKOWANE CYSTAMINĄ: SYNTEZA I WYKORZYSTANIE W SIECIOWANIU I KONIUGACJI PRZEZ WIĄZANIA DISIARCZKOWE

Opracowanie chemicznej metody syntezy oligonukleotydów serii DNA i RNA zrewolucjonizowało świat badań biologii, biochemii i pokrewnych dziedzin. Cząsteczki te oraz ich funkcjonalne modyfikacje pozwoliły na scharakteryzowanie szeregu oddziaływań i mechanizmów funkcjonowania organizmów żywych, których badanie wcześniej nie było możliwe. Obecnie oligonukleotydy stanowią podstawowe narzędzia biologii molekularnej, diagnostyki oraz, w coraz większym stopniu, medycyny.

Chemicznie modyfikowane oligonukleotydy mogą służyć jako użyteczne narzędzia w badaniach nad oddziaływaniami biocząsteczek między sobą. Znanych jest wiele modyfikacji o różnych właściwościach, a przy obecnym stanie wiedzy możliwe jest opracowanie metody funkcjonalizacji bezpośrednio dopasowanej do danego zastosowania. Jedną z użytecznych modyfikacji oligonukleotydów jest wprowadzanie łączników do łańcucha, które dzięki zawartej w swojej strukturze grupie funkcyjnej, pozwalają na kowalencyjne łączenie z inną cząsteczką, np. znacznikiem fluorescencyjnym lub białkiem. Istnieje wiele rodzajów łączników zawierających grupy funkcyjne o różnej reaktywności toteż wybór zależy od zapotrzebowania oraz funkcji, jaką mają pełnić.

Zazwyczaj łączniki umieszczane są w pozycjach terminalnych oligonukleotydu, jednak to rozwiązanie ma ograniczone zastosowanie, szczególnie w sytuacji, kiedy wymagane jest precyzyjne położenie łącznika w określonej pozycji wewnątrz łańcucha. Celem moich badań było opracowanie metody pozwalającej na otrzymanie trwałych oligonukleotydów RNA zawierających łącznik 2,2'-ditiobisetyloaminowy (cystaminowy) na wybranym wiązaniu fosforodiesterowym zlokalizowanym wewnątrz łańcucha kwasu nukleinowego. Sieciowanie i koniugacja poprzez cystaminę jest reakcją odwracalną, co w pewnych zastosowaniach może stanowić dodatkowy atut. Tiol, stanowiący grupę funkcyjną modyfikowanego oligonukleotydu, ulega utlenianiu w reakcji z inną grupą tiolową obecną w drugiej cząsteczce z wytworzeniem mostka disiarczkowego, który z kolei można zredukować powodując uwolnienie obu uprzednio połączonych cząsteczek.

Do otrzymania P-cystaminowych oligonukleotydów wykorzystałam połączenie dwóch podejść syntetycznych: metody amidofosforynowej oraz metody *H*-fosfonianowej. Modyfikacja kwasu nukleinowego łącznikiem następowała na drodze kondensacji odpowiedniego *H*-fosfonianu nukleozydu, który następnie w wyniku oksydatywnego sprzęgania cystaminą (aminacji) poprzez reakcję Athertona-Todda pozwalała na otrzymanie wiązania P-cystaminowego. Początkowe próby otrzymania modyfikowanych RNA z wykorzystaniem *H*-fosfonianów serii rybonukleotydów nie powiodły się, a otrzymany produkt ulegał rozpadowi. Jednym z elementów mojej pracy było określenie produktów i w konsekwencji zaproponowanie mechanizmu hydrolizy łańcucha. Aby otrzymać trwałe cząsteczki P-cystaminowego RNA, zdecydowałam się na wprowadzenie analogu rybonukleotydu w miejscu przyłączenia łącznika; w tym celu wykorzystałam *H*-fosfoniany 2'-deoksyrybonukleotydów lub 2'-deoksy-2'-fluororybonukleotydów. Punktowe wprowadzenie tych modyfikacji do łańcucha pozwoliło na uzyskanie trwałych oligonukleotydów przy minimalnym wpływie na całkowitą strukturę przestrzenną cząsteczki. Następnie, przeprowadziłam optymalizację warunków reakcji otrzymywania P-cystaminowych RNA. W tym celu zbadałam wpływ takich elementów jak czas kondensacji *H*-fosfonianu, rodzaj czynnika kondensującego oraz warunki reakcji sprzęgania oksydatywnego.

Kolejnym z celów moich badań było określenie stereochemii reakcji i produktów. W pierwszym etapie skupiłam się na otrzymaniu uproszczonych modeli dinukleotydowych, co pozwoliło mi na stwierdzenie wpływu zasady heterocyklicznej nukleotydu poprzedzającego modyfikację oraz podstawnika w pozycji C2' *H*-fosfonianu. Dodatkowo przeprowadziłam badanie stereochemii P-cystaminowych RNA celem ustalenia czy dalsze otoczenie modyfikacji może mieć na nią wpływ.

Następnie, skupiłam się na wykorzystaniu modyfikowanych oligonukleotydów w reakcjach sieciowania. Zoptymalizowałam i przeprowadziłam serię eksperymentów interczą steczkowego sieciowania P-cystaminowych RNA o sekwencjach komplementarnych i niekomplementarnych. Podjęłam próby otrzymania kowalencyjnie stabilizowanych spinek RNA poprzez sieciowanie wewnątrzcząsteczkowe. Rozszerzyłam badania nad sieciowaniem wykorzystując dodatkowe homobifunkcjonalne łączniki alkilowe z grupami maleimidowymi.

Jednym z zakładanych zastosowań P-cystaminowych RNA było ich wykorzystanie w badaniach mechanistycznych i strukturalnych białek. Otrzymane przeze mnie modyfikowane oligonukleotydy zostały wykorzystane w celu koniugacji z RNazą H1. We współpracy z

Laboratorium Struktury Białek Instytutu Biologii Molekularnej i Komórkowej otrzymano trwałe kompleksy mutantów RNazy H1 z substratem DNA:RNA, co obrazuje oddziaływania międzycząsteczkowe. Uzyskane kompleksy mogą posłużyć do dalszych badań strukturalnych.

Podsumowując, opracowane przeze mnie metody i uzyskane wyniki mogą posłużyć do dalszych badań nad wykorzystaniem P-cystaminowych RNA jako narzędzi biologii molekularnej, ze szczególnym uwzględnieniem oddziaływań RNA-białko.

Abstract

CYSTAMINE-MODIFIED RNA OLIGONUCLEOTIDES: SYNTHESIS AND APPLICATION IN CROSS-LINKING AND CONJUGATION VIA DISULFIDE BOND

The development of the method of DNA and RNA oligonucleotide chemical synthesis revolutionized the world of biology, biochemistry, and related research areas. These short fragments of nucleic acids allowed for characterization of multitude of interactions and mechanisms which comprise a basis of living organisms that beforehand were impossible to study. Nowadays, oligonucleotides are fundamental tools of molecular biology, diagnostics, and- increasingly- medicine.

Chemically modified oligonucleotides can be very useful in biomolecular research playing vital role in biomolecule intractions. There are numbers of known modifications of different properties and applications and with the current state-of-the-art, it is possible to devise an entirely tailored functionalization method. One of the possible modifications is the introduction of linkers into the nucleic acid chain that allow covalent bonding with another molecule, e.g. fluorescent label or protein, which is owing to the functional groups present in linkers' structure. Diverse types of linkers of different functional group reactivity are available, therefore the choice depends on the application and its function.

Oftentimes linkers are introduced at terminal positions of the oligonucleotide, however such solution has limited applicability, especially if a specific, precise position of the linker within the chain is required. The main goal of my research was the development of a method that would allow for obtaining stable RNA oligonucleotides modified with 2,2'-dithiobisethylamine (cystamine) linker at chosen phosphodiester bond within the nucleic acid chain (P-cystamine RNA). Cross-linking or conjugation via cystamine is reversible, which can be beneficial in certain applications. Thiol, which is a functional group of such modified oligonucleotide undergoes oxidation with a thiol group present in another molecule to form a disulfide bridge. This bond can be in turn reduced resulting in the liberation of the two molecules.

To obtain P-cystamine RNA I have used a combination of two synthetic approaches: the phosphoramidite method and the *H*-phosphonate method. Nucleic acid modification was achieved through condensation of a chosen nucleoside *H*-phosphonate and subsequent oxidative coupling of cystamine (amination) in Atherton-Todd reaction, which yielded P-cystamine bond. Initial attempts to obtain such modified RNA using only ribonucleotide

H-phosphonates had failed since the product underwent cleavage. One of the parts of my work focused on the identification of the products of hydrolysis to suggest the mechanism of the cleavage. In order to obtain a stable P-cystamine RNA, I have decided to introduce ribonucleotide analogs at the site of linker attachment. For that purpose, I used 2'-deoxyribonucleotides and 2'-deoxy-2'-fluororibonucleoitde *H*-phosphonates. Such point modifications yielded stable oligonucleotides with minimal influence on the overall geometry of the molecule. Next, I optimized reaction conditions by examining the impact of such variables as *H*-phosphonate condensation time, type of condensing agent, or oxidative coupling reaction conditions.

Yet another goal of my project was a study of the stereochemistry of reactions and products. At the first stage I focused on obtaining simplified dinucleotide models, which allowed me to identify the influence of heterocyclic base preceding the modification as well as C2' substituent of the *H*-phosphonate. Additionally, I examined the stereochemistry of P-cystamine RNA in order to investigate whether further neighborhood can influence the stereochemistry of the product.

Further, I focused on application of modified oligonucleotides in cross-linking reactions. I optimized reaction conditions and carried out a series of experiments of intermolecular cross-linking of P-cystamine RNA with both complementary and non-complementary sequences. I have also attempted to obtain covalently stabilized RNA hairpins by intramolecular cross-linking. I expanded the studies by using additional homobifunctional linkers with maleimide functional groups.

One of the assumed applications of P-cystamine oligonucleotides is their use in structural and mechanistic studies of proteins. Modified oligonucleotides which I synthesized were used in conjugation with RNase H1. In collaboration with the Laboratory of Protein Structure of the Institute of Molecular and Cell Biology, we obtained stable complexes of RNase H1 mutants with modified DNA:RNA substrate, which proved intermolecular interactions of the two species. Obtained complexes can be used for further structural studies.

To summarize, the methods I have developed and obtained results can serve in future research on the applicability of P-cystamine RNA as molecular biology tools, particularly in studies of RNA-protein interactions.

TABLE OF CONTENTS

Table of contents 14

List of publications 18

List of abbreviations 20

I. The aim of the Thesis 22

II. Introduction 26

1. Oligonucleotide synthesis methods- A historic overview 26

1.1. Phosphodiester approach 26

1.2. Phosphotriester approach 27

1.3. *H*-phosphonate approach 29

1.3.1. Atherton-Todd oxidative coupling 31

1.3.2. Iodine-mediated oxidative coupling 33

1.4. Phosphite triester and phosphoramidite approaches 34

1. 2. Oligonucleotide cross-linking and conjugation strategies 36

2.1. Psoralen cross-linking 38

2.2. Click-chemistry cross-linking 39

2. 3. Oligonucleotide modifications for disulfide cross-linking and conjugation 40

3.1. 5' & 3' end modifications 40

3.2. Internucleotide modifications 41

3.3. Nucleobase modifications 43

3. 4. Thiol and disulfide chemistry 45

4. 5. Oligonucleotide cross-linking via disulfide bridge 46

5.1. DNA cross-linking 47

5.2. RNA cross-linking 48

5.3. Oligonucleotide-peptide conjugates 49

5.4. Oligonucleotide-protein conjugates 49

III. Results and discussion 52

5. 1. Backbone modification of RNA with a disulfide linker 52

1.1. Synthesis of 2,2'-Dithiobis(ethylamine) (cystamine) 52

1.2. Synthesis of 3,3'-Dithiobis(propylamine) (homocystamine) 53

a 1.3. Synthesis of P-cystamine RNA 54

2. Optimization of manual *H*-phosphonate coupling reaction 59
2.1. Study of the activator 59
2.2. Study of the condensation time 61
2.3. Study of the oxidizing agent 62
3. Stereochemistry of P-cystamine modification 65
3.1. Dinucleotide phosphoramidate model 66
3.1.1. Synthesis of 3'-DMT-2'-deoxythymidine 67
3.1.2. Synthesis of 3'-DMT-2'-deoxyadenosine 68
3.1.3. Synthesis of P-cystamine dinucleotides 69
3.1.4,. Influence of the nearest neighborhood on the configuration of P-cystamine oligonucleotides 72
6. 4. Ribooligonucleotide cross-linking via disulfide bridge 74
4.1. Optimization of the cross-linking reaction 74
4.2. Structural studies of cross-linked RNA duplex 77
7. 5. Cross-linking of P-cystamine RNA via homobifunctional linkers 79
8. 6. Cross-linking of RNA hairpin 83
9. 7. Conjugation with RNase H1 via disulfide bridge 87
7.1. Design of RNase H1 mutants 88
7.2. RNase H1- RNA cross-linking 89
7.3. Scale-up of RNase H1-RNA cross-linking 90
IV. Summary 92
V. Materials and Methods 94
10. Materials 94
1.1. Reagents 94
1.1. Consumables 95
1.2. Equipment 95
1.3. Software 96
1.4. List of oligonucleotide samples 96
11. Methods 97
2.1. General methods 97
2.1.1. Buffers composition 97
2.1.2. Chromatographic methods 97
2.1.3. Spectroscopic methods 97
2.2. the Synthesis of dithiobis(a,lkylamine) linkers 98

2.2.1. Synthesis of 2,2'-Dithiobis(ethylamine) (cystamine) **1** 98

2.2.2. Synthesis of 3,3'-Dithiobis(propylamine) (homocystamine) **5** 98

2.3. Synthesis of protected nucleosides 99

2.3.1. Synthesis of 5'-*O*-*tert*-butylmethylsilyl-2'-deoxythymidine **6** 99

2.3.2. Synthesis of 3'-*O*-(4,4'-dimethoxytrityl)- 5'-*O*-*tert*-butylmethylsilyl-2'-deoxythymidine **7** 100

2.3.3. Synthesis of 3'-*O*-(4,4'-dimethoxytrityl)-2'-deoxythymidine **8** 100

2.3.4. Synthesis of N^6-benzoyl-2'-deoxyadenosine **10** 101

2.3.5. Synthesis of 5'-*O*-tert-butylmethylsilyl-N^6-benzoyl-2'-deoxyadenosine **11**. 102

2.3.6. Synthesis of 3'-*O*-(4,4'-dimethoxytrityl)-5'-*O*-tert-butylmethylsilyl-N^6-benzoyl-2'-deoxyadenosine **12** 102

2.3.7. Synthesis of 3'-*O*-(4,4'-dimethoxytrityl)-N^6-benzoyl-2'-deoxyadenosine **13**103

2.3.8. Synthesis of N^6-benzoyl-2'-deoxy-2'-fluoroadenosine **18** 104

2.3.9. Synthesis of 5'-*O*-(4,4'-dimethoxytrityl)-N^6-benzoyl-2'-deoxy-2'-fluoroadenosine **19** 105

2.4. Synthesis of 5'-*O*-(4,4'-dimethoxytrityl)-N^6-benzoyl-2'-deoxy-2'-fluoroadenosine H-phosphonate triethylammonium salt **20** 106

2.5. General procedure for dinucleotide *H*-phosphonate synthesis **14** 107

2.5.1. *O*-(5'-*O*-(4,4'-dimethoxytrityl)-2'-deoxythmidin-3'-yl)-*O*'-(3'-*O*-(4,4'-dimethoxytrityl)-2'-deoxythymidin-5'-yl) *H*-phosphonate **14a** 107

2.5.2. *O*-(5'-*O*(-4,4'-dimethoxytrityl)-2'-deoxythmidin-3'-yl)-*O*'-(3'-*O*-(4,4'-dimethoxytrityl)-N^6-benzoyl-2'-deoxyadenosin-5'-yl) *H*-phosphonate **14b** 107

2.5.3. *O*-(5'-*O*-(4,4'-dimethoxytrityl)-N^4-benzoyl-2'-deoxy-2'-fluorocytidin-3'-yl)-*O*'-(3'-*O*-(4,4'-dimethoxytrityl)-2'-deoxythymidin-5'-yl) *H*-phosphonate **14c** 107

2.6. General procedure for dinucleotide phosphoramidates synthesis **15** 108

2.6.1. *O*-(5'-*O*-(4,4'-dimethoxytrityl)-2'-deoxythmidin-3'-yl)-*O*'-(3'-*O*-(4,4'-dimethoxytrityl)-2'-deoxythymidin-5'-yl)-*N*-(2,2'-dithiobis(ethylamine)) phosphoramidate **15a** 108

2.6.2. *O*-(5'-*O*-(4,4'-dimethoxytrityl)-2'-deoxythmidin-3'-yl)-*O*'-(3'-*O*-(4,4'-dimethoxytrityl)-N^6-benzoyl-2'-deoxyadenosin-5'-yl)-*N*-(2,2'-dithiobis(ethylamine)) phosphoramidate **15b** 108

2.6.3. *O*-(5'-*O*-(4,4'-dimethoxytrityl)-N^4-benzoyl-2'-deoxy-2'-fluorocytidin-3'-yl)-*O'*-(3'-*O*-(4,4'-dimethoxytrityl)-2'-deoxythymidin-5'-yl)-*N*-(2,2'-dithiobis(ethylamine)) phosphoramidate **15c** 109

2.7. Oligonucleotide synthesis 109

2.7.1. 0.2 µmol scale oligonucleotide synthesis 109

2.7.2. 1 µmol scale oligonucleotide synthesis 110

2.7.3. Disulfide linker-modified oligonucleotide synthesis 110
2.7.4. Cleavage from the support and deprotection of oligonucleotides 111
2.7.5. Deprotection of 2'-tert-butylmethylsilyl oligoribonucleotides 112
2.8. Oligonucleotide purification and characterization 112
2.8.1. Polyacrylamide gel oligonucleotide purification 112
2.8.2. Analytical polyacrylamide gel electrophoresis 113
2.8.3. Oligonucleotide desalting/buffer exchange 113
2.8.4. Reversed Phase High Pressure Liquid Chromatography (RP-HPLC) analysis 113
2.8.5. Matrix Assisted Laser Desorption Ionisation Time Of Flight Mass Spectrometry (MALDI-TOF-MS) analysis 114
2.8.6. Optimized protocol for desalting of samples for MALDI-TOF-MS analysis using ZipTip$_{C18}$ pipette tips 114
2.8.7. Melting temperature measurements 115
2.9. Modified oligonucleotide cross-linking and conjugation 115
2.9.1. Reduction of disulfide linker- modified oligonucleotides.....115
2.9.2. General protocol for oligonucleotide-oligonucleotide cross-linking 116
2.9.3. Hairpin-forming oligonucleotide cross-linking 116
2.9.4. Oligonucleotide cross-linking via homobifunctional linkers.....116
2.9.5. Oligonucleotide-RNase H1 cross-linking 116
2.9.6. Protein expression and purification 117
2.9.7. Oligonucleotide-protein cross-linking 118
2.9.8. Purification of cross-linked RNase H1-DNA/RNA complexes 118
VI. Bibliography 120

LIST OF PUBLICATIONS

1. Stasińska Anna R., Putaj Piotr. & Chmielewski Marcin K. Disulfide bridge as a linker in nucleic acids' bioconjugation. Part I: An overview of synthetic strategies. *Bioorg. Chem.* 92, 103223 (2019).

2. Stasińska Anna R., Putaj Piotr. & Chmielewski Marcin K. Disulfide bridge as a linker in nucleic acids' bioconjugation. Part II: A summary of practical applications. *Bioorg. Chem.* 95, 103518 (2020).

3. Hyjek-Składanowska Malwina, Stasińska Anna R., Napiórkowska-Gromadzka Agnieszka, Bartłomiejczak Aneta, Seth Punit P., Chmielewski Marcin K., Nowotny Marcin. Disulfide bridge cross-linking between protein and the RNA backbone as a tool to study RNase H1. *Bioorg. Med. Chem.* 28, 115741 (2020).

LIST OF ABBREVIATIONS

A Adenosine

Ac Acetyl

ACN Acetonitrile

AdCl 1-Adamantanecarboxy chloride

Ade Adenine

APS Ammonium persulfate

B Heterocyclic base

Bz Benzoyl

C Cytosine

CPG Controlled pore glass

Cyt Cytidine

DCA Dichloroacetic acid

DCM Dichloromethane

DMF N,N-dimethylformamide

DMSO Dimethyl sulfoxide

DMT 4, 4'-Dimethoxytrityl

DNA Deoxyribonucleic acid

DTT Dithiothreitol

EDTA Ethylenediaminetetraacetic acid

G Guanosine

Gua Guanine

HCl Hydrochloric acid

HPLC High Pressure Liquid Chromatography

HR-MS High Resolution Mass Spectrometry

iBu *iso*-butyryl

MALDI-TOF-MS Matrix-Assisted Laser Desorption Ionization Time of Flight mass Spectrometry

MeOH Methanol

NaOH Sodium hydroxide

nBuOH *n*-Butanol

NCS N-Chlorosuccinimide

NIS N-Iodosuccinimide

NMP N-Methylpyrrolidone

NMR Nuclear Magnetic Resonance

PAGE Polyacrylamide Gel Electrophoresis

PBS Phosphate Buffer Saline

PivCl Pivaloyl Chloride

Pyr Pyridine

RNA Ribonucleic acid

RP-HPLC Reverse Phase High Pressure Liquid Chromatography

T Thymidine

TBDMS tert-Butyldimethylsilyl

TBE Tris-Borate-EDTA

TEA Triethylamine

TEAA Triethylammonium acetate

TEAx3HF Triethylamine trihydrofluoride

TEMED N,N,N',N'-Tetramethylethylenediamine

TFA Trifluoroacetic acid

THF Tetrahydrofuran

Thy Thymine

TLC Thin Layer Chromatography

Tr Trityl

Tris Tris(hydroxymethylaminomethane)

U Uridine

Ura Uracil

I. THE AIM OF THE THESIS

The overall aim of my scientific research project was to modify and obtain stable RNA oligonucleotides with a disulfide linker, which could then be applied in cross-linking with other oligonucleotides or for conjugation with other biomolecules, e.g. proteins. Modifications, which are synthetically introduced non-native fragments, can be used in order to render properties of oligonucleotides and are widely used tools in contemporary biochemistry, biology and medicine. Starting from labelling in RT-PCR diagnostics through viral RNA mapping up to emerging antisense gene therapies- all these are a consequence of the collective efforts of hundreds of scientists working on chemical nucleic acid functionalization. By modification, several aspects can be controlled, such as thermal stability, susceptibility to enzymes, or cell membrane permeability.

For instance, conjugates of oligonucleotides with carrier molecules such as peptides become increasingly important in antisense therapy, due to their enhanced cell delivery[1]. Moreover, adequate functionalization with linkers allows studying of otherwise transient interactions with other biomolecules, e.g. proteins, frequently providing valuable information about mechanisms underlying processes such as translation, replication, or DNA repair[2,3].

Some of the oligonucleotide functions can be obtained by modification with linkers that allow attachment of another species to form a stable molecule or complex. Conjugation and cross-linking via a disulfide bridge is one prominent method[4]. The disulfide bond is typically formed between two thiolate groups, either naturally occurring or artificially introduced into participating molecules. Whereas proteins or peptides may bear a thiol moiety in their native form owing to the presence of cysteine, oligonucleotides require chemical manipulation that involves the attachment of a disulfide/thiolate linker.

Most strategies of such oligonucleotide functionalization rely on the introduction of a tether either at 3’ or 5’ terminus or at the heterocyclic base, which can be a limiting factor on their utility due to localization in a strand. One interesting strategy involves modification of the internucleotide linkage, which has been used in DNA oligonucleotides but was not reported to be applicable for RNA due to instability of the phosphodiester derivative formed upon the introduction of a linker[5]. This led to a substantial gap in the repertoire of cross-linking and conjugation strategies for oligonucleotide RNA with other molecules.

The first section of my dissertation (*Introduction*) comprises a literature review on oligonucleotide chemistry and conjugation. It provides a brief historical summary of synthetic strategies with a particular focus on *H*-phosphonate chemistry. Moreover, I described matters of oligonucleotide modification, cross-linking, and conjugation. Finally, since the main scope of my research being disulfide-bearing linker modifications, I also included an overview of this approach in the context of conjugation of oligonucleotides and other biomolecules.

In the subsequent section (*Results and discussion*) I described experiments conducted in the course of my research work. Its first chapters focus on the development of RNA oligonucleotides modification with a disulfide linker. Based on *H*-phosphonate chemistry, I proposed a method that allows inserting of a tether at virtually any position of the RNA backbone. I examined the stability of initially obtained molecules and proposed a solution to ensure coherence of the oligonucleotide by replacing modified ribonucleotides with their analogs:
2'-deoxyribonucleotides and 2'-deoxy-2'-fluororibonucleotides. Furthermore, I summarized optimization of the conditions of such modification and investigated stereochemistry of the reaction and products based on dinucleotide models as well as final oligonucleotides.

The second part of this section focuses on the applicability of disulfide linker-modified RNA oligonucleotides. I conducted and discussed a series of disulfide cross-linking reactions, during which I obtained stable RNA duplexes of both complementary and non-complementary sequences and presented their resistance to denaturing conditions. Based on this strategy, I carried out an attempt to obtain mid-stem covalently trapped RNA hairpins. Furthermore, I expanded the cross-linking by using additional homobifunctional linkers in order to suppress the potential impact on the structure of constrained duplex. The use of either alkyl or alkyl-disulfide linkers provided an additional possibility to render reversibility of the cross-linking process.

Finally, I examined the usefulness of cystamine-modified RNA oligonucleotides in structural and mechanistic studies of proteins. For that purpose, functionalized species were conjugated with RNase H1 mutants. Although in native conditions complex between the protein and RNA:DNA substrate is transient, the disulfide bridge conjugated complexes proved to be stable and could be subjected to further studies.

The final section of my dissertation is *Materials and methods* where I collected description of materials used, reaction procedures, and characterization of obtained products.

The research was conducted in a broader context and in collaboration with foreign research centers as part of the implementation of a grant: *Innovative Training Network* supported through EU Horizon 2020 Marie Sklodowska-Curie Action under project number H2020-MSCA-ITN-2016 [DNAREPAIRMAN - 722433].

The main aims of my research were:

1. Developing a method to introduce disulfide linker into RNA oligonucleotide backbone
2. Study of stability of disulfide linker-modified RNA oligonucleotides
3. Optimization of functionalized RNA synthesis conditions
4. Study of the stereochemistry of *H*-phosphonate condensation and oxidative coupling reaction
5. Devising a strategy for inter- and intrastrand cross-linking of RNA oligonucleotide via a disulfide bridge
6. Study of cross-linking influence on RNA duplex structure
7. Application of disulfide linker modified RNA for conjugation with protein in order to obtain stable complex for mechanistic and structural studies

II. INTRODUCTION

1. OLIGONUCLEOTIDE SYNTHESIS METHODS- A HISTORIC OVERVIEW

Humans are curious species and scientists seem to be particularly inquisitive among them when it comes to the surrounding world. People early realized that nature designed the most efficient and flawless systems, where one piece perfectly fits another and processes rely on each other which has been the greatest inspiration for humankind. New discoveries lead to questions, and finding answers gives us an opportunity to mimic nature and thus comfort that we can somewhat control it- or at least think that we can.

It has not been different in the case of nucleic acids. First discovered in 1869 by Friedrich Miescher[6], DNA became slightly forgotten and it took decades until scientists started to characterize and unravel the main functions of DNA and RNA[7–9]. The research of nucleic acids accelerated greatly when in 1953 a groundbreaking finding was announced- the first accurate structure of the B-DNA double helix was published by Watson and Crick[10] based on X-ray crystallographic data collected by Rosalind Franklin and Maurice Wilkins. Finally, the full picture of the structure combined with the realization of the importance of nucleic acids' role was probably what made scientists believe that they can and should make their own, synthetic nucleic acid in a test tube. This is how the concept of oligonucleotides- short chains of nucleic acids up to hundreds of nucleotides- started to emerge. However, for nearly fifty years the key question remained „how". Decades of collective efforts of numbers of prominent researchers allowed for the development of a robust methods of oligonucleotide synthesis, without which modern biology as we know it could not exist. Below, each most crucial approach of oligonucleotide synthesis has been briefly described.

1.1. PHOSPHODIESTER APPROACH

Although not historically first, it was the first approach to be developed to a larger extent and for some years dominated the oligonucleotide synthesis research. The so-called phosphodiester method was introduced by H. G. Khorana and his co-workers in the late 1950s[11,12]. Initial syntheses of thymidine dinucleotide was a reaction between 5'-O-tritylthymidine and 3'-O-acetylthymidine-5'-O-phosphate activated with N,N′-

dicyclohexylcarbodiimide (DCC) or 4-toluenesulfonyl chloride (TsCl) (Figure 1). Upon removal of 3'-*O*- and 5'-*O*- protecting groups, the final product of thymidine dinucleotide (d(TpT)) was obtained. What is important to mention, Khorana's approach did not employ protection of internucleotide phosphate linkage. In fact, he claimed that its protection would mean giving up oligonucleotides' most important feature: its polyanionic nature. Unfortunately, lack of phosphate protection led to the formation of side products (e.g. branched oligonucleotides) and therefore affected overall yield, which was reaching up to 50-70% in case of stepwise synthesis.

Despite some issues, the phosphodiester method underlies several crucial works: Khorana used it for the synthesis of di-, tri-, and tetranucleotide sets, which enabled elucidation of the genetic code[13]. Moreover, using this approach the first gene was synthesized, namely DNA duplex encoding the yeast alanine transfer RNA[14]. Yet another vital contribution of Khorana's group to oligonucleotide chemistry was the introduction of trityl derivatives (methoxytrityl (MMT) and dimethoxytrityl (DMT)) as more labile alternatives for 5'-OH group protection than Tr[15]. The use thereof reduced the risk of glycosidic bond cleavage, especially in the case of purines, since deprotection required milder conditions. Eventually, the phosphodiester method was abandoned in the 1970s thus giving the chance for other approaches to take the lead.

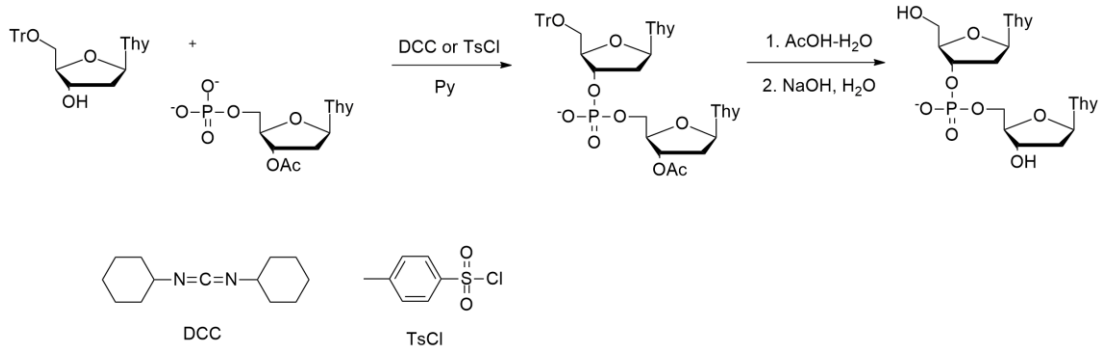

Figure 1. Synthesis of thymidine dinucleotide by Khorana et al. [11,12]

1.2. PHOSPHOTRIESTER APPROACH

This method was used for the first-ever chemical synthesis of dinucleotide in history. In 1955, A. R. Todd and A. M. Michelson published an article in which they described the synthesis of d(TpT) and d(pTpT) dinucleotides[16]. It was also based on coupling between appropriately protected nucleotides, and the key difference between this and the phosphodiester approach was the use of benzoyl-protected phosphate internucleotide linkage. However, in that form of

synthesis the chain elongation did not appear to be possible and the concept was not developed any further for roughly a decade.

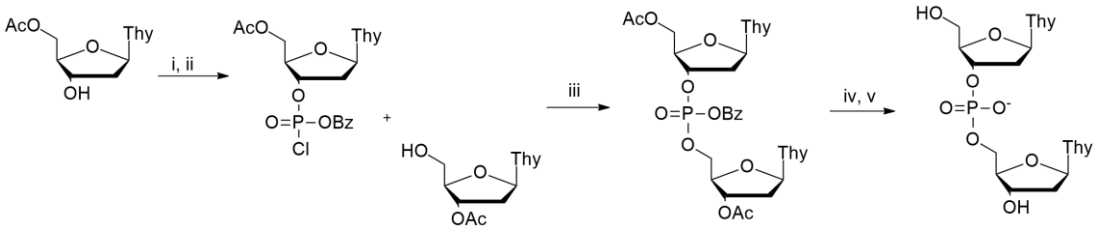

Figure 2. Synthesis of d(TpT) by Todd and Michelson using phosphotriester approach[16]. i) $(PhO)_2P(O)Cl$, 2,6-lutidine, benzene; ii) N-chlorosuccinimide, ACN, benzene; iii) 2,6-lutidine, ACN; iv) H_2SO_4, EtOH, H_2O; v) $Ba(OH)_2$, H_2O

The concept has been revived in the 1960s. R. L. Letsinger and V. Mahadevan reported synthesis of d(CpT) dinucleotide on a polymeric solid support using 2-cyanoethyl as phosphate protecting group[17]. The solid support synthesis concept has been abandoned for quite some time and Letsinger continued using 2-cyanoethyl in his further solution phase synthesis work. Meanwhile, other groups also adopted the strategy of protecting internucleotide linkage. F. Eckstein and I. Rizk reported use of 2,2,2-trichloroethyl group[18,19] whereas C. B. Reese and R. Saffhill applied phenyl group[20]. At that point, however, each of the aforementioned approaches suffered certain drawbacks which prevented an efficient synthesis of long chain oligonucleotides. The 2-cyanoethyl group was too labile to be used in high-yield solution phase synthesis[21], use of 2,2,2-trichloroethyl group gave unsatisfactory yields[22] of deprotected products and phenyl group deprotection resulted in the formation of side products due to cleavage of internucleotide linkage[23]. The latter was then overcome by substitution of the phenyl ring with electron withdrawing groups (e.g. *p*-chloro- moiety)[24]. With many further improvements of phosphorylating and coupling agents, the phosphotriester oligonucleotide synthesis continued to develop throughout the 1970s until the 1990s[25–31]. Using this approach, Itakura and his co-workers, with an aid of enzymatic ligation, synthesized four long DNA sequences forming two double helices corresponding to the genes encoding chains A and B of human insulin[32]. Importantly, their work was then successfully applied for the expression of those genes in *E.coli*[33].

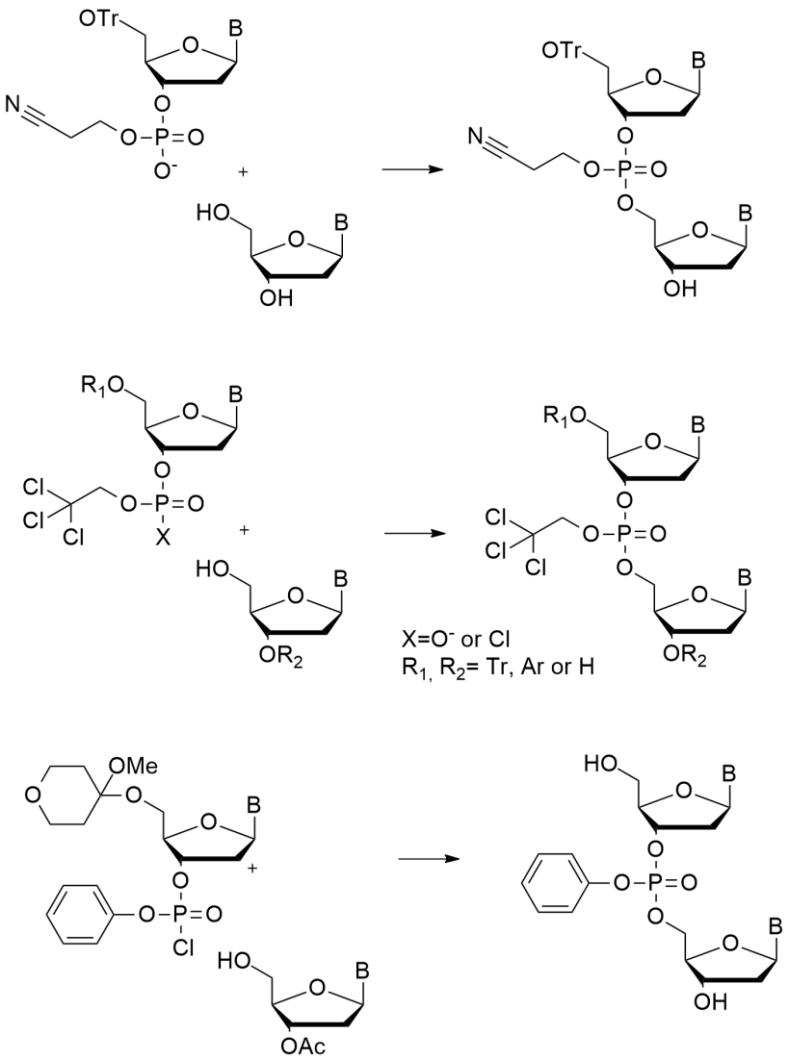

Figure 3. Dinucleotide syntheses using protected phosphate. Approaches applied by (top to bottom) Letsinger et al. [17], Eckstein et al. [18,19] and Reese et al. [20]

1.3. *H*-PHOSPHONATE APPROACH

H-phosphonate method, which is another case of initial attempts to oligonucleotide synthesis was first developed in parallel with the phosphotriester approach in Todd's laboratory[34]. Researchers presented a method of coupling protected nucleotide *H*-phosphonate with appropriately protected nucleoside using diphenyl phosphorochloridate as a coupling agent (Figure 4). However, in this form, the approach seemed like a dead end and further developments were suspended for nearly 30 years.

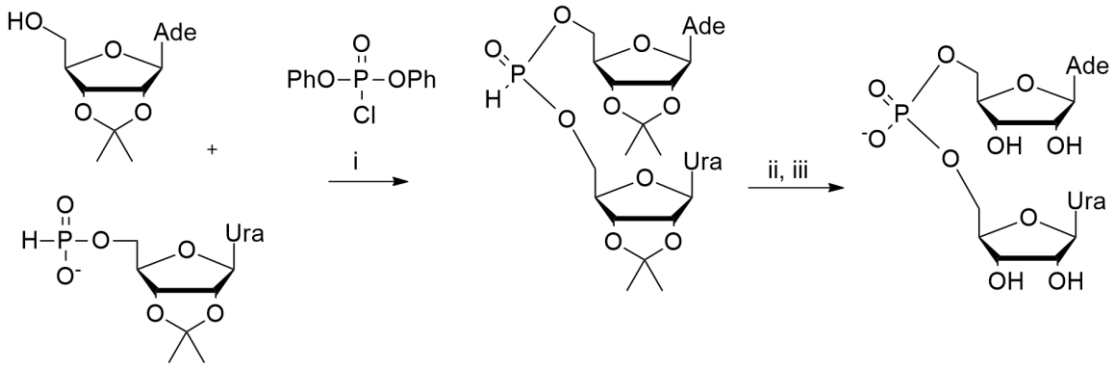

Figure 4. Synthesis of 5'-5'-dinucleotide presented by Hall et al[34]. i) 2,6-lutidine, ACN; ii) N-chlorosuccinimide, 2,6-lutidine, ACN; $NaHSO_3$, H_2O; iii) HCl, H_2O

In the mid-1980s' Foehler[35] and Stromberg's group[36] reinvestigated the *H*-phosphonate strategy and proved its utility in solid phase synthesis of oligonucleotides. They also suggested a series of novel coupling agents, including 2,4,6-triisopropylbenzenesulfonyl chloride (TPSCl), diphenylchlorophosphate (DPCP) and pivaloyl chloride (PivCl)[37,38], all of which afforded excellent coupling yields (> 97%) and therefore- the overall product yield. It was later found that oxidation of *H*-phosphonates into phosphate diesters with iodine in aqueous conditions occurred quantitatively and rapidly[36]. Moreover, when this approach was used instead of oxidizing the sequence after each coupling step, it was possible to carry out oxidation globally as the final step of the synthesis. Application of these findings led to the establishment of a simple synthetic methodology comprising of repetitive cycles (Figure 5), which allowed for the synthesis of long nucleic acid chains on a solid support. This approach also allowed for a convenient synthesis of non-native nucleic acid analogs, such as phosphorothioates[39,40] and phosphoroselenoates[41].

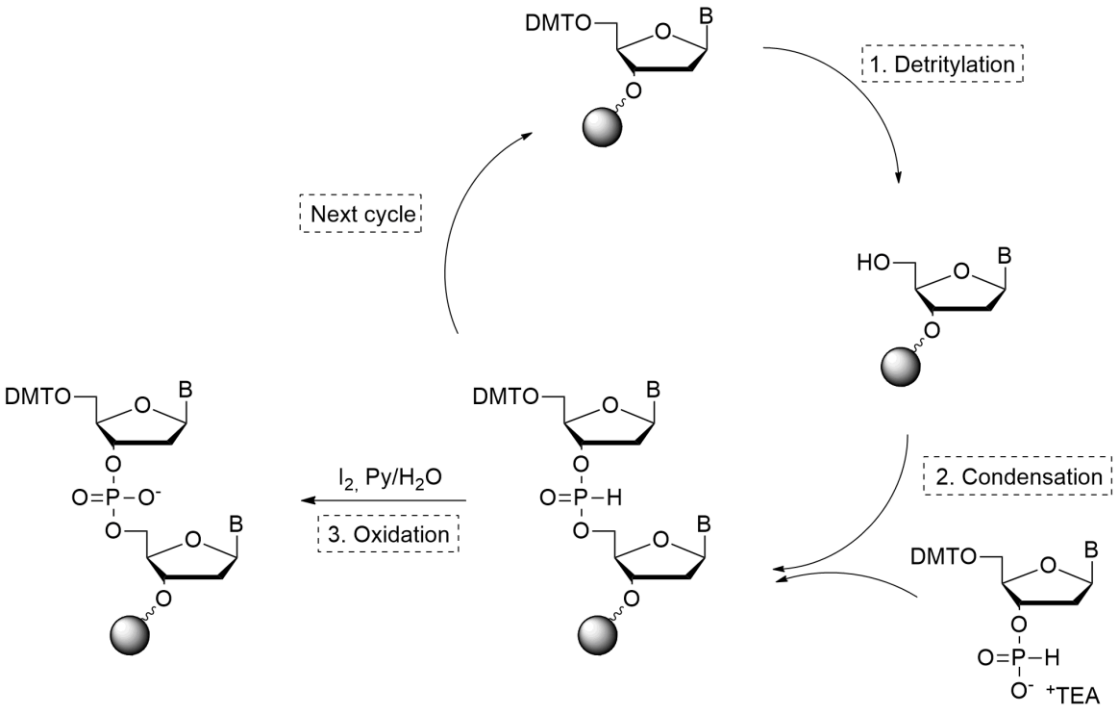

Figure 5. Synthetic cycle using H-phosphonate method of oligonucleotide synthesis.

1.3.1. Atherton-Todd oxidative coupling

In 1945, F. Atherton, H. Openshaw and A. Todd published an article, in which they presented novel methods for two-step amination of dialkyl phosphites via halogenation[42]. The reaction occurred at room temperature under anhydrous conditions within ca. 3 hours. Researchers suggested two possible mechanisms of the reaction. Initially, the authors claimed that in the first step, the phosphite forms an adduct with trichloromethyl group from CCl_4 in the presence of a base, and in the second one, the CCl_3 group gets substituted with primary or secondary amine (Figure 6a). Two years later, they revisited the reaction and suggested another mechanism, which considered the formation of chlorophosphate and subsequent substitution with amine (Figure 6b)[43].

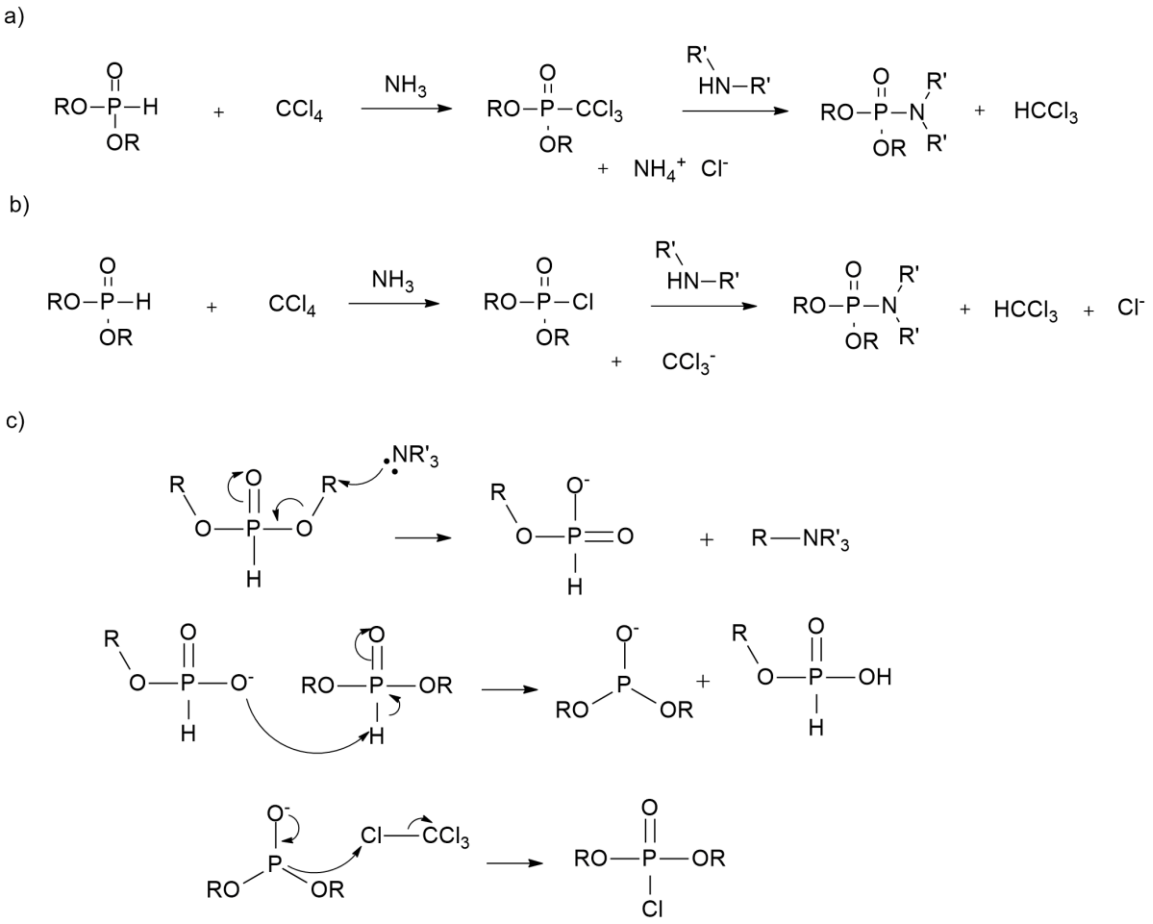

Figure 6. Reaction pathways suggested by Atherton and Todd (a, b)[42,43]. The reaction mechanism established to date (c)[44].

Several years later, Steinberg presented work, where he used trimethylamine as a base to catalyze the reaction, confirmed the latter mechanism to be more plausible, and developed it further[44,45]. The applicability of the Atherton-Todd reaction was later expanded to other nucleophilic species, such as alcohols and thiols, making it a particularly useful tool in phosphorus chemistry. Interestingly, despite its popularity, until now scientists did not fully agree on the exact mechanism of the Atherton-Todd reaction, which is partially due to instability of the transition state[46]. Yet another vital question was the stereochemistry of the reaction. Initial studies indicated that reaction is stereospecific and occurs with inversion of configuration[47,48]. Indeed, in 2010s systematic study showed that for stereochemically pure substrate, regardless of the substituents at the phosphorus center, oxidation product always exhibited inverted stereochemistry[49].

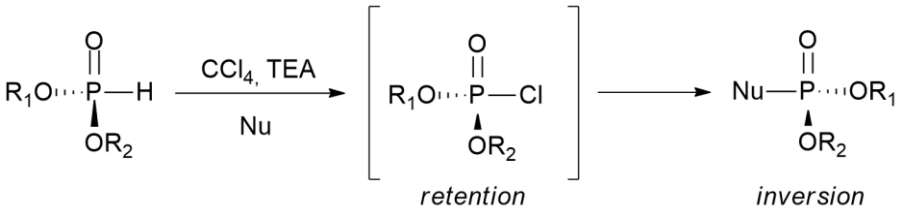

Figure 7. Stereochemistry of Atherton-Todd reaction[47,48].

1.3.2. Iodine-mediated oxidative coupling

Although the Atherton-Todd reaction gained a special status in phosphorus-related chemistry, it was not a convenient solution to use in oligonucleotide synthesis via the *H*-phosphonate approach. As mentioned earlier in Chapter 1.3., Graegg et al. discovered a more efficient way of oligonucleotide *H*-phosphonate oxidation using iodine in aqueous conditions[36]. The reaction was rapid (occurred within minutes) and clean and could be conducted just once as a final step of oligonucleotide synthesis.

While working with *H*-phosphonate analogs, namely *H*-phosphonothioates, Stawiński et al. discovered that depending on the solvent used, one can to a certain extent control the stereochemistry of the product[50]. It was found that in presence of pyridine stereochemically pure substrate undergoes epimerization and therefore the product is a mixture of two diastereoisomers. However, when in analogous reaction pyridine was omitted and acetonitrile was used as a solvent the reaction occurred with full inversion of configuration, yielding a single diastereoisomer. In oxidation reaction pyridine acts as a strong nucleophilic catalyst and it was indicated that the epimerization occurs at the pyridinium intermediate formation step.

Iodine was also applied in *H*-phosphonate amination in a study by Stawiński and Nilsson, where they thoroughly investigated controlling stereochemistry of the oxidative coupling[51]. Similarly as in the case of Atherton-Todd, using iodine in acetonitrile in order to promote amination of stereochemically pure *H*-phosphonate yielded products with inverted configuration (Figure 8a). The main advantage of the latter method was that the reaction occurred in under 5 minutes. Additionally, researchers developed an approach, which allowed for the retention of substrate's stereochemistry: after iodination of the phosphorus, the second step of chloride substitution was introduced, which resulted in a second inversion of configuration. Subsequent phosphorochloridate amination inverted the stereochemistry again yielding phosphoroamidate with configuration retained in reference to the starting *H*-phosphonate (Figure 8b).

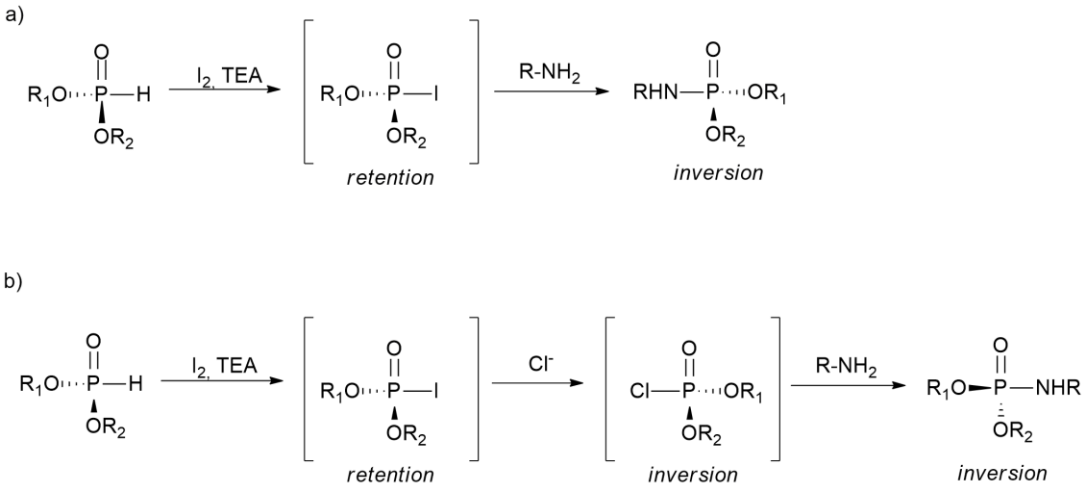

Figure 8. Stereochemistry of iodine-mediated oxidative coupling[51].

1.4. PHOSPHITE TRIESTER AND PHOSPHORAMIDITE APPROACHES

In the 1970s Letsinger and Lunsford suggested a novel method of phosphorylation that employed phosphites rather than phosphates[52], based on their finding that P(III) acylating agents were much more reactive than P(V) compounds used earlier. Reactions of phosphitylation and conjugation between nucleotides occurred much faster and with higher yields than when using phosphates and oxidation to protected phosphotriester could be carried out *in situ* (Figure 9).

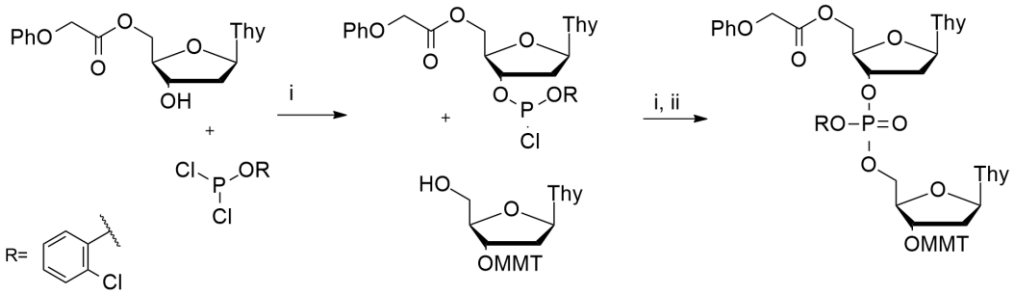

Figure 9. Phosphite triester approach synthesis carried out by Letsinger and Lunsford[52]. i) 2,6-lutidine, THF, -78°C; ii) 2,6-lutidine, I_2, THF, H_2O

Several years later, Caruthers and Beaucage refined Letsinger's method by using additional 1-*H*-tetrazole activation of monofunctional phosphoramidites in order to improve coupling between nucleotides[53]. What is more, this strategy was subsequently implemented for successful solid phase synthesis of oligonucleotides[54]. Further developments of the phosphite triester approach proved that the use of *N,N*-diisopropyl[55], and 2-cyanoethyl[56] protecting groups of phosphoramidites resulted in improved stability thereof and over time it became the most common protecting strategy.

All of the abovementioned can be considered landmark studies, which gave foundations of modern phosphoramidite oligonucleotide synthesis as we now know it. Companies started designing automated synthesizers to facilitate the process of oligonucleotide synthesis and decrease the overall time of the reactions, which opened a new chapter in the history of molecular biology. As a matter of fact, Kary Mullis, during his Nobel Lecture in 1993, mentioned that the first commercial synthesizer SAM I DNA from Biosearch played a crucial role in his research of polymerase chain reaction (PCR)[57]. Nowadays, one can find multiple commercial providers of automated synthesizers, reagents, and phosphoramidites which allow convenient and robust synthesis of oligonucleotides at several scales.

The standard oligonucleotide synthesis occurs from the 3' to 5' end of the chain and comprises the repetitive cycle of 4 steps: detritylation, coupling, capping, and oxidation (Figure 10). During detritylation, the 5'-hydroxyl group is deprotected in acidic conditions, which makes it ready for the coupling step. Coupling takes place between the exposed 5'-OH and a phosphoramidite activated with 1*H*-tetrazole (or its derivatives). Next, all unreacted hydroxyl groups are capped with acetyl group in order to prevent the formation of deletions (missing bases within the sequence). The last step consists of oxidation of the phosphite triester to phosphate triester with iodine in aqueous conditions and the cycle of adding another nucleotide can be repeated. When the final cycle is conducted and the full sequence is synthesized, the oligonucleotide is cleaved from the support and globally deprotected in basic conditions, typically with aqueous ammonia.

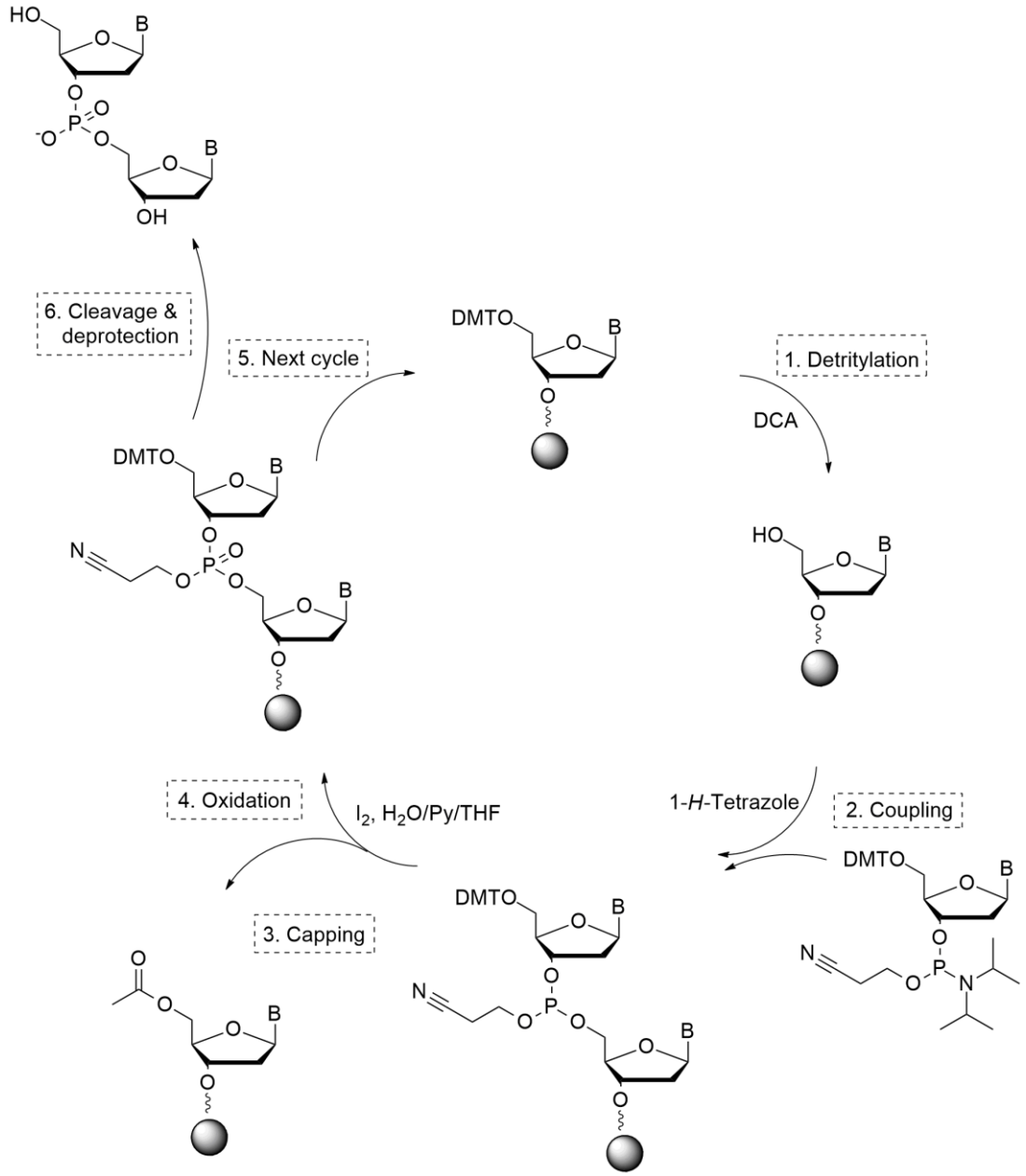

Figure 10. The synthetic cycle of solid phase oligonucleotide synthesis using the phosphoramidite approach.

2. OLIGONUCLEOTIDE CROSS-LINKING AND CONJUGATION STRATEGIES

Over the course of nearly 40 years of modified oligonucleotide synthesis history, numerous examples of functional linker-bearing DNA and RNA derivatives were devised. Some of them gained more attention as they proved to be particularly useful in molecular biology research, often allowing to gain insight into otherwise inscrutable processes. Here, I will give an overview

of several distinct conjugation and cross-linking strategies which play a crucial role in the field of nucleic acid-related research.

Cross-linking between two nucleic acid strands is oftentimes the desired process, especially when it comes to chemotherapy[58]. The formation of DNA lesions where strands are covalently bound to each other in cancer cells causes cytotoxicity which in turn leads to cell apoptosis. Drug resistance of tumor cells, however, arises from the DNA repair pathways of cross-linked lesions. Therefore the investigation of repair mechanisms of cross-linked DNA is a key to the development of novel, efficient antitumor therapies. Below, I am presenting a concise summary of several cross-linking agents (Figure 11).

- Nitrogen mustards are homobifunctional alkylating agents which cause both intra- and interstrand cross-linking in DNA between N^7 atoms of 2'-deoxyguanosines in 5'-GNC (where N is any nucleobase) sites[59]. Even though they were found to cause quite a significant bending of the helix, these cross-links are relatively unstable.
- *Bis*-chloroethylnitrosourea decomposes under physiological conditions to generate an alkylating carbamomnium ion which leads to the formation of an ethyl cross-link between N^1 atom of deoxyguanosine and N^3 atom of 2'-deoxycytidine of the opposing DNA strands.
- Mitomycin C is responsible for cross-linking between exocyclic amine groups of 2'-deoxyguanosines located in the minor groove of dsDNA. The exact mechanism of this reaction is still not fully revealed yet due to its complexity. It was found that mitomycin C cross-link does not cause disruptions in base-pairing, however, it induces local widening of the dsDNA minor groove.
- Platinum-based therapeutics are widely used and highly potent antitumor drugs which cause the formation of inter- and intrastrand cross-linking in both DNA and RNA[60]. Depending on whether the *cis*- or *trans*-platin is used, the linkage is formed between two 2'-deoxyguanosines or 2'-deoxyguanosine and 2'-deoxycytidine, respectively. Platinum cross-link induces significant bending and unwinding of the helix.
- Besides the exogenous cross-linking agents described above, there are several endogenous cross-linkers that also lead to covalent binding between two opposing purine bases of the DNA. Among others, this group includes nitrous acid, formaldehyde, acetaldehyde, acrolein, and crotonaldehyde[61]. In terms of RNA studies, cross-linking via formaldehyde proved useful in tRNA secondary structure determination[62].

Detailed study of described cross-linkers action *in situ* is rather complicated if not impossible and therefore most of these agents have been employed in structural and mechanistic studies in a laboratory setup on a larger scale. Oftentimes synthetic oligonucleotide models are prepared for that purpose. Cross-linking thereof can be conducted in either a post-synthetic manner, where a cross-linking agent is introduced to an oligonucleotide duplex with subsequent purification of the product, or by direct hybridization of two complementary oligonucleotide strands, which are pre-functionalized to form a cross-link as a response to specific stimuli[61].

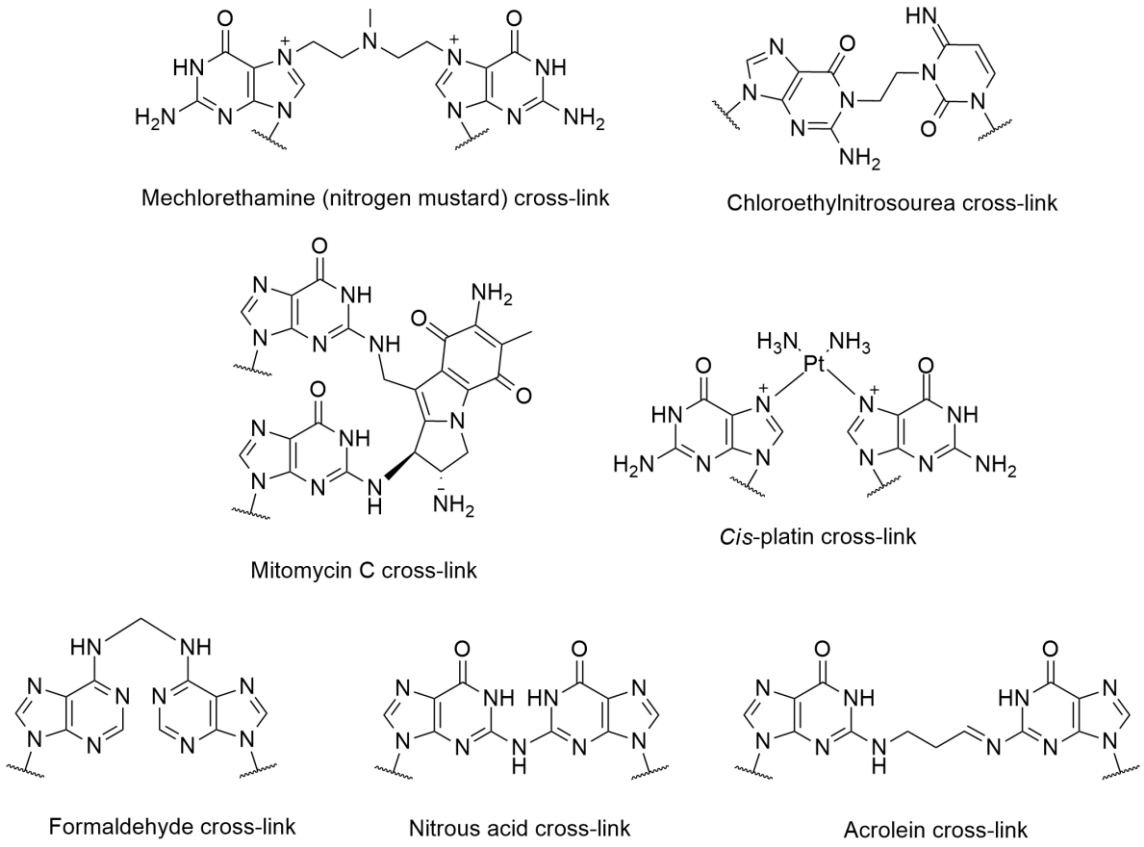

Figure 11. Structures of cross-links formed in nucleic acids upon treatment with exo- and endogenous cross-linking agents.

2.1. PSORALEN CROSS-LINKING

A particular group of cross-linkers which aside from its therapeutic properties found a broad application spectrum is psoralens. They are photoactivated therapeutic agents used particularly in skin disease treatment, which intercalate at the 5'-AT site of the DNA to form a cross-link between the two opposing thymidine residues. The linkage formation is only possible upon UV irradiation and despite the size of the molecule it was found not to cause any significant disruptions of the DNA helix geometry. Oligonucleotides modified with 4,5′,8-

trimethylpsoralen attached at 2'-deoxyadenosine were proven to cross-link to their complementary sequences with very high yields[63]. This DNA cross-linking strategy was found useful in structure studies and mapping of chromatin[64]. Moreover, it was also used as a tool to investigate the topology of tRNA:RNA primer complex in a study of reverse transcription initiation in HIV-1[65]. Furthermore, 4,5',8-trimethylpsoralen cross-linking was applied to increase duplex stability and in consequence enhance antisense oligonucleotides efficiency[66]. In one of the studies, an RNA hairpin-forming sequence was modified with psoralen which upon photoactivation cross-linked with complementary sequence to form a triplex[67]. This strategy showed to drastically suppress target protein expression.

2.2. CLICK-CHEMISTRY CROSS-LINKING

Yet another cross-linking approach that is widely used in molecular biology is so-called "click chemistry" (or click reaction), which is a copper-catalyzed [3 + 2] cycloaddition between terminal alkynes and azides[68]. The versatility of this reaction lies in its operational simplicity and mildness of required conditions. In the field of nucleic acids, it was used for interstrand cross-linking and thermal stabilization of dsDNA oligonucleotides[69]. It was also applied to synthesize branched and cyclic oligonucleotides[70], and in preparation of DNA microarrays[71]. Moreover, DNA conjugates with carbohydrates[72] and proteins[73] were obtained using click chemistry. These days, it is a popular method of fluorescent labeling of oligonucleotides for which reagents are commercially available.

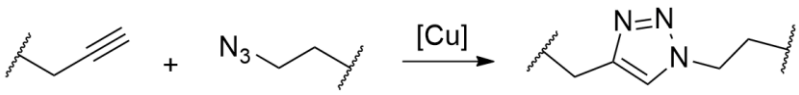

Figure 12. Scheme of the click reaction

An approach that gained valid recognition, especially in studies of RNA, is a photoactivated cross-linking between several modified nucleobases which include 4-thiouridine, 6-thioguanosine, 5-bromouridine, and 5-iodouridine[74,75]. These species can either occur naturally in a ribonucleic acid or can be inserted synthetically into the sequence. Upon UV irradiation, a radical is formed which attacks nearby functional groups forming a so-called "zero-length" linker. However, it is not possible to distinguish a single photoadduct generated as typically there are various pathways in which the cross-links can be formed. This reaction was employed in numerous studies, especially those related to revealing the structure and functional dynamics of ribozymes[76,77], mapping ribosomal RNA[78,79] and investigating interactions between RNA and proteins[80,81].

Last but not least, a plethora of research was reported regarding disulfide bridge cross-linking and conjugation as a tool for studies of nucleic acids and their interactions with other biomolecules, which is described in greater detail in the following chapters.

3. OLIGONUCLEOTIDE MODIFICATIONS FOR DISULFIDE CROSS-LINKING AND CONJUGATION

Half a century ago, scientists started discovering that not all of the nucleosides found in nature are simply adenosine, cytosine, guanosine, thymine, or uridine and that some differ in their chemical structure[82]. Up to date, there are over 170 naturally occurring nucleic acids modifications discovered and described, the majority in RNA[83]. They all exhibit specific properties and as such, they play actual roles in biochemical processes. It seems obvious that at some point in the oligonucleotide synthesis journey researchers started to develop methods to modify them in order to render properties of those synthetic nucleic acids. A plethora of modifications have been devised, some of which became commonly applied solutions over time. The overall structure of nucleotide: the nucleobase, the sugar ring, and the phosphodiester bond allows for the introduction of functional groups at several sites (Figure 13). I gathered and summarized published results in the field of oligonucleotide modifications for disulfide bridge cross-linking in a form of a comprehensive review[84] and below, I introduce the most notable examples in the topic.

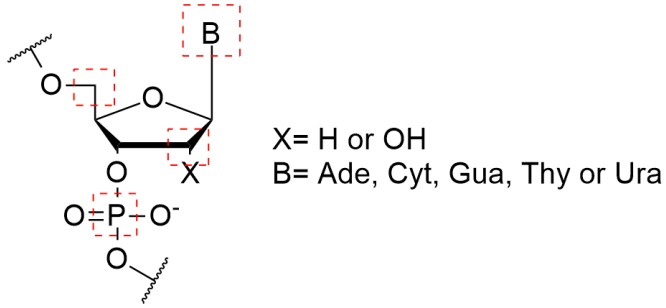

Figure 13. Scheme showing possible modification sites (indicated with red dashed boxes).

3.1. 5’ & 3’ END MODIFICATIONS

Oligonucleotide modification types can be divided in various manners. Criterion, which seems the most intuitive in the context of any modified sequence is the topology of the modification. It groups modifications based on the position in the strand, i.e. whether it is placed on 3’- or 5’-terminus or internally.

Terminal modifications of different kinds are commonly used as handy tools in molecular biology research. Many functional molecules, such as fluorescent dyes, quenchers, or biotin are available commercially and are readily used for labeling either 3'- or 5'- end of an oligonucleotide. It is also possible to decorate the strand termini with a linker bearing a functional group, such as amine or thiol (Figure 14) which allows for further modification of DNA or RNA molecules. This approach is frequently employed for the conjugation of oligonucleotides with other species, in particular with peptides, proteins, or drug carriers due to the ease of preparation and handling.

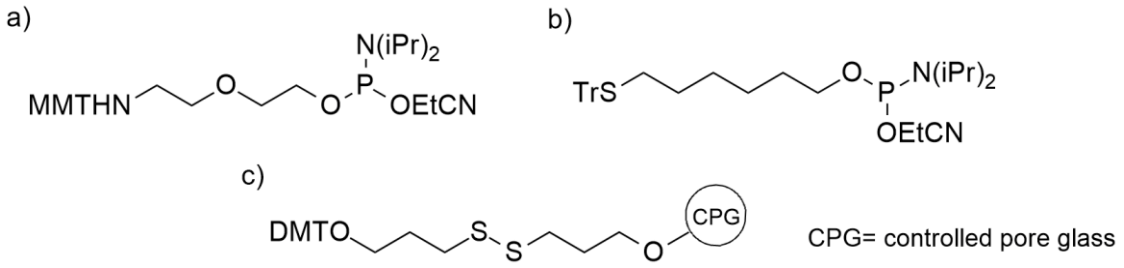

Figure 14. Commercially available terminal modifiers. a) 5'-Amino-Modifier C6; b) 5'-Thiol-Modifier C6; c) 3'-Thiol-Modifier C3 S-S CPG.

3.2. INTERNUCLEOTIDE MODIFICATIONS

Nucleic acid analogs with modified backbone can be of different nature depending on the properties that need to be achieved. Some of them became a standard solution in biochemistry-related research toolbox[85,86], whereas others are meticulously designed in order to serve a particular purpose. Sometimes it can be a seemingly minor modification, such as replacement of a 2'-hydroxyl group of RNA with a fluorine atom or methoxyethyl group to stabilize the oligonucleotide chain. Other times it is a major reconstruction of the entire sugar moiety like in locked nucleic acids (LNA)[87] or even replacement of the entire sugar-phosphate backbone with another moiety as in peptide nucleic acids (PNA)[88,89] or Morpholino (PMO)[90,91]. And then, there is an entire spectrum of possible functionalization in between the two extremes. In this part of the *Introduction*, I will highlight several examples of oligonucleotide backbone modification with tethers for disulfide bridge cross-linking.

The first reported DNA backbone modification with a disulfide linker, which became an inspiration for my project, was an attachment of 2,2'-dithiobis(ethylamine) (cystamine) at the phosphate group. Fidanza and McLaughlin combined automated solid phase phosphoramidite synthesis with the *H*-phosphonate approach. The oligonucleotide sequence was synthesized in a standard manner up to the desired position of the modification. Then, the *H*-phosphonate

was attached as the next building block and subjected to oxidative amination with cystamine, resulting in the formation of phosphoramidate linkage. The sequence was further elongated using automated synthesis. This strategy offered a possibility of introducing the linker at any chosen position within the oligonucleotide strand instead of only at the ends.

Scientists soon realized that another site at which a functional tether can be introduced without significantly affecting inherent nucleic acid properties is the 2'-position of the ribose ring. Manoharan et al. published a study in which he presented a synthesis of a 2′-O-(S-trityl-hexylthio)adenosine phosphoramidite[92]. The idea was followed by Glick and coworkers who synthesized 2'-O-(S-tert-butyl)ethyldithio derivatives of cytidine[93] and guanosine[94] phosphoramidites. Several years later, Jin et al. reported synthesis of the set of all ribonucleotides bearing ethoxythiol linkers in 2'-position[95]. All the above-mentioned phosphoramidites are shown in Figure 15.

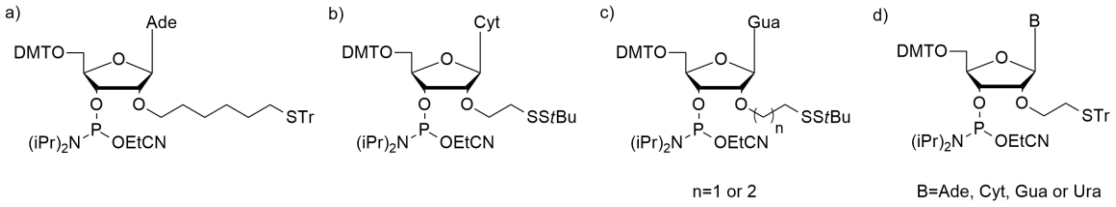

Figure 15. 2'-*O*-substituted nucleotide phosphoramidites obtained by a) Manoharan et al. [92], b) Goodwin et al.[93] c) Gundlach et al.[94] and d) Jin et al.[95].

A different approach to the same concept was used by Sigurdsson et al.[96], and Cohen and Cech[97] which relied on a post-synthetic introduction of a disulfide tether. These strategies assumed incorporation of 2'-amino analogs of uridine or cytidine in a ribozyme sequence followed by treatment with amine-reactive molecules after the RNA synthesis was complete. The nucleic acids were treated with either disulfide-bearing aromatic isothiocyanate yielding a thiourea derivative (Figure 16 top) or with a disulfide maleimide ester to give 2′-O-(S-pirydyl-2-dithio)ethylamide linker (Figure 16 bottom).

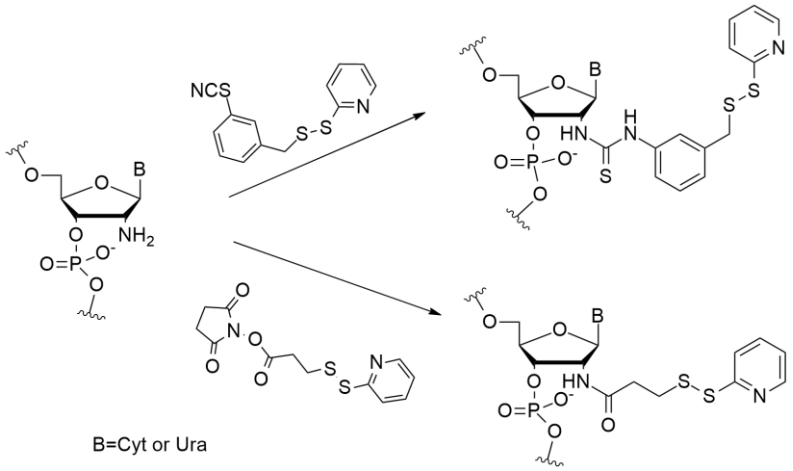

Figure 16. Post-synthetic modification of 2'-position proposed by Sigurdsson et al. [96] (top) and Cohen and Cech[97] (bottom).

Yet another interesting step in the search of solutions for disulfide cross-linking of oligonucleotides was the strategy devised by Hatano et al. They synthesized an abasic nucleotide phosphoramidite where the native heterocyclic nucleobase was replaced with a para-thiophenyl[98] (Figure 17a). Single insertion of such building block did not impair duplex-forming properties of the Dickerson DNA. In a similar manner, another group attached a methylenedisulfide at the C1' position[99] (Figure 17b).

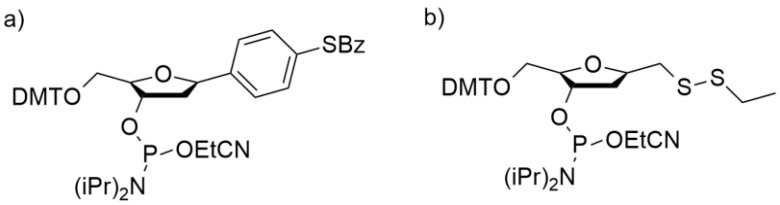

Figure 17. C1-substituted abasic nucleotide phosphoramidites synthesized by a) Hatano et al.[98] and b) Shigdel and He[99].

3.3. NUCLEOBASE MODIFICATIONS

Modified nucleobases bearing a functional tether are a fairly large and important group. Owing to their structure, both purines and pyrimidines offer a possibility of anchoring various linkers at different positions. They typically allow efficient inter- and intrastrand cross-linking of oligonucleotides as the tethers are pointing towards the helix axis and were therefore proven highly useful in studies of secondary structures of DNA and RNA.

The first one to realize the potential of nucleobase functionalization in the early 90s' was Glick, who synthesized an N^3-thioethylthymidine[100], and shortly after, together with Goodwin they obtained a ribonucleotide analog, namely N^3-thioethyluridine[101]. The disadvantage of such

modifications was that they led to disruption of base-pairing in a duplex. To avoid this, pyrimidine was functionalized with a tether at the C^5 position by several research groups[102–105]. The structure of purines is more complex than that of pyrimidines and therefore the introduction of a linker is a more challenging task. Nonetheless, such disulfide tether-modified guanosine syntheses have also been reported[94,106,107].

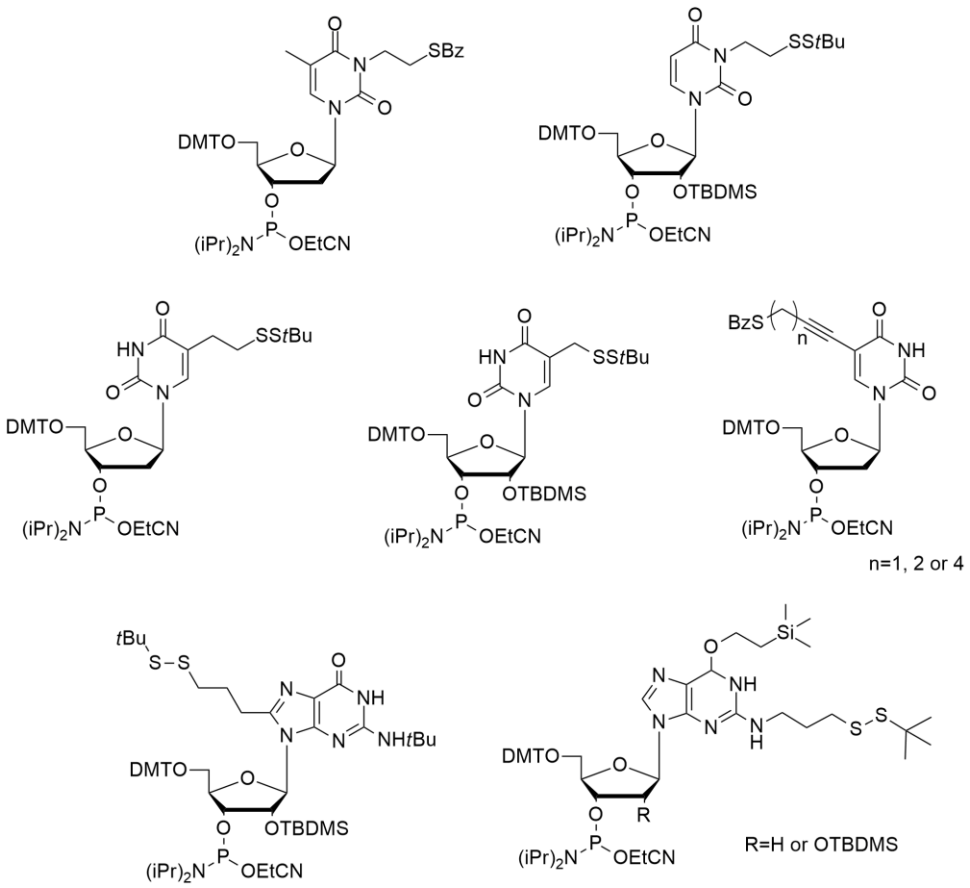

Figure 18. Structures of phosphoramidites modified with thiol and disulfide linker-bearing pyrimidines and purines.

A unique kind of nucleobase modifications that deserves separate characterization is the so-called convertible nucleoside approach[108]. It is an exceptionally neat and convenient method for a single-step post-synthetic modification of oligonucleotides with a tether of preference, including disulfide linkers. It starts with the preparation of building blocks, in which exocyclic functional groups of nucleobases are equipped with good leaving groups, e.g. aromatic rings. These phosphoramidites can be incorporated into the oligonucleotide chain during standard automated synthesis. After cleavage from the support, the product is incubated with a nucleophilic linker, such as cystamine, which attaches at the activated nucleobase position. This strategy was successfully employed for the functionalization of both DNA[109,110] and RNA[111,112] (Figure 19).

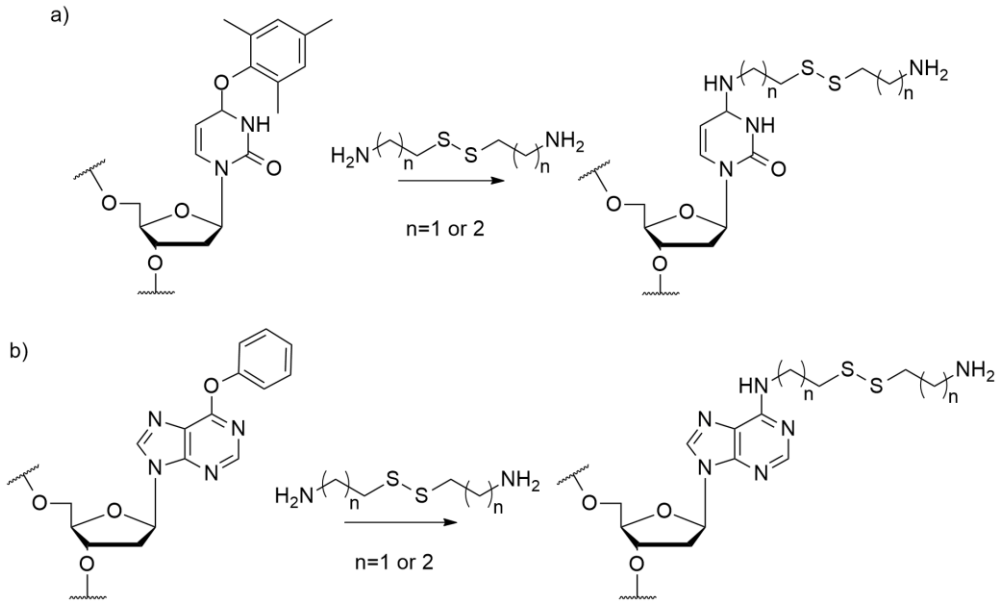

Figure 19. Scheme presenting post-synthetic modification of convertible nucleosides: a) an *O*^{4}-aryl-deoxyuridine[108] and b) an *O*^{6}-aryl-deoxyinosine[109] with cystamine/homocystamine.

4. THIOL AND DISULFIDE CHEMISTRY

Sulfur is a highly abundant element of a great biochemical significance[113]. Interestingly, it makes up 1% of the total weight of a human. In living organisms, it naturally occurs in proteins in form of two amino acids: cysteine (Cys) and methionine (Met), both possessing a thioalkyl side chain. These building blocks can form disulfide bonds which contribute to the stabilization of protein's tertiary and quaternary structure and are oftentimes vital for protein's activity and substrate binding [114,115]. Moreover, sulfur can be also found in multiple cofactors, peptides, and other biologically relevant molecules, such as thiamine, glutathione, or biotin. Sulfur-containing moieties can also be found in nucleic acids in a form of e.g.: 2-thiocytidine, 2-thiouridine, 4-thiouridine, and 2-methylthioadenosine in tRNA[116] or phosphorothioate linkage resulting in bacterial DNA degradation (Dnd) phenomenon[117].

In the periodic table, sulfur is placed in the 3rd period in the VIa group, right below oxygen and therefore thiols (-SH) are considered analogous to alcohols. However, they exhibit slightly different characteristics: in principle, they are more acidic than corresponding alcohols and thiolates

(RS^-) are much more nucleophilic than alkoxides (RO^-). The typical pK_a of thiol ranges from 7 to 9, however it strongly depends on the structure of the compound, for example, the presence of an electron withdrawing group in the vicinity increases the acidity of the RS^-.

One of the biochemically relevant reactions which involve sulfur is the interconversion between thiols and disulfides. This reaction is the basis of drug metabolism and transport phenomena. In this redox reaction, two thiols can be oxidized into the formation of an S-S bond, which can then be reduced again to form thiols, thus making the reaction reversible. The redox potential of the reaction is between -0.2 V to -0.4 V which again is dependable on the chemical structure of reacting molecules. Disulfide bridges are weaker than C-C or C-H bonds. The dissociation energy of the disulfide bond is generally ca. 60 kcal/mol^{-1}, yet the exact value depends on the moiety directly attached to the sulfur and the overall structure of the compound. It ranges from 55 kcal/mol^{-1} for aryl derivatives to over 70 kcal/mol^{-1} for alkyl disulfides[118]. The S-S bonds are flexible and depending on the nature of the molecule, its length can vary from 180 to 260 nm[119].

$$R'SH + R''SH \rightleftharpoons R'SSR'' + 2H^+ + 2e^-$$

Yet another reaction of high biochemical importance is thiol-disulfide interchange (or exchange)[120]. In this heterolytic reaction, the disulfide bond is cleaved with a thiolate, which acts as a nucleophile, in consequence forming a new disulfide and a new thiolate. The reaction follows the S_N2 mechanism, with a nucleophilic attack of the thiolate in the axis of the S-S bond. The presence of thiolate anion is crucial for the reaction to take place and it will not occur with a thiol, so the pH of the reaction needs to be kept above the pK_a of -SH. Moreover, steric factors also play a role: compounds substituted at alpha carbon react slower than unsubstituted. Additionally, the reaction rate depends on the used solvent: in polar aprotic solvents such as DMF, it is 1000-fold faster than in polar protic ones, like water.

$$RSSR + R'S^- \rightleftharpoons R'SSR + RS^-$$

5. OLIGONUCLEOTIDE CROSS-LINKING VIA A DISULFIDE BRIDGE

The disulfide bridge cross-linking and conjugation is a broad topic and a plethora of studies that utilize this strategy has been and still are being published. During the course of my research for this thesis, I have collected and analyzed articles about the most remarkable and often innovative examples of the disulfide bond cross-linking applications and combined them into a review, which summarizes this broad topic[4]. Below, I present the most interesting and relevant among them in the context of my research.

5.1. DNA CROSS-LINKING

Cross-linking via disulfide bridge has been widely exploited in studies of DNA secondary structures. Ferentz and Verdine were the pioneers who used the disulfide tethers- cystamine and homocystamine in order to covalently join together two complementary oligonucleotides[109,121]. They found that it greatly stabilized the structure, increasing the melting temperature of the duplex by over 16°C as compared to the native B-DNA helix. Similar results were achieved later by Milton et al.[122] and Coleman et al.[123], who cross-linked two DNA strands without using any linker but rather by introducing 4-thio-2'-deoxyuridine/thymidine and 6-thio-2'-deoxyinosine into the sequence. In the aforementioned experiments, the cross-linking did not notably distort the helical structure of the duplexes. In fact, it was used as a tool for a study of the mechanism of dsDNA interconversion from B to Z form[124].

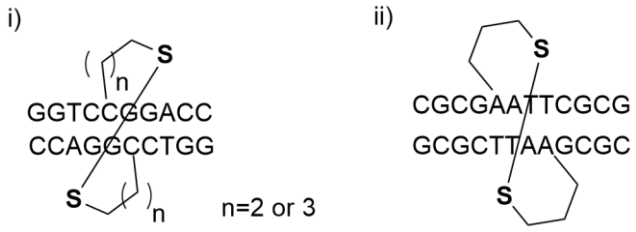

Figure 20. Disulfide cross-linked DNA duplexes obtained by Wolfe and Verdine[110,125].

On the other hand, some other studies looked into the disulfide cross-linking of dsDNA as means of inducing structural disruption in a controlled manner. For instance, Wolfe and Verdine investigated whether the introduction of a short interstrand cross-linker could induce torsional stress and lead to unwinding yet they found only local disruption in base-pairing[125]. Disulfide cross-linking was also applied in studies of bending of the DNA helix, either artificially forced[110] or caused by exogenous factors, such as cisplatin[126].

Although hairpins are much more abundant in the RNA world, some experiments were conducted in order to investigate the influence of a covalent cross-link on DNA hairpins, also leading to the conclusion that it stabilizes the structure[100]. Using NMR spectroscopy, Glick's laboratory managed to compare a solution structure of a native and disulfide cross-linked DNA hairpin confirming that the overall geometry of its stem was retained in the presence of the linker[127,128]. (Bis)disulfide cross-linked DNA was also used in a study of DNA hairpin-dumbbell interconversion[129,130] (Figure 21a). Some more complex, non-canonical DNA secondary structures have been obtained as well and stabilized through disulfide cross-linking. That includes triple helices formed by a single[131] or more separate strands[104,132], looped and

branched oligonucleotides[133] or DNA double crossover tiles (abbreviated DAE, Figure 21b)[134]. Endo and Majima obtained a large, self-assembling formation of cross-linked DNA double helices[135,136] whereas more recently Wolfrum et al. managed to synthesize a DNA nanostructure comprising 704 nucleotides using 34 oligonucleotides linked with a disulfide bridge in 19 cross-linking sites[137] (Figure 21c).

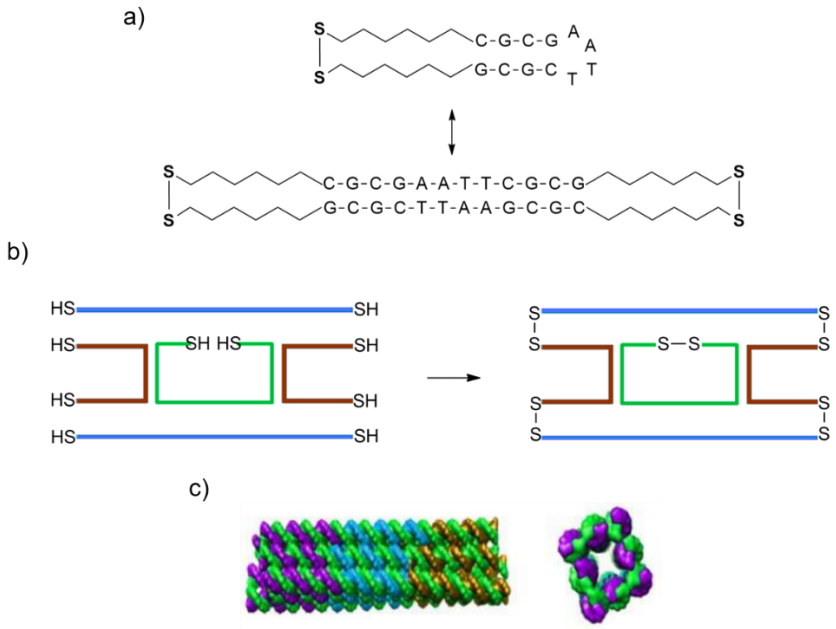

Figure 21. Scheme representing a few DNA secondary structures obtained using disulfide cross-inking. a) DNA hairpin-dumbbell interconversion by Gao et al.[129,130]; b) DNA double crossover tiles by De Stefano and Vesterager Gothelf[134]; c) DNA nanotube (reproduced from Wolfrum et al. [137].

5.2. RNA CROSS-LINKING

While the DNA naturally prefers a double helix conformation, the RNA may fold into multiple distinctive secondary structures, all of which can have different functionality which imposes their activity *in vivo*. That is why the cross-linking strategy was found particularly useful for studies and mapping of RNA structural motifs. It enables identification of either inter- or intramolecular interactions or induction of non-native structural constraints, often allowing for elucidation of the structure-activity relations[74].

Disulfide cross-linking was also used to covalently restrain certain RNA secondary structures. When applied in a duplex, it induced a great stabilization thereof increasing its melting temperature by 40°C[138]. The analogous effect was achieved for hairpins: cross-linking between two opposite strands of the stem[101] as well as between two adjacent nucleobases in the loop[139] caused a significant increase in thermal stability of the species.

The strategy was applied in studies of larger and far more complex RNA structures. In the late 90s,' it was used for intrastrand cross-linking in yeast $tRNA^{Phe}$ proving no disruptions of the native structure and opening a way for further experiments over its folding and conformational dynamics[93,140]. Cohen and Cech used a similar approach in their research of thermal motions dynamics of group I ribozyme from *Tetrahymena thermophila*[97]. Furthermore, the disulfide cross-linking played a pivotal role in studies of hammerhead ribozyme by helping to resolve a disagreement over the structure of its catalytically active form through elucidating a relative orientation between helices I and II[96,141]. Later, it was also used in a clever experiment where the catalytic activity of the hammerhead ribozyme was inverted. The introduction of a flexible disulfide crosslink between the ribozyme and a substrate showed to greatly increase ligation rate as compared to native structure[142].

5.3. OLIGONUCLEOTIDE-PEPTIDE CONJUGATES

Conjugates between oligonucleotides and peptides usually serve one fundamental purpose-enhanced cellular delivery of the former and in consequence improved therapeutic activity. Antisense nucleic acids in native form suffer from very poor cell membrane uptake due to their significant hydrophilicity arising from the negatively charged backbone. One possible way to overcome this issue is to decorate them with a moiety that would allow membrane permeability without impairing their activity. A class of peptides known as cell penetrating peptides (CPPs) are cationic species built of 5-30 amino acids and for over 30 years are extensively investigated as carriers for antisense oligonucleotides[143]. What makes disulfide cross-linking a particularly useful strategy for CPP-ASO conjugation is the fact that the disulfide bridge is cleaved after cellular internalization due to the reducing conditions of the environment[144,145], and thus a free, fully functional antisense strand can be released. There is a number of studies reporting the applicability of peptide-oligonucleotide conjugates in gene silencing, inhibition of protein expression, and splicing correction[146–154]. Nucleic acids successfully delivered using this approach range from unmodified single-stranded DNA[152,155–160], phosphorothioates[147,153,161], RNA[150,162,163] as well as PMO[164] and PNA[151,165–171].

5.4. OLIGONUCLEOTIDE-PROTEIN CONJUGATES

Nucleic acids interact with proteins in numerous fundamental biological processes. Gene expression, transcription, replication, DNA repair: they all rely on interactions between DNA or RNA and an enzyme. These interactions are oftentimes transient as interspecies contacts are momentary which sometimes makes them very challenging to monitor and study. Covalent

cross-linking offers a way of trapping otherwise temporary complexes in a sort of preserved static state, often allowing mechanistic and structural insight. The disulfide cross-linking is particularly convenient since one of the protein-building amino acids- cysteine- bears a thiol side chain, which may be naturally present at the site of cross-linking or introduced employing molecular engineering at the chosen position.

Conjugation via disulfide linkage has been successfully used in mechanistic studies of nucleic acids- protein complexes. By using this strategy scientists determined a minimal RNA hairpin substrate for RNA glycosylase ricin[111] and figured out the mechanism of substrate unwinding by RNase P[172]. It also allowed investigation of human immunodeficiency virus 1 reverse transcriptase (HIV-1 RT) interactions with the template:primer which illustrated conformational changes upon substrate binding[173,174] and gave some implications for the roots of HIV's drug resistance[175,176]. Moreover, disulfide cross-linking proved useful in studies of DNA repair, serving as a tool for revealing the mechanism of DNA lesions detection by several DNA glycosylases[3,177–180] and DNA transferases[99,181–186] (Figure 22).

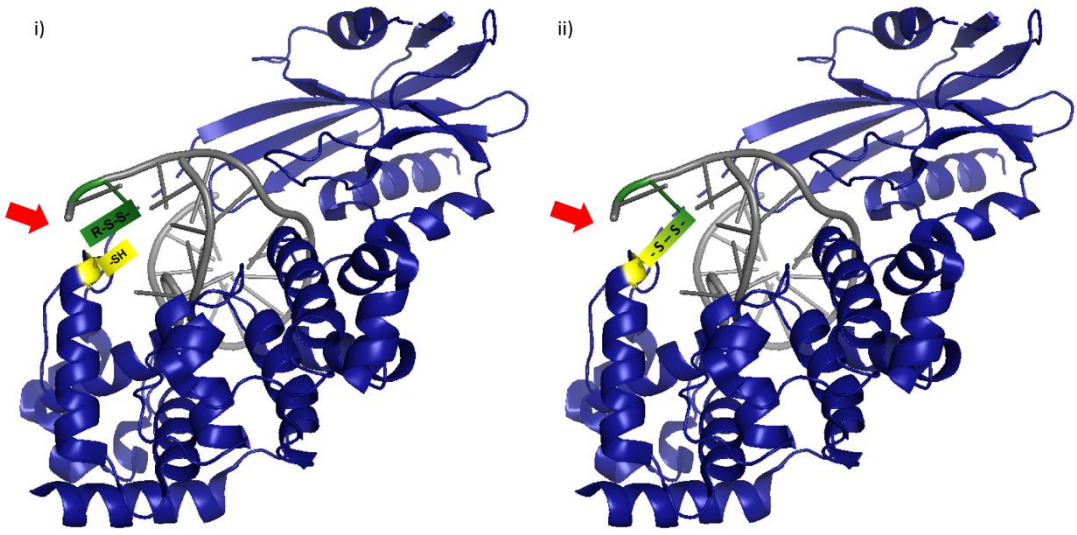

Figure 22. Crystal structure of MutY glycosylase with anti-substrate dsDNA: i) before and ii) after disulfide cross-linking[3]. The conjugation site is indicated with a red arrow.

Additionally, in some cases not only did the cross-linking give mechanistic indications but also allowed for solving a crystal structure of a protein-nucleic acid complex. For example, it helped to obtain crystals of bovine poly(A) polymerase conjugated with RNA[187] and elucidated how mouse p53 tumor suppressor protein is assembled on DNA duplex[188]. Sometimes, even seemingly non-specific binding may afford crystal structures. It was presented in an elegant, systematic study of DnaG primase[2]. The method employed, named FASTDXL, assumed no

detailed knowledge of intermolecular interactions. 20 disulfide tether-bearing oligonucleotides were cross-linked with 16 protein variants with single cysteine mutations yielding 320 combinations. As a result, two novel crystal structures of DnaG primase were resolved.

Some researchers found that by conjugating with nucleic acids, one can impose some non-native features on proteins. Corey and Schultz engineered otherwise non-specific deoxynuclease so that once covalently linked to an oligonucleotide, the hybrid enzyme would cleave ssDNA at the preferred site[189]. Imposing tailored properties was shown in a study of sequence-targeted toxin:RNA aptamer complex linked by a disulfide bridge, which proved targeted toxicity against prostate tumor cells[190,191]. Other times, it was the protein that served as a carrier for therapeutically potent oligonucleotides. In the 90s', antisense DNA conjugated with mannosylated serum albumin or streptavidin exhibited increased internalization in comparison with unmodified nucleic acid[192–194]. More recently, immunoconjugate consisting of antisense oligonucleotide and monoclonal antibody presented promising results in the treatment of acute lymphoblastic leukemia (ALL)[195].

III. RESULTS AND DISCUSSION

1. BACKBONE MODIFICATION OF RNA WITH A DISULFIDE LINKER

The first reported modification of phosphodiester moiety of an oligonucleotide with disulfide linker, namely cystamine, was carried out in the early 90s' by Fidanza and McLaughlin[196]. Based on findings of Atherton and Todd[2], and Froehler[3] they presented a method that allowed functionalization of DNA with a thiol tether at any chosen phosphodiester linkage of an oligonucleotide strand between two automated synthesis cycles. Original protocol assumed conjugation of *H*-phosphonate activated by 1-adamantanecarbonyl chloride followed by oxidative coupling of cystamine (Figure 23). This allowed the attachment of other functional compounds to the backbone of DNA, e.g. thiol specific fluorescent labels.

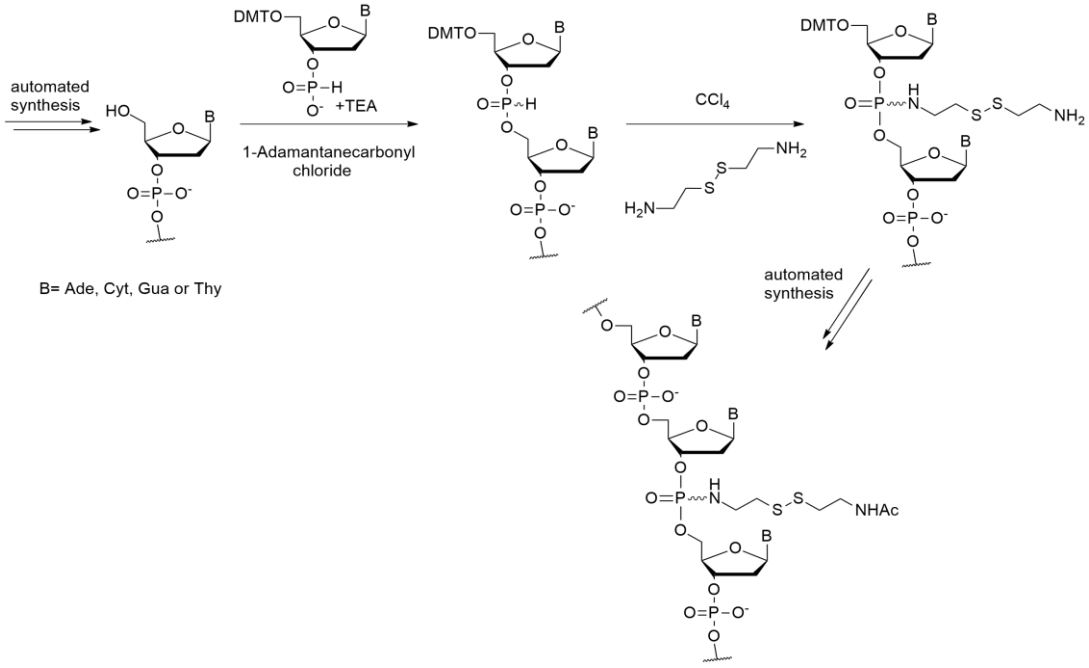

Figure 23. Scheme of the synthesis of cystamine-modified oligonucleotides presented by Fidanza and McLaughlin[196]

1.1. SYNTHESIS OF 2,2'-DITHIOBIS(ETHYLAMINE) (CYSTAMINE)

Despite being a simple molecule, cystamine is not commercially available in a free amine form. It can be obtained in two pathways: by oxidation of 2-aminoethanethiol (cysteamine) or by extraction from cystamine hydrochloride salt. The first method is highly convenient and very efficient, however, it is relatively expensive, whereas the latter is cost-effective yet does not give high yields. For the purpose of my project, I used both methods interchangeably.

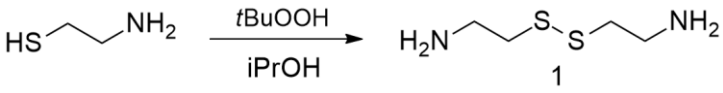

Figure 24. Oxidation of cysteamine to cystamine

To obtain the disulfide linker, cysteamine was dissolved in isopropanol and treated with *tert*-Butyl hydroperoxide solution. The reaction was stirred at reflux until completion for 3 hours yielding cystamine **1**. Importantly, any traces of water in the product were removed by thorough lyophilization. The yield of the reaction was around 94-96%.

Alternatively, cystamine can be obtained in form of a free amine from cystamine hydrochloride. In this pathway, cystamine hydrochloride was dissolved in water and a 6N sodium hydroxide solution was added for neutralization. The change of pH of the solution was monitored until it became alkaline to ensure that all the hydrochloride was consumed. Water was then evaporated to dryness and the resulting white precipitate was immersed in dichloromethane for 24-48 hours to extract the cystamine (**1**). The solution was then dried over anhydrous sodium sulfate, filtered and solvents were removed under vacuum to yield a yellow oil. The typical yield of this process was 40-60%. If the extraction step was repeated, an additional 15% of the product could be obtained.

1.2. SYNTHESIS OF 3,3'-DITHIOBIS(PROPYLAMINE) (HOMOCYSTAMINE)

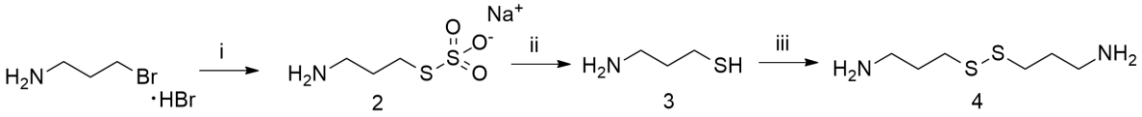

Figure 25. Synthesis of homocystamine. i) sodium thiosulfate, MeOH/H_2O; ii) MeOH/H_2O; iii) I_2, MeOH/H_2O

It was clear to me that for the future purpose of cross-linking and conjugation the linker length is an important factor. Shorter linkers did not appear to have much applicability, therefore I decided to synthesize a linker that would be longer than cystamine and retain the flexibility of an alkyl chain. Therefore, 3,3'-dithiobis(propylamine) (**4**) was chosen as an appropriate solution. Homocystamine was synthesized in a one-pot, three-step synthesis. The first step in fact comprises two stages. In the first stage, 3-bromopropylamine hydrobromide was treated with sodium thiosulfate in methanol-water to obtain Bunte salt of propylamine (**2**). The first stage of this reaction occurs rapidly, after around 2 hours of refluxing, the substrate is consumed. The reaction mixture was then refluxed for additional 12 hours. In consequence, Bunte salt hydrolyzed after around 6 hours yielding 3-aminopropanethiol (**3**). In the second

step, thiol was oxidized to form a disulfide. This was done by dropwise addition of iodine in methanol, which typically took up to 8 hours until completion. Lastly, the free homocystamine was extracted in a similar manner as cystamine described above- the crude product was first transformed to homocystamine hydrochloride and then after neutralization with 6N sodium hydroxide, the final product (**4**) was extracted with dichloromethane. Finally, the solution was dried over anhydrous sodium sulfate, filtered and solvents were removed under vacuum to yield orange oil (70-80% yield).

1.3. SYNTHESIS OF P-CYSTAMINE RNA

The method of obtaining such P-cystamine modified oligonucleotides has only been limited to DNA. In early studies, the introduction of alkylamine tether in RNA dinucleotide at the phosphorus was found to result in hydrolysis of the internucleotide linkage[35,42]. I chose to obtain RNA sequence 5'-AGUGCGACAC***C****UGAUUCC-3' (**O1**, *-cystamine **1**) using the following semi-automated approach. First, the oligonucleotide chain was extended by automated solid-phase synthesis using phosphoramidite chemistry. Once the nucleotide preceding the site of modification was attached, the 5'-hydroxyl group was deprotected on the synthesizer and the column was removed from the synthesizer. An empty syringe was attached to one side of the column. A mixture of cytidine *H*-phosphonate and 1-adamantanecarbonyl chloride in acetonitrile-pyridine (1:1) was prepared, drawn into another syringe, which was then mounted on the other side of the column and the support was carefully washed back and forth with the solution for 15 minutes, resulting in the formation of *H*-phosphonate diester. The solution was then discarded and the column was flushed thoroughly with acetonitrile. Next, the support was washed for 1 hour with the solution of cystamine in pyridine with addition of carbon tetrachloride in a similar manner as the previous step to allow oxidative coupling of the amine to the *H*-phosphonate diester. Finally, the reaction mixture was discarded, support was washed with pyridine and the column was again mounted on the synthesizer, and flushed with acetonitrile. Oligonucleotide chain extension was then carried out automatically, starting with a 5'-OH capping step. After the first detritylation step, a bright orange color was observed proving that the nucleotide was indeed attached to the chain. After the synthesis was finished, oligonucleotide was cleaved from the support and deprotected using standard procedures (Chapters 2.7.4 & 2.7.5 of *Materials and methods*) and the crude product was subjected to analysis. Unfortunately, oligonucleotide **O1** appeared to degrade rapidly after the final deprotection of 2'-hydroxyl groups with triethylamine trihydrofluoride. The analysis of **O1**

(Figure 26) using ion-pairing RP-HPLC showed the presence of multiple peaks, including two shortmers, and none of them could be assigned to the intended final product. In order to study the fragmentation pattern, I separated species corresponding to major peaks via RP-HPLC and subjected them to MALDI-TOF-MS analysis for identification. Masses found during the analysis and assignment of sequences corresponding to peaks are presented in Table 1.

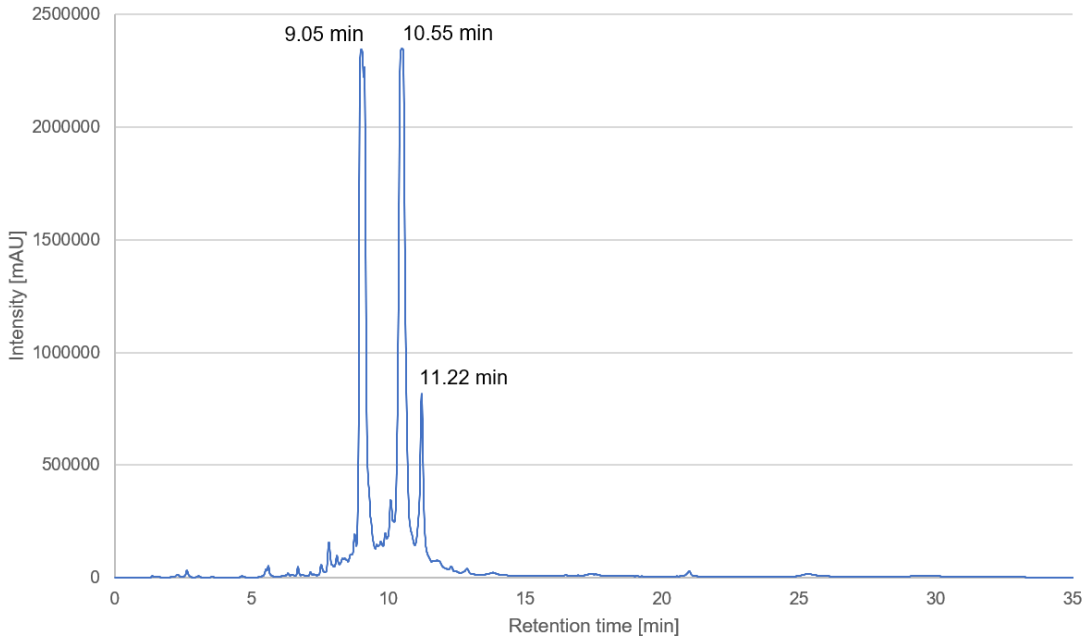

Figure 26. RP-HPLC chromatogram of the crude oligonucleotide **O1**.

Among the separated fragments it was possible to identify the following masses: the two main peaks were corresponding to the first part of the sequence (from the 3'-terminus to the site of its modification, t_r= 9.0 min) and to the second part (from the modification site to the 5'-terminus, t_r =10.5 min) bearing a 3'-phosphate group. Both of these species were formed in equal amounts. Additionally, trace amounts of a full yet unmodified sequence were identified as well (t_r = 11.2 min).

It is a widely known fact that the RNA is less stable than DNA and requires more delicate handling to avoid its cleavage[197]. Over the years, multiple mechanisms of the hydrolysis of internucleotide linkage in RNA were suggested and considered different steric factors and cleavage conditions[198]. In principle, it is believed that the RNA cleavage is a result of an intramolecular nucleophilic attack of the 2'-hydroxyl moiety on the phosphorus which leads to the formation of unstable 2',3'- cyclic phosphate intermediate. In basic and highly acidic aqueous conditions (pH<2)[198], the cyclic intermediate rapidly undergoes cleavage yielding a mixture of 2'- and 3'- ribonucleic acid phosphate, and 5'-hydroxy nucleic acid.

Table 1. Peak assignment of fragmentation products of **O1**.

Retention time [min]	M_{exp} [Da]	Corresponding fragment sequence and description (5' → 3')		M_{calc} [Da]
9.0	2140.0	UGA UUC C	From 3'-end to modification site	2141.3
10.5	3563.8	AGU GCG ACA CCp	From modification site to 5'-end	3568.2
11.2	5694.9	AGUGCGACACCUGAUUCC	Full length chain without cystamine	5691.5

Removal of TBDMS protecting group using triethylamine trihydrofluoride in presence of triethylamine exposes the 2'-OH group, which subsequently conveys nucleophilic attack on adjacent phosphorus leading to the formation of a cyclic 2',3'-phosphate transition state. Unlike in native RNA, in the case of P-cystamine modification, the phosphoramidate lacks the negative charge, which would typically add to the stability of the phosphodiester. An additional factor, which promotes cleavage of the strand is the fact that from all of the substituents at the phosphorus, the only one which is a good leaving group is the primary alcohol, i.e. the 5'-hydroxyoligonucleotide. To further support the notion that the RNA cleavage occurs at the site of modification the chromatographic analysis of **O1** showed that the two main products-shortmers corresponding to the first and the second part of the sequence were produced in equal amounts. According to mass spectroscopy, none of the shortmers carried a linker, which means that it either dissociates further after the strand hydrolysis or upon ionization during the analysis itself. The presence of the full length RNA sequence without the linker can be explained by the fact that the oxidative coupling of cystamine to *H*-phosphonate diester intermediate is not quantitative. It means that the remaining *H*-phosphonate diester gets oxidized with iodine in the next coupling step, further down the automated chain extension. In Figure 27, a plausible cleavage mechanism is presented with an indication of possible fragmentation patterns leading to an obtained mixture of **O1** fragmentation products.

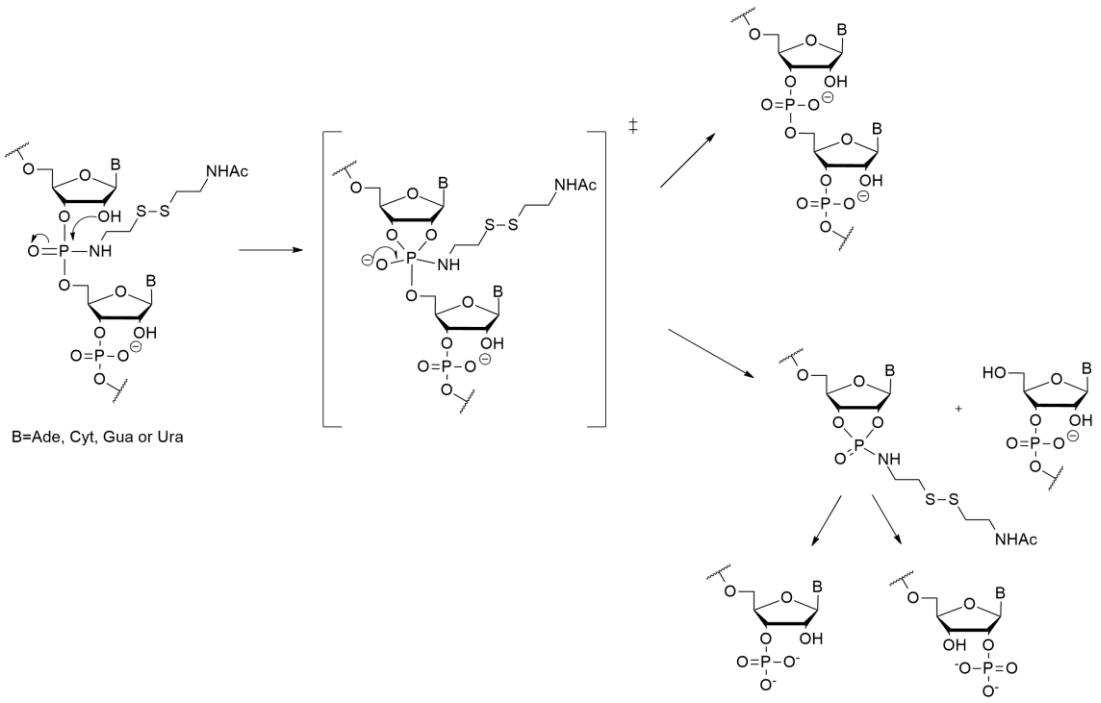

Figure 27. The mechanism pathways of P-cystamine RNA cleavage

At that point, it became clear that the disulfide linker functionalization of RNA oligonucleotides at the phosphorus center is not feasible using ribonucleotide *H*-phosphonates. In order to overcome the issue and to obtain a stable modified RNA sequence, I decided to replace the ribonucleotide at the site of modification with its analog which does not comprise the 2'-OH group, hence is less susceptible to hydrolysis.

The primary choice was 2'-deoxyribonucleotide, which appeared as the most straightforward and intuitive being a natural ribonucleotide analog. In principle, the insertion of a single 2'-deoxynucleotide in the RNA sequence should not affect the overall geometry of the oligonucleotide strand. It was, however, presented that it causes local disruptions of the structure[199], which in particular cases, such as e.g. interactions with other biomolecules, can be unfavorable. It is a consequence of the ribose ring puckering difference between the DNA and the RNA as, due to steric factors, the first prefers C2'- endo conformation whereas the latter takes C3'- endo (Figure 28)[200].

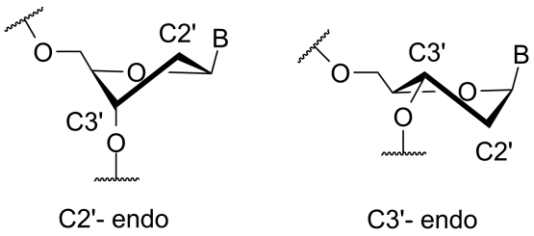

Figure 28. Ribose ring conformations of 2'-deoxyribonucleotides in B-DNA helix (C2'-endo) and ribonucleotides (C3'-endo) in A-RNA helix.

To minimize the effect of ribonucleotide replacement, 2'-deoxy-2'-fluororibonucleotide was chosen as an alternative solution. 2'-substituted ribonucleotide analogs such as 2'-O-methyl- (2'-OMe) 2'-fluoro- (2'-F) and 2'-O-methoxyethylribonucleotides (2'-MOE) are often used to stabilize the oligonucleotide while retaining C3'- endo conformation of native RNA. Out of these, 2'-F analogs are considered to be the most efficient at mimicking RNA since the fluorine atom is of a size similar to the hydroxyl group and these two groups are, to large extent, bioisosteric[201,202]. It was also proved that even point insertions of 2'-fluororibonucleotides into oligonucleotide strand results in a significant increase in thermal stability of DNA-DNA or DNA-RNA duplexes compared to unmodified sequences[203].

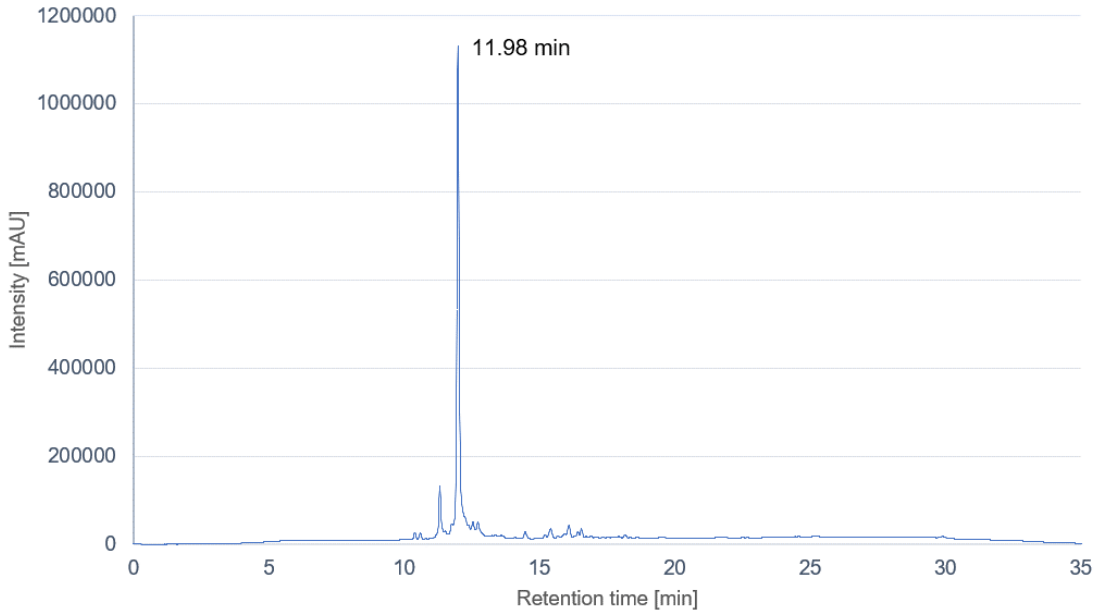

Figure 29. RP-HPLC chromatogram of the oligonucleotide **O2.**

To prove the abovementioned rationale, I synthesized an RNA sequence 5'-AGUGCGACAC**2'FC***UGAUUCC-3' (**O2**, 2'FC- 2'-deoxy-2'-fluorocytidine) using the same procedure as **O1** but replacing the cytidine *H*-phosphonate with 2'-deoxy-2'-fluorocytidine *H*-phosphonate. The oligonucleotide was cleaved and deprotected according to standard

procedures and the crude product was subjected to initial analysis. After the presence of the intended sequence was confirmed, the oligonucleotide was purified using urea-polyacrylamide gel electrophoresis and characterized using RP-HPLC (Figure 29) and MALDI-TOF-MS (M_{exp}=5871.9, M_{calc}= 5869.5).

2. OPTIMIZATION OF MANUAL *H*-PHOSPHONATE COUPLING REACTION

Even though the synthesis of P-cystamine-modified oligonucleotides was carried out nearly three decades ago and initially appeared as potential multi-purpose candidates for further functionalization, the strategy did not seem to be fully optimized.

Using the approach presented by Fidanza and McLaughlin[196], the yield of products has been relatively low and there was nearly no data presented on the systematic study of the synthesis or development of the methodology. In order to achieve higher efficiency, it was necessary to carry out a consistent examination of possible variants of the P-cystamine oligonucleotide synthesis. Pilot sequence **O2** was chosen for the study and the influence of several factors was examined: the activator used, the condensation time, and the halogenating agent used in the oxidation step.

Table 2. Synthesis conditions variants used during optimization

Sequence	Activator	Condensation time	Halogenating agent
O2A	AdCl	15 min	CCl_4
O2B	PivCl		
O2C	AdCl	5 min	CCl_4
O2D		15 min	
O2E	AdCl	10 min	I_2
O2F			NIS
O2G			NCS

AdCl- 1-Adamantanecarbonyl chloride; PivCl- Pivaloyl chloride; NIS- N-iodosuccinmide; NCS- N-chlorosuccimide

2.1. STUDY OF THE ACTIVATOR

In order to achieve the best coupling yield between the free 5'-hydroxyl group and the *H*-phosphonate, two activators were chosen to be examined based on the literature, namely 1-Adamantanecarbonyl chloride (AdCl) and Pivaloyl chloride (PivCl)[204,205]. These reagents had

been once successfully applied as condensing agents in the *H*-phosphonate approach of oligonucleotide synthesis when this strategy was considered a viable alternative to the phosphoramidite method. Although no noticeable differences in the coupling efficiency observed between PivCl and AdCl were observed, the latter became the most standard activator[206]. At that point, the main reason for that was the increased stability of the AdCl solution in pyridine-acetonitrile as compared to PivCl. Moreover, AdCl appears as a solid at room temperature whereas PivCl is a fuming, highly toxic liquid with a pungent odor, which makes it much less convenient to handle.

Yet another factor, which has a significant impact on the reaction yield is the preactivation time between the *H*-phosphonate and the activating agent prior to the condensation. It was found that it should be reduced as much as possible since extended preactivation times lead to the formation of trivalent side products such as phosphite triesters and acyl phosphites[207]. Therefore, it is crucial that the *H*-phosphonate solution is mixed with the activator immediately before the condensation reaction.

For this study, I have decided to examine how the choice of the condensing agent influences the overall yield in the cases where only a single nucleotide is introduced to the growing oligonucleotide chain in the form of *H*-phosphonate. To maintain consistency of the results, I simultaneously ran two semi-automated oligonucleotide syntheses of identical sequence (**O2**) at 1 µmol scale according to the general protocol (Chapters 2.7.2 & 2.7.3 of *Materials and Methods*), using either 1-adamantanecarbonyl chloride or pivaloyl chloride as activators for the synthesis of **O2A** and **O2B**, respectively. Cleavage from the support and deprotection of both samples was carried out using standard procedures. Crude products were analyzed using RP-HPLC and the samples were purified with denaturing urea-PAGE. The bands on the gel of both samples were migrating with a similar pattern (Figure 30). Each clearly visible band was cut out, the oligonucleotide was eluted and samples were analyzed with RP-HPLC and MALDI-MS to identify the products. The broadest bands (indicated with red arrows) were identified as target product oligonucleotide **O2**.

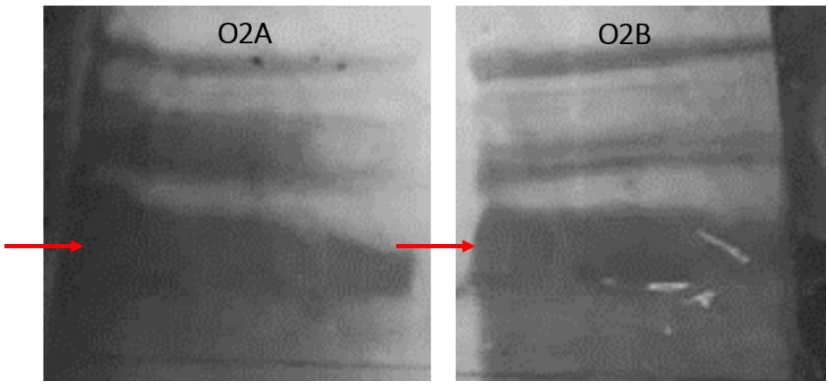

Figure 30. Urea-PAGE purification of samples O2A and O2B.

The amounts of the final products were obtained by absorbance measurement on a spectrophotometer. There was nearly no difference in the efficiency of the two condensing agents compared in this study. In this case, I concluded that the final factor to be taken into consideration when choosing the activator is simply personal preference since both PivCl and AdCl have their advantages and disadvantages. The first one is rather unpleasant to work with, mainly due to its vapors, but on the other hand, is less hygroscopic and therefore less susceptible to decomposition in contact with water than AdCl. For my further studies, I preferred using 1-Adamantanecarbonyl chloride, which I found more convenient to handle.

2.2. STUDY OF THE CONDENSATION TIME

Established protocols for automated *H*-phosphonate solid phase oligonucleotide synthesis included clear indications of the time of the coupling stage. It was previously discovered that the effective condensation time between the *H*-phosphonate and 5'-OH group is ca. 2 min when the reaction mixture is recycled in a closed loop[206]. It is reasonable to believe that the same reaction rate can be achieved using the manual coupling method, however, it was decided to verify whether it is possible to achieve better efficiency by extending the reaction time.

For that purpose, two semi-automated oligonucleotide syntheses of identical sequence **O2** were run simultaneously at a 1 µmol scale according to general protocol, the only variation being the time of the condensation reaction- namely 5 min or 15 min for **O2C** and **O2D**, respectively. Cleavage from the support and deprotection of both samples was carried out using standard procedures. Crude products were analyzed using RP-HPLC and samples were purified with denaturing urea-PAGE. Both oligonucleotides had a nearly identical migrating pattern, with the main product appearing as the widest band (Figure 31). Each clearly visible band was cut out, the oligonucleotide was eluted and samples were analyzed with RP-HPLC

and MALDI-MS in order to identify products. The analysis confirmed that the main bands in the gel corresponded to a full length sequence with cystamine **O2**.

Amounts of the final products were obtained by absorbance measurement on a spectrophotometer. 3-fold extension of coupling time resulted in a minor increase of the final product yield, however, the difference cannot be claimed significant. The study led to the conclusion that the initial minutes of coupling are indeed the most crucial and dictate the overall yield, yet an additional extension of reaction time may be beneficial. Eventually, 10 minutes was chosen as the most optimal compromise and applied for all the following syntheses carried out for this project.

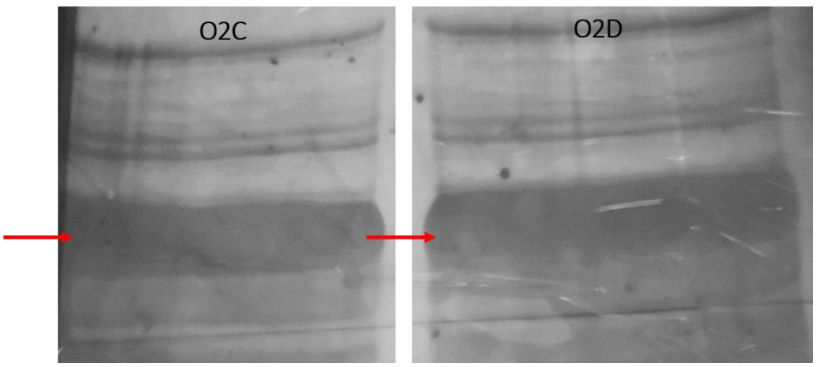

Figure 31. Urea-PAGE purification of samples O2C and O2D.

2.3. STUDY OF THE OXIDIZING AGENT

Once the *H*-phosphonate is condensed with the 5'-OH of the oligonucleotide strand, the oxidative coupling needs to be carried out to attach the cystamine to the phosphonate. Principles of oxidative coupling reaction are described in more detail in Chapter 0. In brief, oxidative coupling of the *H*-phosphonate is a two-step reaction: (i) halogenation of the phosphorus and (ii) subsequent substitution with nucleophilic species, e.g. water or amine. The most common method involves the use of iodine in pyridine or acetonitrile[51], but historically the first one to be described was the Atherton-Todd reaction in which coupling is mediated by chlorine from carbon tetrachloride[42]. Besides the mechanisms, another difference between these two approaches is the rate of the reaction- oxidation with I_2 happens within minutes whereas coupling via CCl_4 takes over 30 minutes to be completed. Therefore, it seemed rather counterintuitive that in their original publication Fidanza and McLaughlin decided to choose the Atherton-Todd approach as the primary oxidative coupling method. I decided to investigate whether it is possible to accelerate the process and at the same time to evaluate the choice of

the methodology. Three halogenating agents other than CCl_4 were tested as its alternatives - iodine, N-iodosuccinimide (NIS), and N-chlorosuccinimide (NCS).

In order to do so, three semi-automated oligonucleotide syntheses of identical sequence **O2** were run simultaneously at a 1 µmol scale. They were carried out according to general protocol, the only variation being the oxidative coupling step. Iodine, N-iodosuccinimide and N-chlorosuccinimide was chosen as halogenating agents for **O2E**, **O2F,** and **O2G** respectively. 0.1 M solutions of these reagents were prepared in anhydrous pyridine. The support was first washed with just the halogenating solution and then with cystamine in pyridine. The support slowly and continuously flushed with the reaction mixture for 10 min. After that time, syntheses were continued according to standard procedures. Cleavage from the support and deprotection of all three samples was carried out using standard procedures. Crude products were analyzed using RP-HPLC and samples were purified with denaturing urea-PAGE. Samples **O2E**, **O2F,** and **O2G** had similar migrating patterns (Figure 32). The chromatograms of crude products revealed the presence of several additional peaks as compared to other syntheses carried out with CCl_4 as an oxidizing agent.

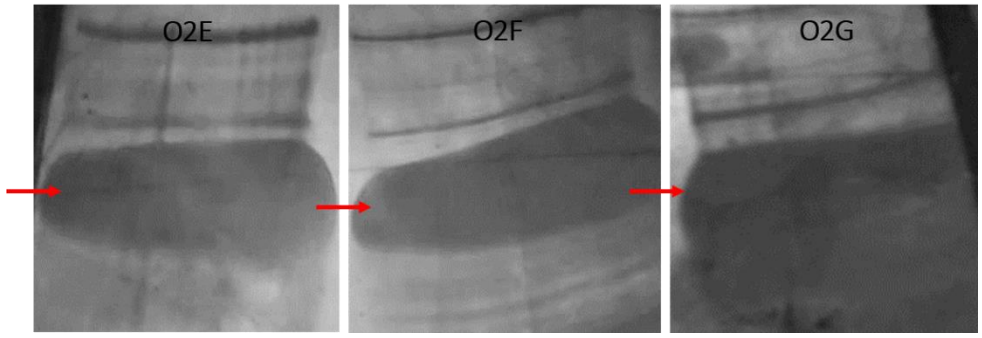

Figure 32. Urea-PAGE purification of samples O2E, O2F, and O2G.

For product identification, purified oligonucleotides were subjected to RP-HPLC and MALDI-TOF-MS analyses. In the case of each sample, the widest bands were identified as a mixture of the two full length oligonucleotides: the main product (P-cystamine RNA) and the unmodified oligonucleotide. Moreover, chromatograms of **O2E** and **O2F** showed that the unmodified sequence was actually the main fraction of the product (Figure 33). In the case of **O2G,** the amount of the modified oligonucleotide was significantly higher than in the two previous samples, yet still, nearly half of the material comprised unmodified RNA (Figure 34).

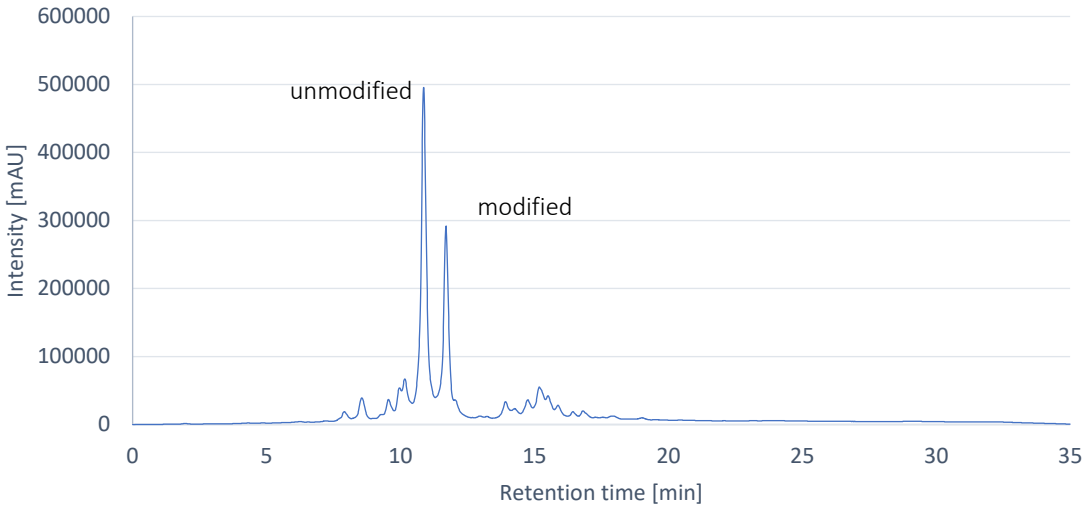

Figure 33. Chromatogram of crude **O2E** oligonucleotide.

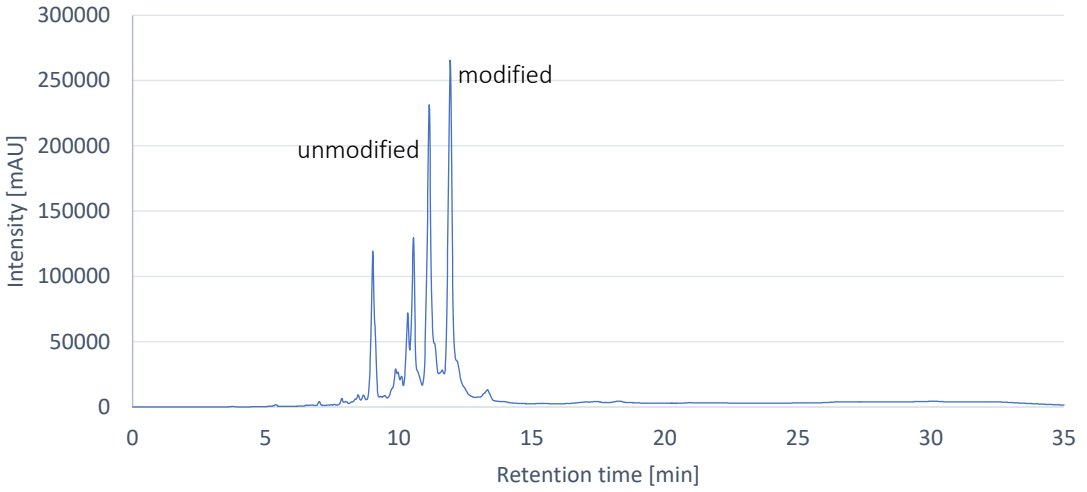

Figure 34. Chromatogram of crude **O2G** oligonucleotide.

An explanation lies presumably in different oxidation mechanisms and reaction rates. In principle, the iodine-mediated oxidation occurs more rapidly than the amination via the Atherton-Todd reaction. Iodine is an excellent leaving group and therefore there is little discrimination between the nucleophiles attacking the phosphorus. It means that the traces of water in the reaction mixture compete with the amine leading to substitution with the hydroxyl group and consecutive formation of the phosphodiester instead of phosphoramidate. After finding out that no other approach than the Atherton-Todd reaction gave satisfactory results in obtaining desired P-cystamine RNA, the latter has been chosen for future syntheses of modified oligonucleotides.

After a series of experiments described in this chapter, I concluded the following for the most optimal conditions of P-cystamine oligoribonucleotides synthesis:

(i) use of 1-adamantanecarbonyl chloride as a condensing agent,

(ii) condensation time should be 10 minutes

(iii) Atherton-Todd should be used for oxidative amination.

3. STEREOCHEMISTRY OF P-CYSTAMINE MODIFICATION

DNA and RNA oligonucleotides in their native form do not exhibit chirality at the internucleotide linkages. However, anytime one of the oxygens is substituted with another atom or moiety at the phosphorus, the phosphodiester derivative becomes chiral (Figure 35).

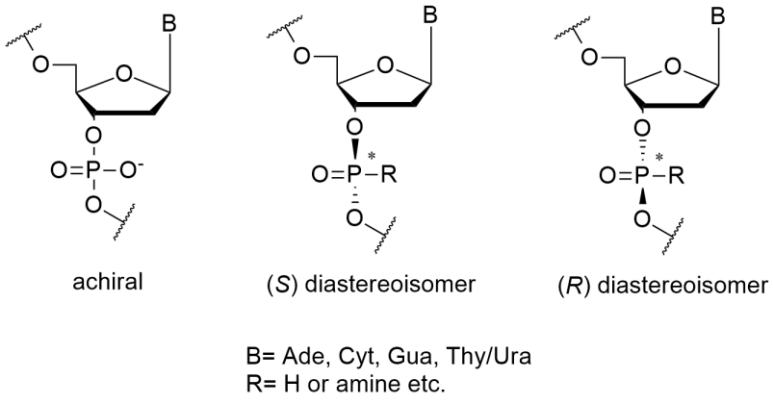

Figure 35. Scheme showing the conformation of substituted phosphodiesters as compared to the native internucleotide bond (left).

This is exactly the case with P-cystamine oligonucleotides, which may confer either *R* or *S* stereochemistry. The arrangement of specific fragments of P-cystamine RNA in a single stranded form is presented in Figure 36. The study of the stereochemistry of the cystamine-modified RNA was an inherent element of this project, since depending on the application, the exact spatial position of the linker can play a crucial role in the functionality of the modified oligonucleotide. It occurred relevant to find out what is the stereospecificity and stereoselectivity of reactions leading to obtaining P-cystamine oligoribonucleotides.

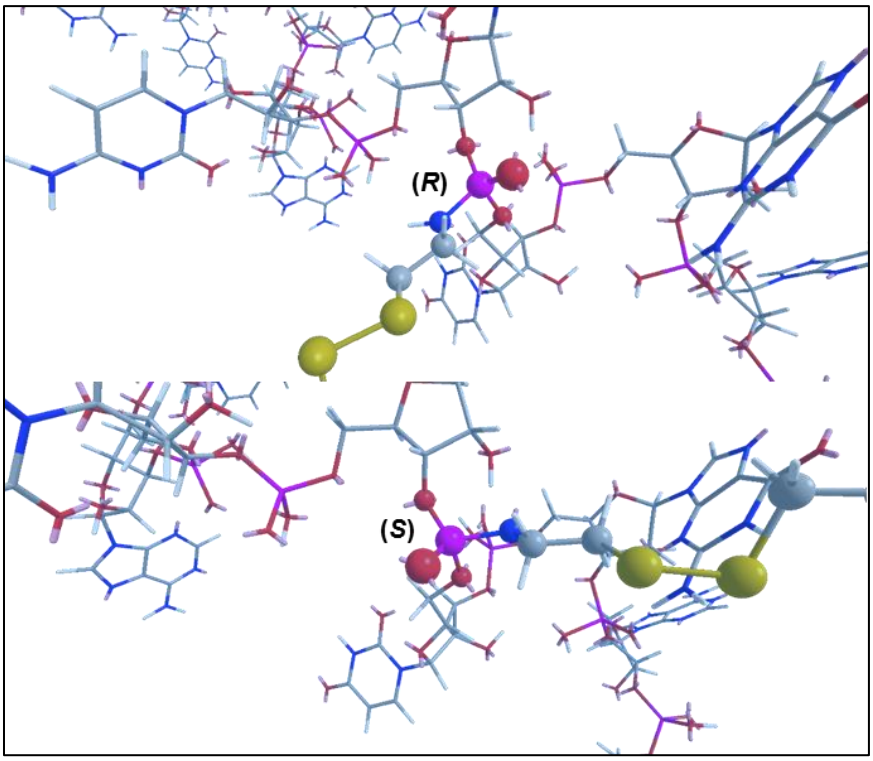

Figure 36. 3D models showing the spatial arrangement of (R)- (top) and (S)-P-cystamine RNA (bottom). The oligonucleotide chain is shown in sticks, the chiral phosphoramidate with the linker is shown in balls. Carbons are shown in grey, oxygens in red, phosphorus in magenta, nitrogen in blue, and sulfur in yellow. Models were built in Chem3D Pro 12.0.

3.1. DINUCLEOTIDE PHOSPHORAMIDATE MODEL

To examine the stereochemistry of the phosphoramidates obtained upon substitution with cystamine, I decided to carry out syntheses of dinucleotide models. First and foremost, the main advantage of such a model is that it is chemically and structurally more simple and can be obtained in large quantities as compared to oligonucleotides. That in consequence allows more convenient and accurate analysis. For the study, I synthesized four dinucleotides using different *H*-phosphonate and nucleosides.

3.1.1. Synthesis of 3’-DMT-2’-deoxythymidine

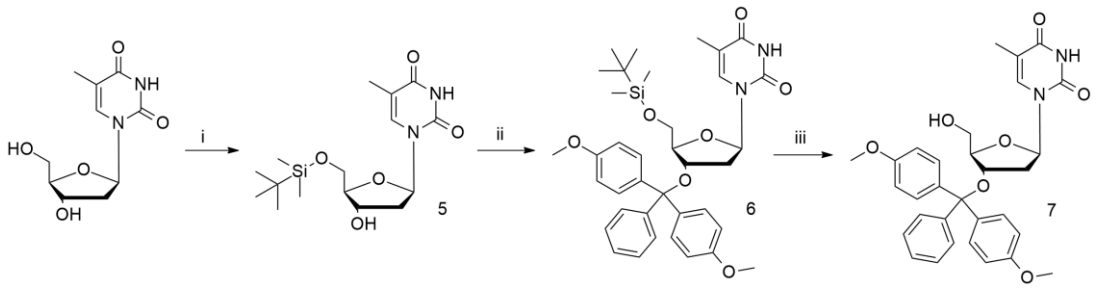

Figure 37. Scheme of the synthesis of 3'-O-(4,4’-dimethoxytrityl)--2'-deoxythymidine 7. i) *tert*-butylmethylsilyl chloride, imidazole, DMF; ii) 4,4’-dimethoxytrityl chloride, Pyr; iii) triethylamine trihydrofluoride, triethylamine, THF

First, I decided to synthesize a 3’-protected deoxynucleoside namely 3’-O-4,4’-dimethoxytrityl-2’-deoxythymidine **7**. It was synthesized in three steps which included appropriate protection and deprotection reactions of hydroxyl groups. Straightforward protection of the 3’-hydroxyl group of the nucleoside, which is a secondary alcohol is not possible due to the presence of unprotected primary alcohol, namely the 5’-hydroxyl group which reacts substantially faster. The starting material was unprotected 2’-deoxythymidine. In the first step, the 5’-hydroxyl group was blocked using *tert*-butylmethylsilyl chloride (TBDMSCl) and imidazole in dimethylformamide. The reaction was complete within 1 hour giving **5** with 80-90% yield. In the next step, the 3’-hydroxyl group was protected with 4,4’-dimethoxytrityl chloride (DMTCl), which is an acid labile protecting group, commonly used in the automated oligonucleotide synthesis. Since 3’-OH is less reactive than primary alcohols the reaction was carried out for 18-20 hours to increase the efficiency. Obtained nucleoside **6** was protected with two orthogonal protecting groups. To allow the nucleoside to participate in dimer synthesis, the 5’-OH protecting group had to be selectively removed. TDBMS group is labile under treatment with fluoride ions, which exhibit a very high affinity towards silicon. The final step, namely the deprotection of the 5’-hydroxyl group was done by trimethylamine trihydrofluoride in the presence of trimethylamine in tetrahydrofuran. The reaction was complete after 6-8 hours and occurred quantitatively yielding 3’-O-4,4’-dimethoxytrityl-2’-deoxythymidine **7**.

3.1.2. Synthesis of 3’-DMT-2’-deoxyadenosine

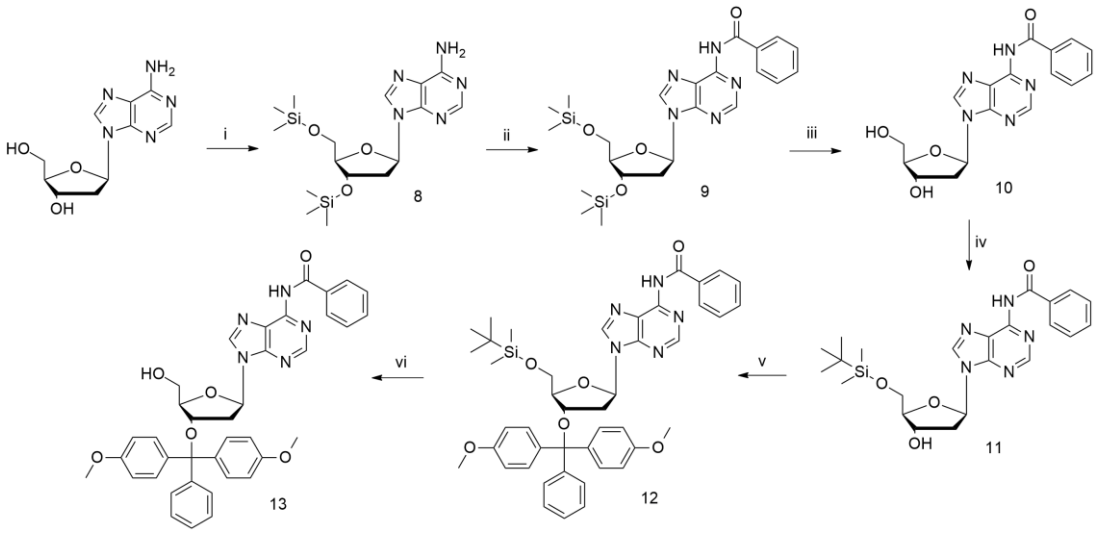

Figure 38. Scheme of the synthesis of 3'-O-(4,4’-dimethoxytrityl) -2'-deoxy-N^6-benzoyl-adenosine 13. i) trimethylsilyl chloride, Pyr; ii) benzoyl chloride, Pyr; iii) ammonium hydroxide, Pyr; iv) tert-butylmethylsilyl chloride, imidazole, DMF; v) 4,4'-dimethoxytrityl chloride, Pyr; vi) triethylamine trihydrofluoride, triethylamine, THF

In order to verify if the heterocyclic base type has any influence on the stereochemistry of P-cystamine dimer, I decided to synthesize also a 3’-DMT-2’-deoxyadenosine **11**, which is a purine base. Synthesis of 3’-DMT-2’-deoxyadenosine is carried out analogously to 3’-DMT-thymidine **7**, however, it requires additional steps at the beginning of the synthetic pathway, which ensure appropriate protection of the adenine exoamine group. For that purpose, I chose a convenient, one-pot synthesis that comprises three steps[208]. In the first one, 3’- and 5’-hydroxyl groups are transiently protected with the highly labile trimethylsilyl group (**8**). The reaction between the nucleoside and trimethylsilyl chloride (TMSCl) in pyridine was completed after 25 minutes. Next, benzoyl chloride was added to the reaction mixture, after ca. 2 hours forming an amide with exoamine of the heterocyclic base (**9**). The TMS groups are highly labile in both basic and acidic conditions, so it is possible to remove them in rather mild conditions. The addition of concentrated aqueous ammonia to the reaction mixture results in the complete removal of the TMS from hydroxyl groups after 30 minutes, while leaving the benzoyl group at the amine intact (**10**). Once the product was purified, the rest of the synthesis of 3’-DMT protected adenosine **13** was carried out analogously as in the case of thymidine described above.

3.1.3. Synthesis of P-cystamine dinucleotides

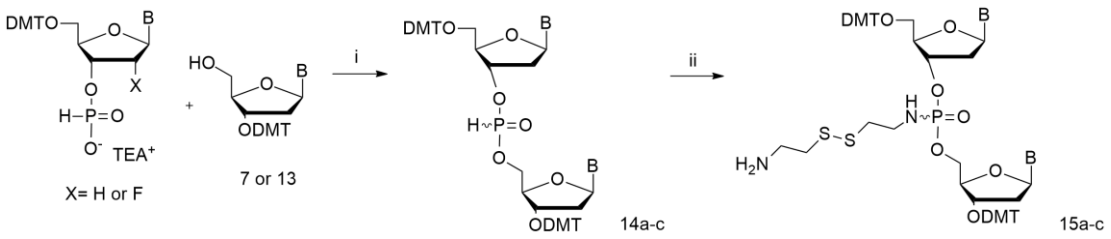

Figure 39. Scheme of the synthesis of P-cystamine dinucleotides 15a-c. i) 1-Adamantanecarbonyl chloride, Pyr-ACN; ii) cystamine, carbon tetrachloride, Pyr.

The synthesis method of P-cystamine-modified dinucleotide was carried out in the same conditions for every dinucleotide combination presented further. First, I obtained dithymidine model **15a** molecule in a two-step synthesis. The condensation reaction, which is the first step, occurred between 3'-DMT-2'-deoxythymidine **7** and 5'-DMT-2'-deoxythymidine *H*-phosphonate triethylamine salt in a pyridine-acetonitrile mixture, in the presence of 1-adamantanecarbonyl chloride (AdCl) as activating agent. It is crucial that all reagents and solvents are anhydrous since the activator decomposes in the presence of water. The reaction was completed within 15 minutes yielding two diastereoisomers of *H*-phosphonate diester **14a**, according to the analysis of the reaction mixture with ^{31}P NMR spectroscopy (Figure 40). Diastereomers *Rp* and *Sp* were separated via silica gel chromatography and their configuration was assigned based on their mobility ("fast" and "slow") according to the literature[209,210].

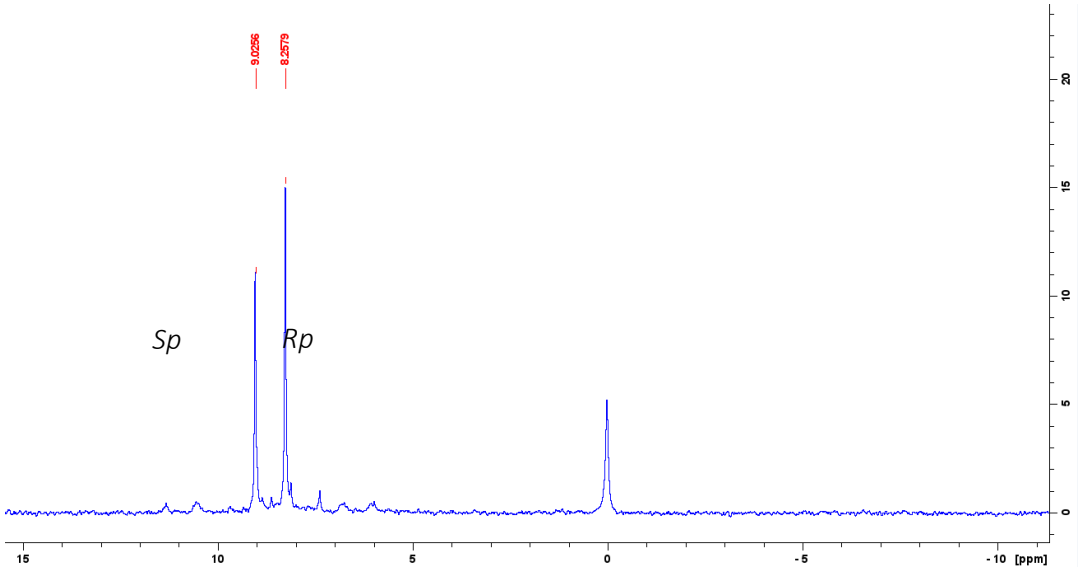

Figure 40. ^{31}P NMR spectrum of dithymidine *H*-phosphonate diester showing the presence of two diastereoisomers.

In the next step, the diester undergoes oxidative coupling via the Atherton-Todd reaction. For that purpose, the mixture of *H*-phosphonate diester stereoisomers **14a-c** was treated with cystamine **1** in pyridine with the addition of carbon tetrachloride and again all of the components have to be anhydrous to avoid oxidation to dinucleotide phosphodiester. Moreover, to increase the efficiency of the amination and reduce side products formation, 15 equivalents of cystamine were used[209]. The reaction progress was monitored with ^{31}P NMR spectroscopy and it was complete after 1 hour yielding a mixture of two dinucleotide phosphoramidate diastereoisomers **15a-c** (Figure 41).

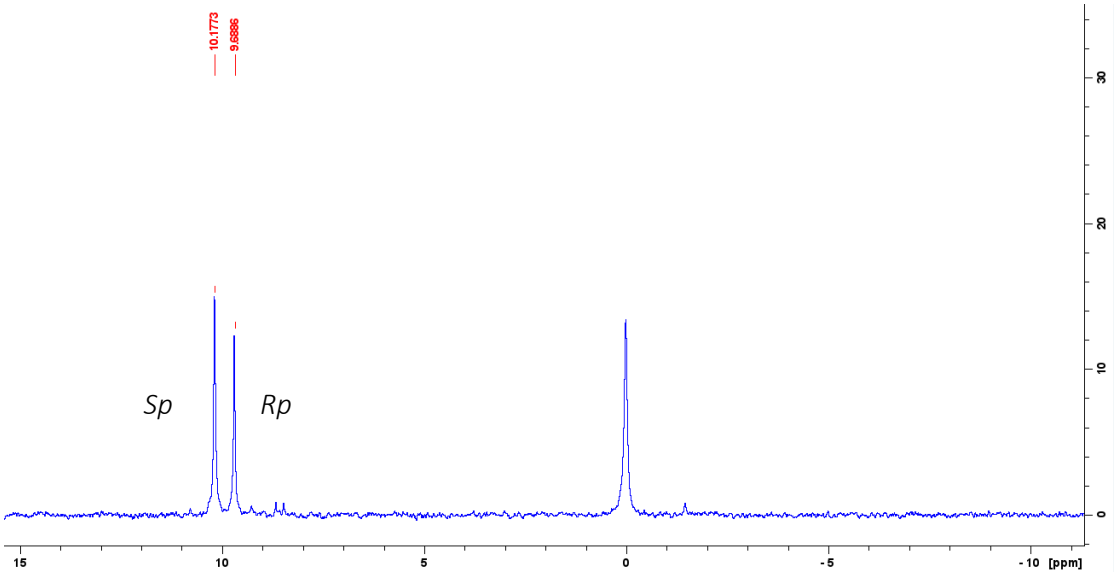

Figure 41. ^{31}P NMR of dithymidine cystamine phosphoramidate showing inversion of stereochemistry after oxidative coupling of amine.

I have decided to investigate the stereochemistry of both reactions: *H*-phosphonate condensation and oxidative coupling of cystamine linker. ^{31}P NMR spectra of dinucleotides- TT, TA, and 2'FCT recorded after the condensation demonstrated that reaction can be considered stereoselective since the *Rp* diastereoisomer was produced in excess in each case. However, a difference in ratio between *Sp* and *Rp* *H*-phosphonate diester formed was observed, depending on the composition of dinucleotide. TT and TA diastereoisomers were produced in 3:4 (*Sp:Rp*) whereas 2'FCT yielded a higher amount of the *Rp* product (3:5). Obtained results suggest that the nucleobase preceding modification site does not have an impact on condensation product configuration. On the other hand, substitution on C2' and in consequence conformation of ribose affects the stereochemistry of the reaction to some extent, making it more stereoselective towards the *Rp* product. Since 2'-deoxy-2'-fluorocytidine geometrically resembles cytidine it is in agreement with previous findings from Almer and Stawiński, who

showed that the synthesis of diribonucleotide H-phosphonates was stereoselective, yielding 4-times more of the *Sp* stereoisomer than *Rp*[211].

Table 3. ^{31}P NMR shifts of dinucleotide models

Dinucleotide *H*-phosphonate	*Sp* ^{31}P NMR shift [ppm]	*Rp* ^{31}P NMR shift [ppm]	*Sp:Rp* ratio
14a TT	9.38	8.17	3:4
14b TA	9.03	8.26	3:4
14c 2'FCT	9.74	8.51	3:5
P-cystamine dinucleotide	*Sp* ^{31}P NMR shift [ppm]	*Rp* ^{31}P NMR shift [ppm]	*Sp:Rp* ratio
15a TT	10.18	9.69	4:3
15b T*A	9.61	9.52	4:3
15c 2'FC*T	10.17	10.06	5:3

Analysis of products of oxidative coupling showed that regardless of the dinucleotide phosphoramidate variant the reaction occurred with inversion of configuration and therefore is stereospecific. An additional control experiment verifying the stereochemistry of the oxidative coupling reaction was conducted. It was found previously that the stereochemistry of oxidation with iodine depends heavily on the solvent used in the reaction. It has been previously demonstrated that when pyridine is present during the oxidation of *H*-phosphonothioate diesters, the reaction occurs in a stereoselective manner[50]. Stawiński et al. proved that even when stereochemically pure *H*-phosphonate (or *H*-phosphonothioate) diesters were subjected to oxidative coupling with alcohols in acetonitrile the reaction occurred stereospecifically with complete inversion of configuration. However, when the solvent was replaced with pyridine, epimerization occurred and two diastereoisomers were produced for each of the diesters. That is because pyridine acts as a strong nucleophilic catalyst and as such forms a mixture of pyridinium intermediate diastereoisomers[212]. For the purpose of my research, two syntheses of dithymidine *H*-phosphonate oxidation with cystamine via Atherton-Todd reaction were conducted in either pyridine or acetonitrile. Reaction mixtures were then examined with ^{31}P NMR spectroscopy. The results showed that irrespective of the presence or absence of pyridine, the ratio between *Sp* and *Rp* diastereoisomers formed was the same meaning that in both conditions oxidative coupling was stereospecific and occurred with

complete inversion of the configuration. The choice of solvent in this step does not play any crucial role in controlling reaction stereochemistry.

3.1.4. Influence of the nearest neighborhood on the configuration of P-cystamine oligonucleotides

Studies of the dinucleotide model gave solid confirmation of the stereoselectivity of *H*-phosphonate condensation reaction and stereochemistry of the P-cystamine modification. However, the key research focus of this project is oligonucleotide functionalization, which is in principle much more complex molecules than the aforementioned models. It means that many interactions can possibly occur within a single strand during the synthesis which can affect the stereochemistry of the final P-cystamine product.

I decided to systematically approach the issue and create several P-cystamine oligonucleotide variants, each containing a single variation in the sequence. It appeared the most relevant to assess the influence of steric factors in the closest vicinity of the modification site. Therefore, two following elements have been screened: (i) the nucleobase preceding the modified nucleotide and (ii) the *H*-phosphonate analog type used. In the case of the preceding nucleotide, the aim was to compare between pyrimidine (adenine and guanine) and purine base (cytosine, thymine, and uracil). Purines are bulkier than pyrimidines which can impose steric hindrance during condensation of activated *H*-phosphonate[200,213]. Another factor that was examined was the effect of the *H*-phosphonate analog used for the condensation, namely 2'-deoxyribonucleotide and 2'-deoxy-2'-fluororibonucleotide. These two analogs possess different ribose conformation (C2'-endo vs. C3'-endo), which could also affect the stereoselectivity of the reaction. The sequences chosen for the study are presented in Table 4. To achieve consistency of the results three sequences were chosen in which the only variable was the nearest neighborhood of the modification site. All variants were synthesized and purified using standard procedures (Chapter 2.7.3. of *Materials and methods*).

Table 4. Oligonucleotide sequence variants were synthesized for the study of stereochemistry. Varying fragments are underlined.

Factor	Sequence (5'→3')		Analog
preceding base	AGUGCGACAC2'FC*UGAUUCC	O3A	pyrimidine
	AGUGCGACAC2'FC*AGAUUCC	O3B	purine
deoxy vs. 2'F	AGUGCGACAC2'FC*UGAUUCC	O3A	2'-deoxy-2'-fluoro
	AGUGCGACACdC*UGAUUCC	O3C	2'-deoxy

The NMR spectroscopy of oligonucleotides may be more challenging than those of small molecules due to the fact that the amounts of synthetic DNA or RNA obtained in laboratory settings do not exceed 1-2 mg. Therefore, high purity of the sample and solvents are required and the spectrum needs to be recorded for at least 16 to 20 hours (typically overnight). In the case of O3, each oligonucleotide was purified with gel electrophoresis, which ensured high purity but at the same time decreased the final yield. Between 25 to 35 OD_{260} of each sample was dissolved in 500 µL of autoclaved MiliQ water and 100 µL of deuterium hydroxide was added. All of the three ^{31}P NMR spectra were recorded overnight.

Table 5. ^{31}P NMR shifts of P-cystamine modified oligonucleotides diastereoisomers.

Sample number	*Sp* shift [ppm]	*Rp* shift [ppm]	*Sp:Rp* ratio
O3A	10.29	10.16	3:2
O3B	10.09	9.93	3:1
O3C	10.08	9.92	2:1

Due to the absence of data on the stereochemistry of such modified oligonucleotides in reported literature, I assumed that the results can be analyzed based on dinucleotide models data that I obtained previously. ^{31}P NMR spectra recorded for oligonucleotide samples showed an analogous pattern as in dinucleotide models analyzed earlier- in each case *Sp* diastereoisomer was the predominant product of the synthesis, which further confirms that *H*-phosphonate condensation is stereoselective. However, quite noticeable differences between *Sp:Rp* formation ratio were observed between all three species. The lowest amount of Rp diastereoisomer was observed in O3B, where cystamine was accommodated between 2'-deoxy-2'-fluorocytidine and adenosine. Among others, this variant is the most sterically hindered which can be the determining factor in the stereochemistry of this reaction. Analysis of sample O3A showed that when pyrimidine nucleotide is followed by 2'-deoxy-2'-

fluorocytidine the stereoselectivity of the reaction is less strikingly evident, which again is in agreement with dinucleotide model results.

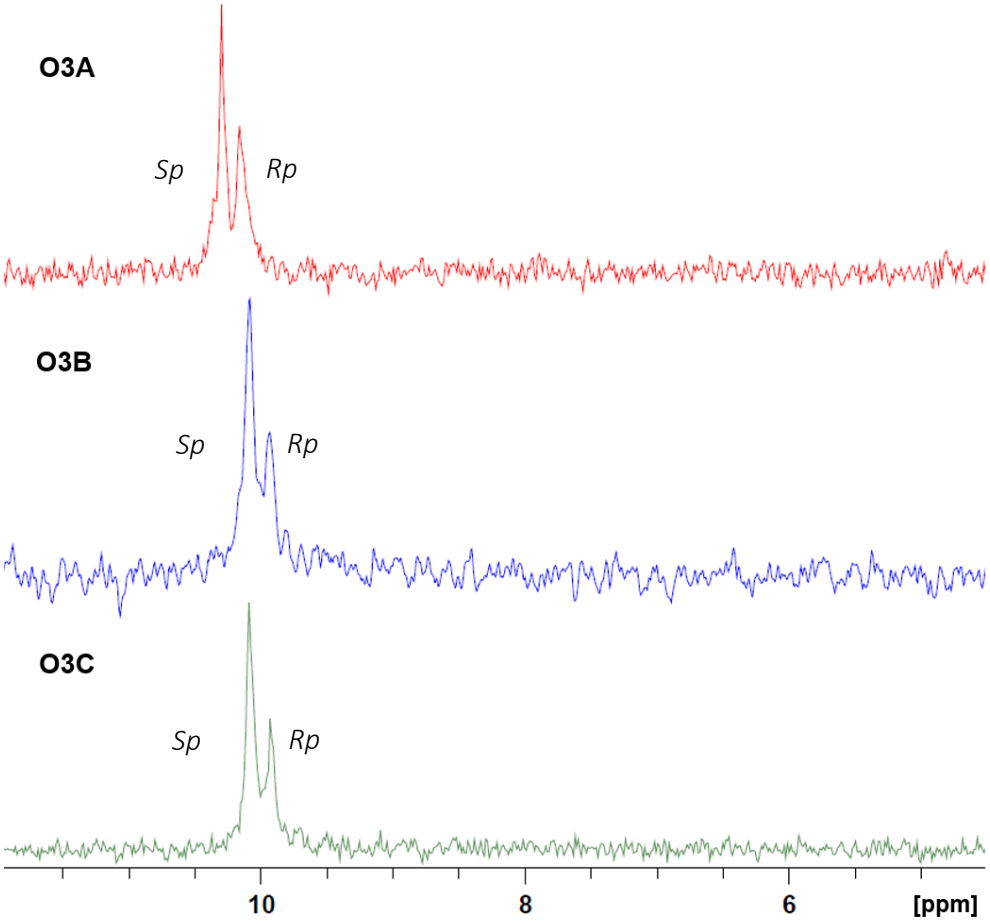

Figure 42. Stacked 31P NMR spectra of oligonucleotides O3A-C.

4. RIBOOLIGONUCLEOTIDE CROSS-LINKING VIA A DISULFIDE BRIDGE

4.1. OPTIMIZATION OF THE CROSS-LINKING REACTION

One of the tentative applications of RNA modification with a disulfide tether was the possibility to obtain oligonucleotides capable of forming secondary structures stabilized by the covalent linkage between two strands.

From the literature, one cannot easily extract a single, universal method of disulfide nucleic acid conjugation. Quite the contrary, among studies in which the authors used disulfide bridge formation in the context of oligonucleotides a multitude of approaches was reported with little consistency among them. The strategies employed several buffers at different pH, such as Tris-

HCl[173,182], Tris-EDTA (TE)[121,155], or sodium phosphate buffer[100,130], a range of oligonucleotide concentrations, reaction times, and temperatures. Furthermore, some scientists reported the use of aromatic disulfides as activating agents which in principle are meant to increase the efficiency of disulfide bridge formation[110,214,215]. Before writing my dissertation, I have prepared and published a review article, which gathers the knowledge on this topic to date[84].

Considering previously reported results, I decided to carry out a systematic optimization of the P-cystamine RNA cross-linking reaction. After literature research and careful consideration of reported results, I assumed that the cross-linking should be carried out (i) in aerobic conditions and (ii) at room temperature. To eliminate the factor of duplex formation tendency of an oligonucleotide, which is an inherent characteristic depending on the sequence complementarity, the study was carried out using non-complementary sequence 5'-AGUGCGACACdC*UGAUUCC-3' (O4).

Prior to the disulfide bridge formation, the cystamine linker should be reduced into cysteamine to expose the thiol moiety. I chose to use dithiothreitol (DTT), which is one of the most popular reducing agents in nucleic acid and protein research. It is more efficient and less toxic than 2-mercaptoethanol, however, it also exhibits a shorter half-life[216], therefore it needs to be prepared fresh before carrying out the reduction. Moreover, DTT thiols exhibit pKa of 9.2 and 10.1[217], therefore for the reduction to be efficient the pH of the reaction needs to be maintained alkaline. I found that after incubation of P-cystamine oligonucleotide with a significant excess of DTT (100 mM in Tris-Borane-EDTA buffer pH 8.3), the linker was completely reduced. Although the reducing agent is not stable, every time before the cross-linking reaction, the oligonucleotide-DTT solution was extracted with ethyl acetate and then desalted with Sephadex NAP columns.

The following buffers were used in the optimization of the cross-linking reaction:

i. Phosphate buffer pH 6.0
ii. PBS pH 7.2
iii. Phosphate buffer pH 8.0
iv. TBE pH 8.3

The concentration of each buffer was 100 mM. Autoclaved MiliQ water was used as a control (O4X-5). Additionally, I conducted an experiment in which some of the P-cystamine oligonucleotides were activated with 5,5'-dithiobis-(2-nitrobenzoic acid) (DTNB) prior to the

cross-linking reaction (O4X-6). Aliquots of each sample were taken after 12, 24, 48, and 72 hours of incubation and then analyzed using denaturing PAGE.

The cross-linking was observed in all experiments, however with different yields (Figure 43). It was found to be the most efficient in phosphate buffer pH 8.0 (O4X-3, lane 3) and in these conditions, it was nearly complete after 48 hours. The second most efficient cross-linking was observed for samples incubated in PBS pH 7.2 (O4X-2, lane 2) and in the case of oligonucleotide preactivated with DTNB (O4X-6, lane 6) yet it was still not quite as good as for O4X-3. The reactions conducted in phosphate buffer pH 6.0 (O4X-1, lane 1), TBE buffer pH 8.3 (O4X-4, lane 4) and MiliQ water (O4X-5, lane 5) did not reach satisfying cross-linking rates even after 48 hours of incubation.

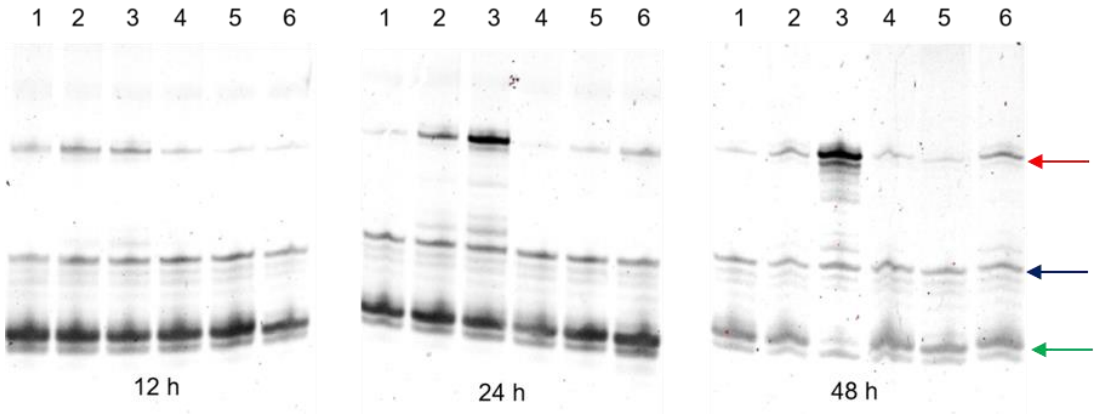

Figure 43. Denaturing gel electrophoresis of O4 cross-linking progress after 12, 24, and 48 hours. The green arrow indicates the substrate, the navy blue arrow indicates unidentified impurity, the red arrow indicates the cross-linked species. Lane 1. Phosphate buffer pH 6.0; lane 2. PBS pH 7.2; lane 3. phosphate buffer pH 8.0; lane 4. TBE pH 8.0; lane 5. MiliQ water; lane 6. DTnB activated/TBE pH 8.3

After finding the most optimal conditions for efficient cross-linking of P-cystamine oligonucleotides, I decided to carry out an experiment to examine whether an addition of an oxidizing agent could accelerate the reaction and therefore decrease the overall cross-linking time. For that purpose, reduced and desalted O4 was incubated for 24 hours with a 2-fold molar excess of iodine in methanol (O4X-7). Aliquots were taken after 12 and 24 hours and then analyzed using denaturing gel electrophoresis. It was found that not only did not the addition of iodine increase the cross-linking rate but it also seemed to inhibit the reaction. After 24 hours only a small fraction of cross-linked oligonucleotide could be observed.

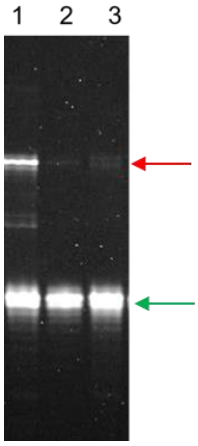

Figure 44. Denaturing gel electrophoresis of samples 4X-3 and 4X-7. The green arrow indicates the substrate, the red arrow indicates the cross-linked species. Lane 1. 4X-3; lane 2. 4X-7 after 12 hours incubation; lane 3. 4X-7 after 24 hours incubation.

4.2. STRUCTURAL STUDIES OF CROSS-LINKED RNA DUPLEX

Once the cross-linking strategy via P-cystamine has been tested and established, in the next step I focus on examining the influence of such modification on the helix geometry. Several studies have been conducted and published in order to assess the structural consequences of the introduction of interstrand covalent cross-linking in dsDNA. It was found that with the proper design when disulfide linkers are placed on nucleobases, the influence on the overall geometry of the strand is negligible. Simulations, NMR, and CD data showed virtually undistorted structure and dynamics of native B-DNA helix[109,123,218]. On the other hand, there are cases, where researchers exploited the disulfide cross-linking of oligonucleotides for the exact opposite purpose, namely controlled destabilization of the helix. For example, Wolfe and Verdine examined how the use of different linkers to form the linker between opposite nucleobases affects base-pairing in dsDNA[125]. They found that by using cystamine instead of homocystamine induced torsional stress, which led to disrupted base-pairing in the vicinity of the modification. Yet another study used the disulfide cross-linking strategy to enforce bending of Dickerson-Drew dodecamer dsDNA[110]. The linkers, displaced by 2 nucleotides between the two strands, formed a linkage on the outside of the helix, which caused bending of the entire molecule. Interestingly, it was achieved without affecting the overall B-DNA geometry.

Considering the facts that sequences used in my studies are mostly RNA analogs, they also have a tether attached at phosphorus, but also comprise ribonucleotide analogs (2'-deoxyribonucleotides or 2'-fluoro-2'-deoxyribonucleotides), it was necessary to investigate the consequences of introducing such modifications. One of the possible issues of direct cross-linking of RNA via built-in cystamine linkers is their length. In principle, the RNA duplex adapts an A conformation in which phosphorus centers are placed on the outside of the helix, 9.5 Å

from the axis[219]. The linkages created upon disulfide bridge formation for cystamine and homocystamine have a length of 9.33 Å and 10.86 Å respectively[a]. Considering these facts, I presumed that if the cross-linking via P-cystamines takes place, it is going to affect the local geometry of the RNA duplex.

To examine any conformational changes, I chose crystallography as one of the most reliable and popular methods of determining the structure of a molecule. However, nucleic acids are highly challenging species for structural studies, especially when it comes to RNA. Up to date, less than 1500 RNA-only structures were released on RCSB PDB, which is below 1% of all structures available in the database[b].

The sequence of oligonucleotide subjected to experiments was designed in such a way to ensure high self-affinity in order to increase the likelihood of crystal formation. This dsRNA consists of two self-complementary, GC-only 11-nucleotide strands. First, sequences 5'-GCG**2'FC***GCGCGCG-3' (**O5A**, *-cystamine) and 5'-GCG**2'FC****GCGCGCG-3' (**O5B**, **-homocystamine) were synthesized. They were fully self-complementary with a relative linker position shift of 2 nucleotides between the two duplex-forming strands, which was previously found to be the most optimal strategy[104].

Such GC-rich sequences are not easy to synthesize and handle. Rather than that, they are very "sticky" and tend to form secondary structures. Their duplexes exhibit significantly higher melting temperatures compared to oligonucleotides of the same length comprising all four nucleobases. I found that even upon denaturation with 7M urea for gel electrophoresis analysis there were bands present at the height corresponding to dsRNA indicating that denaturation was not complete (Figure 45, lanes 2 and 4). Cross-linking of **O5A** and **O5B** was conducted according to standard procedures to yield **O5AX** and **O5BX** respectively. First, samples were treated with DTT, then the reducing agent was removed by extraction and desalting, and samples were lyophilized. Next, each oligonucleotide was reconstituted in reaction buffer to a final concentration of 100 mM, heated to 95°C, and then let to cool down to room temperature at which it was incubated for another 48 h. After that time, aliquots of **O5AX** and **O5BX** were taken and analyzed via denaturing gel electrophoresis.

[a] Calculated with Chem3D Pro 12.0
[b] https://www.rcsb.org/stats [access: 08/09/2020]

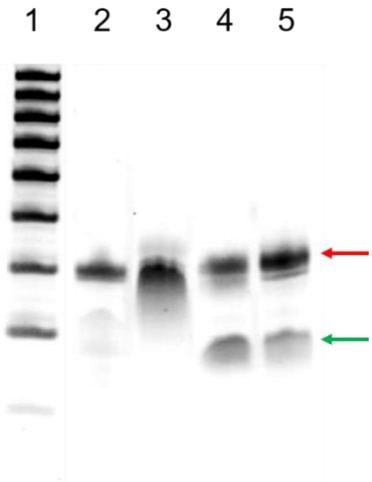

Figure 45. Denaturing gel electrophoresis of RNA duplex 5. The red arrow indicates double stranded RNA (cross-linked species), Green arrow indicates single stranded modified RNA. Lane 1. marker; lane 2. O5A; Lane 3. O5AX; Lane 4. O5B; lane 5. O5BX.

Cross-linked species were subjected to structural studies. Upon the first attempt, the **O5AX** dsRNA formed a crystal, however, there was no deviation from native structure or any indication that the cross-linking is present. Moreover, there was no visible evidence of the presence of the fluorine atom at the 2'-position of C^4. The **O5BX** did not form any crystals.

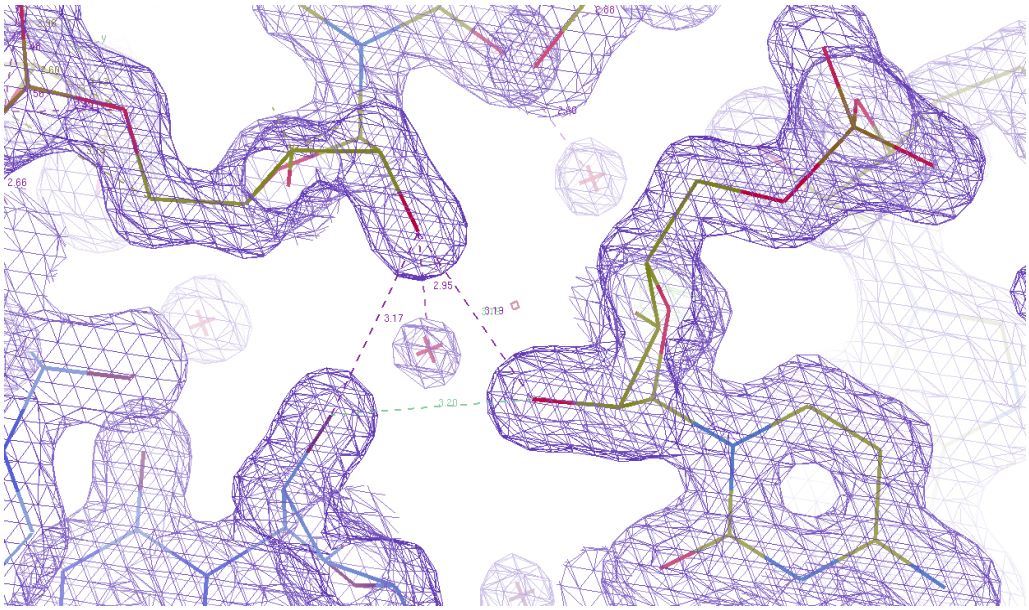

Figure 46. Fragment of a structural model obtained in crystallization studies

5. CROSS-LINKING OF P-CYSTAMINE RNA VIA HOMOBIFUNCTIONAL LINKERS

Studies of direct disulfide bridge cross-linking between two P-cystamine RNA strands, which I initially conducted showed that even though it does take place, it is not as efficient as initially assumed. It is presumably a consequence of two factors: (i) the geometry of the linker-bearing phosphate and therefore the spatial arrangement of the linker and (ii) the length of cystamine

and homocystamine, which is not sufficient to cover the distance between phosphoramidates of the two opposing RNA strands. One of the hypotheses in my research project assumed that the interstrand cross-linking could be more efficient with the aid of an additional linking agent.

For the experiments, two linkers were chosen, namely bismaleimidohexane (BMH) and dithiobismaleimidoethane (DTME). Both of them comprise of two maleimide functional groups tethered by flexible alkyl (BMH) or alkyl-disulfide (DTME) chain (Figure 47). Depending on the pH of the reaction mixture, maleimides may react with thiols or amines, yet the reaction with thiols has a significantly higher rate[220]. BMH and DTME have a similar length, but the latter thanks to the presence of a disulfide bridge in its structure offers reversibility of the cross-linking. A general comparison of the two linkers can be found in

Table 6. An initial experiment to verify the feasibility of this strategy, I decided to carry out cross-linking of an oligonucleotide which is not self-complementary and therefore is not prone to the formation of secondary structures. For that purpose, the pilot sequence 5'-AGUGCGACAC2'FC*UGAUUCC-3' (O6) was chosen.

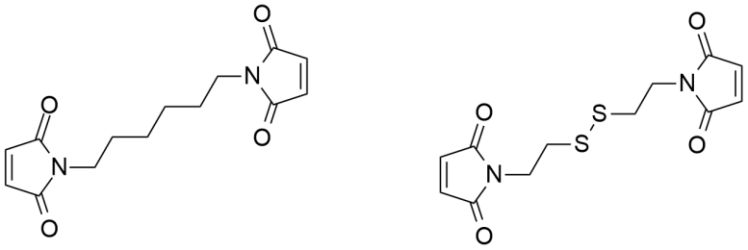

Figure 47. Structure of bismaleimidohexane (BMH) and dithiobismaleimidoethane (DTME)

Before cross-linking, the cystamine-modified oligonucleotide was reduced with DTT to expose the thiol moiety and desalted. Maintaining the right pH is crucial for reaction to occur selectively between maleimide and thiol, therefore the oligonucleotide was reconstituted in phosphate buffer saline (PBS) pH 7.2, denatured by heating to 95°C for 5 minutes and after cooling down to room temperature it was mixed with a 2-fold excess of cross-linker dissolved in DMF and incubated for 3 hours, and eventually desalted. 2 OD_{260} of both BMH and DTME cross-linked species were taken, incubated with DTT for 3 hours and finally desalted. After every stage, aliquots of each sample were taken for comparison on denaturing gel electrophoresis.

Table 6. Comparison between Bismaleimidohexane and Dithiobismaleimidoethane

Linker	Functional group	Reactivity	Length	Cleavable
BMH	Maleimide	Thiols (pH 6.5-7.5) Amines (pH>8.0)	13.0 Å	No
DTME	Maleimide	Thiols (pH 6.5-7.5) Amines (pH>8.0)	13.3 Å	Yes (Reducing agents)

Urea-PAGE analysis shows that the cross-linking using both BMH and DTME occurred with very high yields (Figure 48). In lanes 3 and 4, a band referring to **6** (lane 1) or its reduced version (lane 2) disappeared nearly entirely, and instead, a band corresponding to double the oligonucleotide length became visible (**O6X-BMH** and **O6X-DTME**). Moreover, after incubation of cross-linked species with DTT, the oligonucleotides migrated according to initial presumption: the **O6X-BMH** + DTT (lane 5) still appeared at the height of cross-linked oligonucleotide and **O6X-DTME** + DTT migrated at the level of non-cross-linked species proving the reversibility of the disulfide bridge formation.

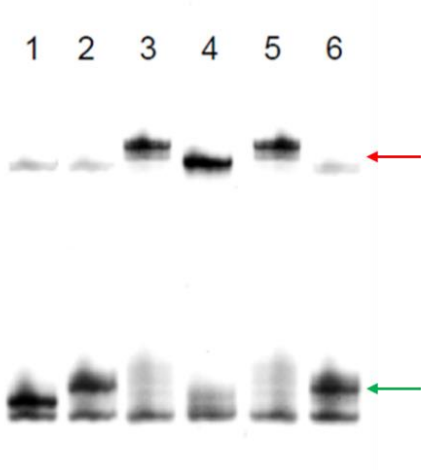

Figure 48. Gel migration of 6 cross-linked oligonucleotides. The green arrow indicates the substrate, the red arrow indicates the cross-linked species. Lane 1. O6; lane 2. O6 + DTT; lane 3. O6X-BMH; lane 4. O6X-DTME; lane 5. O6X-BMH + DTT; lane 6. O6X DTME + DTT.

In the next step, I decided to carry out an analogous cross-linking experiment of two partially complementary P-cystamine RNA strands. For this purpose, two oligonucleotides 5'-**2'FA***AACACCGGUGGAGG-3' (**O7A**) and 5'-AAACACCGGUGG**2'FA***GG-3' (**O7B**) were synthesized and purified according to standard procedures. The sequence was designed in such a way to comprise an internal self-complementary 8-nucleotide region with 3- and 4-nucleotide non-complementary flanking regions, where P-cystamine modifications were located.

10 OD_{260} samples of purified **O7A** and **O7B** were subjected to reduction with DTT according to standard procedures. After removal of the reducing agent, each oligonucleotide was divided and aliquoted into three separate tubes and lyophilized. Next, a set of three samples containing an equimolar mixture of **O7A** and **O7B** were prepared by diluting them with a buffer to the final concentration of 0.1 mM. Finally, three cross-linking reactions were conducted according to standard procedures: (i) **O7X-SS** (ii) **O7X-BMH** and (iii) **O7X-DTME**, for which the detailed conditions are given in Table 7. Once the cross-linking reactions were finished a sample of each entry was taken and treated with DTT for 2 hours. Analogously as for **O6**, aliquots at different stages were taken for analysis using denaturing gel electrophoresis.

Table 7. Conditions of each RNA duplex 7 cross-linking reaction entry.

Entry	Buffer	Linker	Reaction time
O7X-SS	phosphate buffer pH 8.0	cystamine	48 hours
O7X-BMH	PBS pH 7.2	BMH	2 hours
O7X-DTME	PBS pH 7.2	DTME	2 hours

Cross-linking occurred in each entry, however out of all three, direct cross-linking via disulfide bridge formation (**O7X-SS**, lane 3) was the least efficient (Figure 49). Moreover, from the gel, it can be deduced that more than one cross-linked product was formed since the sample migrates as two bands at the height corresponding to double the length of oligonucleotide **O7**. In both entries that were cross-linked via homobifunctional linkers, the reaction occurred with a very high yield (lanes 4 and 5). No additional bands with slower migration were present in neither **O7X-BMH** nor **O7X-DTME**. Control reduction reactions were also in agreement with the expected outcome: the **O7X-SS** (lane 7) and **O7X-DTME** (lane 8) were reduced upon treatment with DTT whereas **O7X-BMH** (lane 6) remained intact.

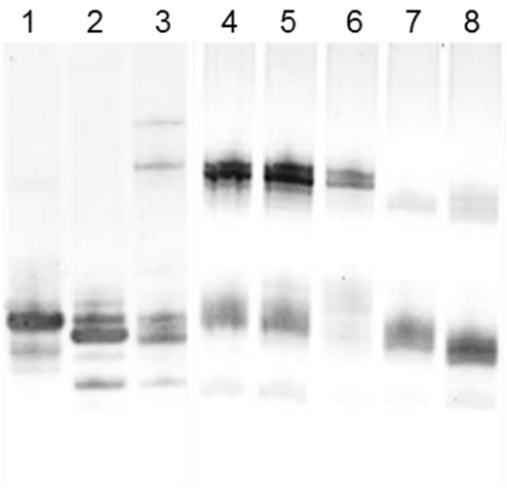

Figure 49. Gel electrophoresis of partially complementary RNA duplex O7. Lane 1. O7A; Lane 2. O7B; lane 3. O7X-SS; lane 4. 7X-BMH; lane 5. O7X-DTME; lane 6. O7X-BMH + DTT; lane 7. O7X-DTME + DTT; lane 8. O7X-SS + DTT. In the case of sample O7B, a band coming from a degraded sequence is visible at the bottom, which unfortunately could not be fully removed during purification.

The poor yield of cystamine cross-linking of **O7X-SS** can be explained by the fact that the linker was placed in a position, which highly disfavored the formation of a linkage. The disulfide bridge in order to be formed would have to overcome strong repulsive forces in the non-complementary region of the sequence. In this case, unlike in a situation when the entire sequence is non-complementary and hence retains its full flexibility, the internal part of the oligonucleotide **O7** formed a duplex, and therefore molecule was locally constrained in a specific geometry (Figure 50). After annealing, this constraint is likely to prevent the thiol moieties to come together close enough to form the disulfide bond. Presumably, the species which migrated higher on the gel were a mixture of dimer combinations (O7A-A, O7A-B, and O7B-B) formed before the annealing was finished.

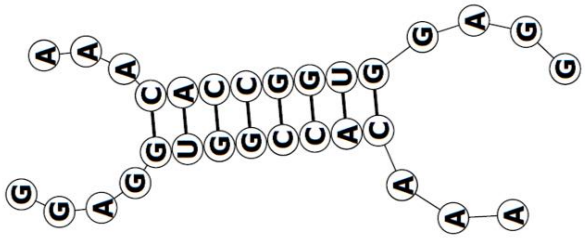

Figure 50. Scheme showing RNA duplex formed by annealing sequence O7. The model was obtained using RNAstructure 6.2 Bimolecular structure prediction.

6. CROSS-LINKING OF RNA HAIRPIN

RNA hairpins are undoubtedly the most characteristic features of RNA. This secondary structure plays a vital role in the process of RNA folding, in gene expression, preventing mRNA from degradation, or often acts as a substrate for enzymes or recognition site for proteins[219,221]. In principle, an RNA hairpin is built of a stem and an apical loop (hence, is interchangeably

called stem-loop). The loop is formed by several unpaired nucleotides, tetraloops (i.e. loops comprising 4 nucleotides) being particularly common[222], and the stem is a double-stranded RNA (dsRNA), which is not necessarily fully complementary and often contains bulges or mismatches. Owing to their versatility, synthetic RNA hairpins are commonly used tools for molecular biology serving as aptamers[223] or biosensors[224]. Moreover, RNA hairpins are challenging motifs for structural studies due to their reduced thermodynamic stability and tendency to refold forming duplexes at high concentrations, required for e.g. NMR or crystallography.

Obtaining an RNA hairpin, which exhibits more thermodynamic stability than native structures would be highly advantageous. Scientists have been working on that for decades now and most of the strategies are based on intramolecular cross-linking[100,139,225].

I decided to use disulfide cross-linking between the two strands of the stem. Using the The P-cystamine approach allows the cross-linking to take place at any chosen site of the RNA oligonucleotide, i.e. internally, which is advantageous to strategies that employ cross-linking between 3' and 5' end. The presence of the cross-link between termini has previously shown that the final structure formed is often circular species instead of a hairpin. Presumably, this is the consequence of the fact that such oligonucleotide is not completely conformationally restricted and dsRNA to some extent retains flexibility. I assumed that covalently bonding the two strands of the stem nearer to the loop can stabilize the hairpin more efficiently.

First, to assess whether the hairpin intramolecular cross-linking will occur using P-cystamine RNA, the sequence with two modification sites was designed in a way to maximize the stability of the stem-loop structure: 5'-GC**dC***GACCAGUCCUUCGGGACUG**dG***UCGGC-3' (**O8**). The loop consisted of UUCG, which is the most stable and among the most abundant tetraloops in 16S ribosomal RNA[226] with C-G closing pair, and the stem comprised two 11 nucleotide strands with 72.7% GC content for elevated thermal stability. P-cystamine modifications were positioned at C^3 and G^{23} and were inserted as deoxynucleotides. For this initial study, the sequence was designed in such a way as to promote the hairpin formation and concomitant cross-linking. Indicative melting temperatures were calculated using OligoAnalyzer provided by Integrated DNA Technologies, which is based on UNAFold software (previously known as mFold)[12]. For the following conditions: 100 mM oligonucleotide **O8** and 100 mM Na^+, the calculated melting temperature was 106.5°C for the hairpin. Indeed, in an attempt to measure actual melting temperatures using the spectrophotometric method showed that using 100 mM Na^+ melting

buffer no transition could be observed between 20 and 90°C. Results demonstrated superior stability of the hairpin structure even prior to the cross-linking reactions.

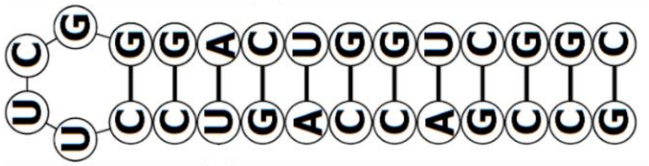

Figure 51. Scheme of RNA stem-loop structure formed by O8. The structure was obtained with RNAstructure 6.2 using RNA single sequence structure prediction.

The disulfide cross-linking was carried out according to general procedures (Chapters 2.9.1 & 2.9.3 of *Materials and methods*). The modified oligonucleotide was first treated with DTT for cystamine reduction. The reducing agent was then removed by extraction with ethyl ether and the oligonucleotide was desalted and lyophilized. Next, **O8** was reconstituted in phosphate buffer pH 8.0 and due to high melting temperature, it was thermally denatured by 10 minute incubation at 98°C. Finally, the oligonucleotide was incubated for 48 h at room temperature gently shaking to allow air oxidation. Finally, the sample **O8X** was desalted and subjected to analysis using denaturing gel electrophoresis. The results of gel visualization were not as initially expected yet they presented an interesting picture (

Figure 52). The sample **O8** (lane 2) prior to the cross-linking reaction was migrating at the expected height, namely slightly slower than the unmodified control **O8C** (lane 1). Additionally, a band corresponding to a dimer was visible thus indicating that the sequence has unusually high self-affinity and tends to form a self-dimer even under denaturing conditions. According to the literature, a circular or a hairpin structure should migrate faster in the gel than a single-stranded RNA[139,225]. After the cross-linking reaction, I observed that the entire substrate was consumed, however, the **O8X** (lane 3) sample migrated as multiple bands at heights corresponding to oligomers rather than a hairpin, which implies that as a result of cross-linking several stable tertiary structures were formed.

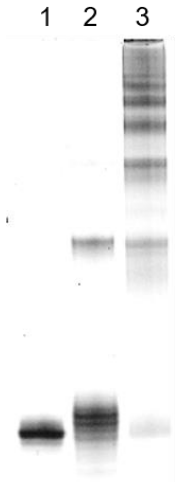

Figure 52. Denaturing gel electrophoresis of RNA hairpin O8 cross-linking experiments. Lane 1. O8C; lane 2. O8; lane 3. O8X.

Having obtained these results, I have decided to carry out an analogous experiment using a shorter sequence with a lower melting temperature. I designed and synthesized RNA oligonucleotide 5'-AGU**2'FC*** CUUCGGGA**2'FC*** U-3' (**O9**) as well as unmodified oligonucleotide 5'-AGUCCUUCGGGACU-3' (**O9C**) as a control. Both syntheses were done according to general procedures at 1 µmol and 0.2 µmol scales respectively. According to indicative thermal parameters based on UNAfold software predictions using 100 uM oligonucleotide and 100 mM Na^+ concentrations, the melting temperature of **O9C** 85.6°C. Thermal stability measurements conducted as described in general methods (Chapter 2.8.7. of *Materials and methods*) determined the actual melting temperature of **O9C** as 83.0°C. The cystamine linkers of oligonucleotide **O9** were reduced with DTT, the reducing agent was then removed and the sample lyophilized. Next, it was reconstituted in phosphate buffer pH 8.0, incubated for 5 minutes at 90°C, and let to gradually cool down to room temperature. The cross-linking reaction was conducted for 48 hours. Aliquots of the sample before the reaction **O9** and the cross-linked sample **O9X** were taken and analyzed with denaturing gel electrophoresis (

Figure **53**). Similarly, as in the case of oligonucleotide **O8,** no species migrating at the height corresponding to the hairpin structure was observed (lane 3), instead a stable duplex was formed. This time, however, no additional bands were visible above the duplex, indicating that no other tertiary structures were formed during the reaction.

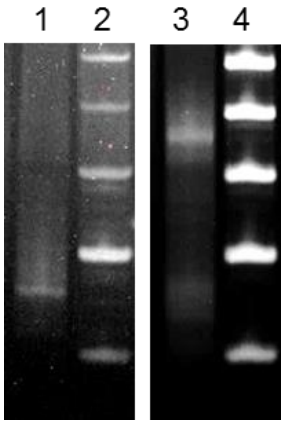

Figure 53. Denaturing gel electrophoresis of RNA hairpin O9 cross-linking experiments. Lane 1. O9; lane 3. O9X; lanes 2 & 4. marker.

The results are not as unexpected as they might seem at the first glance and the reason for that is the fact that spontaneous thiol oxidation reaction is unspecific. The predominant factor that determines the formation of a disulfide bridge is the mutual position between the two reacting thiol moieties. My initial assumptions regarding the location of intrastrand cross-linking of oligonucleotide's stem were based on the fact that the sequence exists exclusively as a hairpin in standard reaction conditions. Clearly, the cross-linking was somewhat incidental and occurred between separate strands leading to the formation of tertiary structures.

One way to promote intra- instead of interstrand cross-linking would be a significant decrease in RNA concentration in order to ensure that oligonucleotide strands do not neighbor each other within the linker range. Additionally, lowering the reaction temperature could aid the process as well by impairing RNA molecule's mobility in the solution and concomitantly decrease the probability of incidental interstrand cross-linking. On the other hand, the latter approach could significantly extend the time required for thiol oxidation to form a disulfide bridge.

7. CONJUGATION WITH RNASE H1 VIA A DISULFIDE BRIDGE

In previous chapters, I focused on the results of P-cystamine-modified RNA-RNA oligonucleotide cross-linking studies. In this chapter, I am demonstrating the applicability of such RNA in conjugation with other biomolecules, namely protein. In Chapter 5.4. of the *Introduction*, I described several examples of the use of covalent conjugation between proteins and oligonucleotides. This strategy is often required to provide information about the structure of the protein-nucleic acid complex or the mechanism of interaction between the two species.

P-cystamine modified RNA appeared as an excellent tool for the study of proteins which in principle interact with the nucleic acid backbone since the linker is placed directly at the backbone and points outwards of the helix. In collaboration with prof. M. Nowotny's lab, we decided to use it for cross-linking of RNase H1 with RNA/DNA heteroduplex. Eukaryotic RNase H1 is an endonuclease, which hydrolyses the RNA strand of the RNA/DNA chimera during the process of mitochondrial DNA replication[227]. Involved in the R-loop processing, it prevents the development of mitochondrial disease[228]. This enzyme was also found useful in antisense oligonucleotide therapy based on directed RNA cleavage[229]. Obtaining a stable complex between RNase H1 and nucleic acid substrate was conducted to get insight into the mechanism of their interaction.

The design of the experiment to test the feasibility of the cross-linking strategy was based on the previously resolved crystal structure of human RNase H1-RNA/DNA complex[230]. The active site of the protein interacts with the RNA strand of heteroduplex in the minor groove. Therefore, the modified oligonucleotide sequence **O10** was designed so that the cystamine-bearing phosphoramidate moiety was localized close to the RNA binding region of the protein. The modification site was chosen between C^8 and C^9 of the sequence, which is placed 1 nucleotide away from the scissile phosphate. Two variants of P-cystamine RNA were synthesized (**O10A** and **O10B**, sequences given in Table 8) the former having a 2'-deoxyribonucleotide and the latter 2'-deoxy-2'-fluororibonucelotide insertion at the modification site. The DNA strand of the substrate chimera was complementary to the sequence **O10** and comprised 5-methylated cytosines.

Table 8. Oligonucleotides used for RNase H1 conjugation

	Sequence 5' → 3'
O10A	AGUGCGACA**dC*** CUGAUUCC
O10B	AGUGCGACA**2'FC*** CUGAUUCC

7.1. DESIGN OF RNASE H1 MUTANTS

The RNase H1 structure was studied and the conclusion was made that the native cysteine residue Cys147 could form a linkage with modified RNA. There was a great concern that it could impose significant steric hindrance in nearby active site which in consequence could impair the activity of the protein. Thus, Cys147 was replaced with serine, and instead, three other residues further from the active site were substituted with cysteine, namely serine 149 (S149C), serine 150 (S150C), and arginine 278 (R278C). The proteins were expressed in *E.coli* and purified with

liquid chromatography as described in detail in Chapter 2.9.8. of *Materials and methods*. As presented in Table 9, the expression yield of the R278C mutant was very low, below 1 ug.

Table 9. RNase H1 mutants used in RNA cross-linking experiments

Name and species	Mutations	Expression yield [ug per 1g of bacterial pellet]
hsRH1 S149C (human)	C147S S149C D210N	7.35
hsRH1 S150C (human)	C147S S150C D210N	7.04
hsRH1 R278C (human)	C147S D210N R278C	0.67
rnRH1 R277C (rat)	C146S D209N R277C	54.08

7.2. RNASE H1- RNA CROSS-LINKING

All three RNase H1 variants were subjected to cross-linking with two modified RNA/DNA heteroduplexes with the ration 1:1.1 (protein-substrate). The cross-linking buffer consisted of 50 mM Tris pH 7.4, 45 mM NaCl, 25 mM KCl, 30% glycerol (v/v) and 5 mM $MgCl_2$. No reducing agent was added because it would prevent disulfide bridge formation between the P-cystamine RNA and the protein. Control reactions on the other hand were carried out in the same conditions with the addition of DTT. The conjugation products were analyzed on 15% non-reducing sodium dodecyl sulfate polyacrylamide gel electrophoresis (SDS-PAGE). The analysis of the complexes showed that for the first two variants (S149C and S150C) very low cross-linking yield was achieved, however, the remaining variants (R278C and R277C) achieved cross-linking efficiency reaching ca. 50% compared to unreacted protein. There was no significant difference in reactivity observed between substrates **O10A** and **O10B** implying that a single nucleotide modification does not affect the cross-linking efficiency.

7.3. SCALE-UP OF RNASE H1-RNA CROSS-LINKING

To make use of the full potential of this conjugation strategy, it was necessary to scale it up. Unfortunately, the very poor expression yield of the human RNase H1 mutant which exhibited the best cross-linking efficiency prevented upscaling in its current form. Instead, we decided to employ rat RNase H1 ortholog, which could serve as a good substitute for the human variant as all of its vital binding region amino acids are conserved. This protein mutant (rnRH1 R277C) was expressed with a nearly 80-fold increased yield of its human ortholog. Moreover, its cross-linking efficiency was just as high. Eventually, conjugation reaction was conducted in scale-up and the cross-linked product was purified with size exclusion chromatography followed by affinity chromatography. After confirmation of obtained product's purity with SDS-PAGE and its concentration to ca. 7 mg/mL, the cross-linked RNase H1- RNA/DNA complex could be then subjected to crystallization. Unfortunately, no crystals have been obtained up to date.

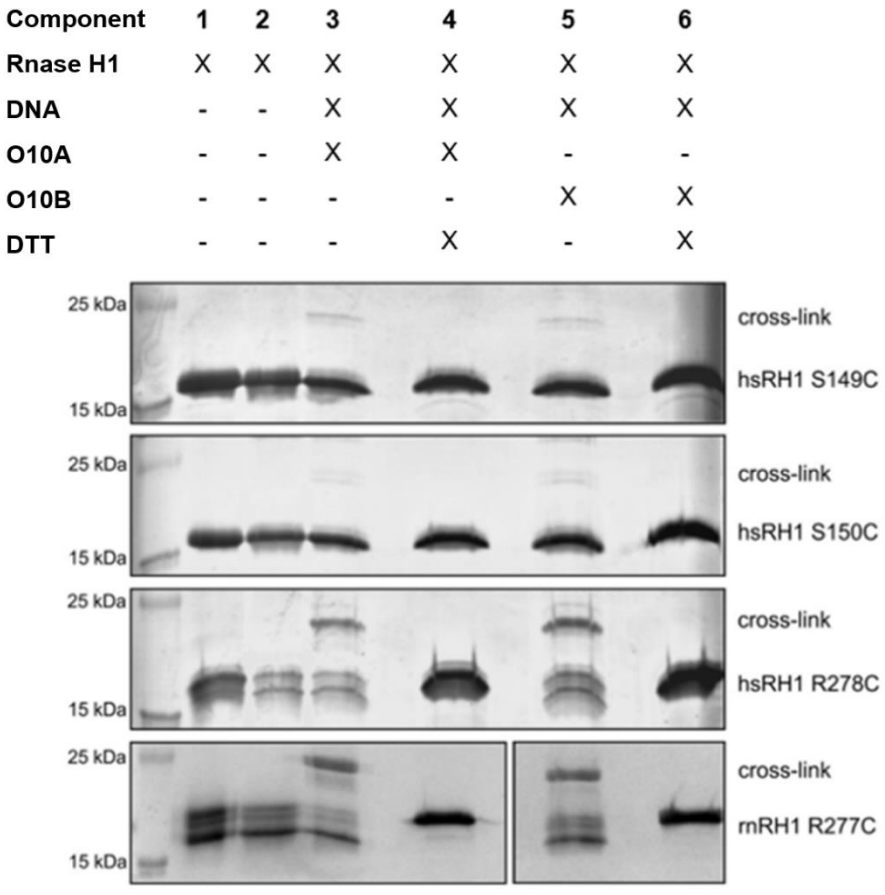

Figure 54. The SDS-PAGE analysis of RNase H1 variants cross-linking reactions with reaction composition indicated on top of each lane. Lane most to the left is a mass marker.

IV. SUMMARY

Oligonucleotide modifications are a broad and ever-growing field of biology-related research. By introducing changes into nucleic acids structure we can manipulate their properties to great extent, making them versatile tools in molecular biology or potent therapeutic agents. The chemical complexity of a single building block, i.e. nucleotide offers a wide range of functionalization possibilities at different sites. One can alter the sugar ring, modify the heterocyclic base and phosphate group or even replace the entire sugar-phosphate backbone with an alternative, non-native polymeric chain.

My research was focused on the development of RNA oligonucleotides modified in a way that would allow for their reversible cross-linking as well as conjugation with other biomolecules.

During my studies, I managed to find a way of introducing cystamine linker at any chosen phosphate of RNA oligonucleotide without impairing its stability, by combining phosphoramidite and *H*-phosphonate chemistry. Although initial experiments showed that the P-cystamine RNA oligonucleotides were unstable and underwent rapid cleavage, I found that the issue can be overcome by replacing the ribonucleotide at the site of modification with 2'-deoxy- or 2'-deoxy-2'-fluoronucleotides. The synthesis was then optimized to achieve the highest yields of cystamine-modified oligonucleotides.

Furthermore, I have studied the stereochemistry of *H*-phosphonate condensation and cystamine coupling reactions and their products. Using dinucleotide models, I investigated the ratio between diastereoisomers formed depending on which ribonucleotide analog is used and whether nearby nucleobases have any effect. Moreover, I also verified obtained results in the context of full oligonucleotide sequence by subjecting several variants to ^{31}P NMR analysis.

I have optimized conditions of oligonucleotide cross-linking via disulfide bridge between cystamine tethers and synthesized several linked bimolecular species. I have obtained stable dimers of disulfide cross-linked non-complementary oligonucleotides, which could potentially serve as a scaffold for creating more complex RNA nanostructures. Such dimers could be also useful in the structural mapping of large RNA molecules e.g. as triplex-forming probes. Furthermore, I synthesized covalently trapped RNA duplexes, which were subjected to structural studies in order to examine the impact of the cross-link on a molecule's geometry.

Additionally, I expanded cross-linking capabilities by applying external homobifunctional linkers, which increases the spatial range of linkage formation as well as provides the possibility to choose between reversible and non-reversible linking.

I synthesized RNA hairpin oligonucleotides with two P-cystamine modifications for intrastrand cross-linking. Sequences were designed in a way that the disulfide bridge could form a mid-stem between the opposing strands. Unfortunately, I did not manage to obtain cross-linked hairpins using this strategy as instead multiplex structures were formed. Results achieved in several experiments clearly exposed one of the major drawbacks of disulfide bridge-based cross-linking, namely the limited ability to control its formation specificity.

The final stage of my research covered the application of P-cystamine RNA in protein conjugation. During experiments, RNase H1 mutants were successfully linked via disulfide bridge with modified RNA:DNA substrate forming stable complexes. It proved the utility of disulfide linker functionalized oligonucleotides as tools in mechanistic and structural studies of interactions between proteins and nucleic acids.

One of the biggest challenges in P-cystamine oligonucleotide synthesis would be to develop a method in which one could obtain products with defined stereochemistry of modified phosphate. The ability to control the stereochemistry of products means placing the linker in the most desired position, which in turn would lead to maximal inter- and intrastrand cross-linking and protein conjugation efficiency.

To summarize, during my studies I devised a way to synthesize RNA oligonucleotides bearing a cystamine linker at the backbone in a reproducible manner and proved that these species can be used for interstrand cross-linking as well as conjugation with other biomolecules.

V. MATERIALS AND METHODS

1. MATERIALS

1.1. REAGENTS

Reagents that were used in my research project were purchased from the following suppliers:

Merck/Sigma-Aldrich

Molecular sieves 4Å, silica gel 60 (0.04-0.063 mm), 40% methylamine in water, 2,2'-dithiobis(ethylamine) dihydrochloride, 2-aminoethanethiol, tert-butyl hydroperoxide, triethylammonium trihydrofluoride, phosphate buffered saline (PBS) pH 7.2 tablets, 4,4'-dimethoxytrityl chloride, sodium bicarbonate, iodine, sodium thiosulfate, 2',4',6'-trihydroxyacetophenone monohydrate, ammonium citrate dibasic, triethylammonium acetate buffer 1 M pH 7.0, ammonium persulfate, 10x Tris-Borate-EDTA (TBE) buffer pH 8.3, tris(hydroxymethylaminomethane (Tris), sodium cacodylate, trimethylacetyl chloride, dithiotreitol, 5,5'-dithiobis-(2-nitrobenzoic acid), carbon tetrachloride, N-chlorosuccinimide, N-iodosuccinimide

Chem Genes (oligonucleotide synthesis)

DNA and RNA phosphoramidites, 2'-deoxyribonucleotide *H*-phoshonate triethylamine salts, 2'-deoxy-2'-fluorocytidine *H*-phosphonate triethylamine salt, Controlled Pore Glass (CPG) beads solid supports

emp Biotech (oligonucleotide synthesis)

Activating solution (0.2 M Hyacinth benzoylmercaptotetrazole in anhydrous acetonitrile, Capping A solution (THF/2,6-lutidine/acetic anhydride 80:10:10 v/v/v), Capping B solution (16% N-Methylimidazole in THF), Oxidation solution (0.1 M Iodine in THF/pyridine/water 78:20:2 v/v/v)

VWR

Acetonitrile <30 ppm water, N-methyl-2-pyrrolidone ninhydrin monohydrate

ACROS Organics

Acetonitrile Extra dry <10 ppm water, 1-butanol, 1-adamantanecarbonyl chloride

Chempur

Benzene, pyridine, acetonitrile 30% ammonia in water, methanol, glacial acetic acid, monosodium phosphate hydrate, disodium phosphate heptahydrate

POCH

Sodium hydroxide, hydrochloric acid, pyridine, dichloromethane, methanol, n-hexane

Bio-Rad

40% Acrylamide/Bisacrylamide 29:1 w/w solution, tetramethylethylenediamine (TEMED), urea

Fluorochem

3-Bromopropan-1-amine hydrobromide

Metkinen Chemistry

2'-deoxy-2'-fluoroadenine

Thermo Fisher Scientific

Dithiobismaleimidoethane, bismaleimidohexane

1.1. CONSUMABLES

Gel-Pak desalting columns	GlenResearch
Illustra NAP Sephadex DNA Purification columns	Cytiva/GE Healthcare
ZipTip with 0.6 µL C_{18} resin	Merck

1.2. EQUIPMENT

H6 DNA/RNA/LNA Synthesizer	K&A Laborgeraete GbR
miniSpin centrifuge	Eppendorf
TS-100C Thermo-Shaker with cooling	Biosan
High Pressure Liquid Chromatography	Shimazu
NanoDrop UV-VIS spectrophotometer	Thermo Scientific
SpeedVac vacuum centrifugal concentrator	Eppendorf
Genevac miVac centrifugal concentrator	Fisher Scientific
Gel electrophoresis system	Custom made
Gel Doc XR+ Gel Documentation System	BioRad
ScanVac CoolSafe freeze dryer	LaboGene
Liquid Chromatography Mass Spectrometer	Shimazu
Autoflex MALDI-TOF-MS	Bruker

UltrafleXtreme MALDI-TOF/TOF	Bruker
400 MHz AVANCE II NMR Spectrometer	Bruker
500 MHz AVANCE II NMR Spectrometer	Bruker
UV-VIS spectrophotometer V-650	JASCO

1.3. SOFTWARE

ChemDraw Ultra 12.0, Chem 3D Pro 12.0, TopSpin 4.0 Bruker, flexAnalysis 3.4 Bruker, UNAFold, RNAstructure 6.1, MeltWin 3.5

1.4. LIST OF OLIGONUCLEOTIDE SAMPLES

Name	Sequence (5' → 3')
O1	AGUGCGACACC*UGAUUCC
O2A-G	AGUGCGACAC2'FC*UGAUUCC
O3A	AGUGCGACAC2'FC*UGAUUCC
O3B	AGUGCGACAC2'FC*AGAUUCC
O3C	AGUGCGACACdC*UGAUUCC
O4	AGUGCGACACdC*UGAUUCC
O5A	GCG2'FC*GCGCGCG
O5B	GCG2'FC**GCGCGCG
O6	AGUGCGACAC2'FC*UGAUUCC
O7A	2'FA*AACAC CGGUGGAGG
O7B	AAACACCGGUGG2'FA*GG
O8	GCdC*GACCAGUCCUUCGGGACUGdG*UCGGC
O9	AGU2'FC*CUUCGGGA2'FC*U
O10A	AGUGCGACAdC*CUGAUUCC
O10B	AGUGCGACA2'FC*CUGAUUCC

2. METHODS

2.1. GENERAL METHODS

2.1.1. Buffers composition

1X Phosphate buffer saline (PBS) pH 7.2	137 mM NaCl, 2.7 mM KCl, 10 mM Na_2HPO_4, 1.8 mM KH_2PO_4
1X Tris-borate-EDTA (TBE) pH 8.3	100 mM Tris, 90 mM boric acid, 1 mM EDTA
Phosphate buffer pH 6.0	13.7 mM $Na_2HPO_4 \cdot 7H_2O$, 86.3 mM $NaH_2PO_4 \cdot H_2O$
Phosphate buffer pH 8.0	94 mM $Na_2HPO_4 \cdot 7H_2O$, 6 mM $NaH_2PO_4 \cdot H_2O$
Melting buffer pH 7.0	20 mM sodium cacodylate, 100 mM NaCl, 0.2 mM Na_2EDTA

The pH of all buffers was adjusted using appropriate acids and bases.

2.1.2. Chromatographic methods

Synthesis reactions were monitored using thin-layer chromatography (TLC) technique using silica 60 gel-coated aluminum plates without or with F_{254} fluorescent indicator (Merck). Plates were visualized using UV lamp λ=254 nm. Staining was done using an iodine chamber (thiols), 2% m/v ninhydrin in n-butanol (amines), or 10% H_2SO_4 in ethanol with heating (4,4'-dimethoxytrityl, ribose, and 2'-deoxyribose).

Synthesis product chromatographic purifications were done by standard column chromatography using silica gel 60 (0.04-0.063 mm).

2.1.3. Spectroscopic methods

Nuclear magnetic resonance spectra were recorded in the Laboratory of Biomolecular NMR IBCh using Bruker Avance 400 and 500 MHz spectrometers. In spectra descriptions, chemical shifts are given in ppm in relation to TMS for ^{1}H and ^{13}C and H_3PO_4 in D_2O for ^{31}P. Most of the analyzed samples were prepared directly in deuterated solvents or with the addition of deuterated solvents.

Mass spectroscopy (MS) analysis was done using Shimazu Liquid Chromatography Electrospray Mass Spectrometer (LC-ESI-MS) in the Department of Molecular Probes and Prodrugs High-

resolution mass spectroscopy (HRMS) analysis was done in Laboratory of Mass Spectroscopy IBCh using electrospray ionization (ESI) method.

2.2. SYNTHESIS OF DITHIOBIS(ALKYLAMINE) LINKERS

2.2.1. Synthesis of 2,2'-Dithiobis(ethylamine) (cystamine) **1**

1 g of 2-aminoethanethiol (cysteamine) (26 mmol) was dissolved in 5 mL of isopropanol and mixed with 2.7 mL of *tert*-Butyl hydroperoxide (28.5 mmol). The reaction was stirred and heated under reflux for 2.5 h until the entire cysteamine was consumed and the color of the solution turned brown. Next, solvents were evaporated under vacuum, and the remaining brown oil was lyophilized overnight. Reaction yield was virtually stoichiometric yielding pure cystamine **1**.

Alternative protocol

15 g of cystamine dihydrochloride (67 mmol) was placed in a round bottom flask and was dissolved in 12 mL of 6 N sodium hydroxide. When necessary, 5 mL of water was added to facilitate solubilization. The mixture was thoroughly stirred at room temperature for 15 min and then the water was evaporated to dryness. The white residue was immersed in 100 mL of dichloromethane, shaken vigorously, and incubated for 48 h at room temperature. After that time, the organic layer was decanted from the solid residue, dried over anhydrous K_2CO_3 and after filtration, the solvent was evaporated under vacuum. The remaining yellow oil was lyophilized overnight, yielding 6.4 g (63% yield) of cystamine **1**.

HR-MS m/z: $[M+H]^+$ Calcd for $C_4H_{12}N_2S_2$: 153.0442, found 153.0445.

^{1}H NMR (DMSO, 400 MHz, δ): 2.81-2.69 (dt, 8H, CH_2)

^{13}C NMR ($CDCl_3$, 100 MHz, δ): 39.8, 36.4

2.2.2. Synthesis of 3,3'-Dithiobis(propylamine) (homocystamine) **5**

2.0 g of 3-Bromopropylamine hydrobromide (9 mmol) and 1.59 g of sodium thiosulfate (10 mmol, 1.1 eq) were dissolved in 18 mL of methanol-water solution (4:5) and the reaction was stirred and heated under reflux for 12 h. The first step, namely the formation of Bunte salt **2** occurred rapidly, after around 2 h the substrate was entirely consumed. The second step,

namely salt hydrolysis, is much slower and it starts after ca. 6 h. The reaction was monitored using TLC (MeOH-1% AcOH, 3:2) stained with ninhydrin until **3** was fully transformed into **4**.

After reaction completion, the solution of iodine (1.27 g, 5 mmol) in 20 mL MeOH was added dropwise over the course of 5 h until the brown color of the mixture stopped disappearing. Any excess of unreacted iodine was quenched with a few drops of saturated sodium thiosulfate solution.

Solvents were evaporated under vacuum resulting in brown oil. The residue was dissolved in 3 mL of 6 N NaOH and extracted with dichloromethane (2x 50 mL). The organic phase was collected and the solvent was evaporated under vacuum. The obtained oil was dissolved in 4 mL of 4N HCl and concentrated under vacuum again. The resulting suspension was dissolved in 4 mL of water and a few drops of 6 N NaOH were added to adjust pH to alkaline. Water was evaporated under vacuum and the resulting residue was immersed in 50 mL of DCM and after shaking thoroughly was left for 16-48 h at room temperature. After that time, the organic layer was decanted from the solid residue, dried over anhydrous K_2CO_3 and after filtration, the solvent was evaporated under reduced pressure to give **5**. The remaining yellow-brown oil was lyophilized overnight.

HR-MS m/z: $[M+H]^+$ Calcd for $C_6H_{16}N_2S_2$: 181.0755, found 181.0763.

^{1H} NMR ($CDCl_3$, 400 MHz, δ): 2.76-2.72 (t, 4H, CH_2-N), 2.61-2.57 (t, 4H, CH_2-S), 1.70-1.63 (quin, 4H, C-CH2-C)

^{13}C NMR ($CDCl_3$, 100 MHz, δ): 40.3, 36.8, 31.3

2.3. SYNTHESIS OF PROTECTED NUCLEOSIDES

2.3.1. Synthesis of 5'-*O*-*tert*-butylmethylsilyl-2'-deoxythymidine **6**

2'-Deoxythymidine (2.42 g, 10 mmol), *tert*-butylmethylsilyl chloride (TBDMSCl) (1.81 g, 12 mmol) and imidazole (1.63 g, 24 mmol) were dissolved in 20 mL of dry DMF and stirred at room temperature under argon atmosphere for 1 h. The reaction was monitored by TLC (DCM-MeOH, 95:5). After the reaction was completed, the remaining TBDMSCl was quenched with 1 mL of MeOH and stirred for 10 min. The mixture was evaporated to dryness and lyophilized overnight. Obtained crude oil was dissolved in 20 mL of DCM and washed with H_2O (3x 60 mL). The organic layer was collected and evaporated to dryness. The obtained white solid was

recrystallized from boiling benzene (50 mL per each 1 g of crude material) by addition of n-hexane and the mixture was immediately filtered.

HR-MS m/z: $[M+H]^+$ Calcd for $C_{16}H_{28}N_2O_5Si$: 357.1767, found 357.1781.

^1H NMR (DMSO, 400 MHz, δ): 11.31 (s, 1H, NH), 7.46 (s, 1H, C6), 6.18-6.14 (t, 1H, H1'), 5.26-5.25 (d, 1H, H4'), 4.19 (m, 2H, H5', H5''), 3.81-3.70 (m, 2H, H3', OH), 2.08-2.06 (m, 2H, H2'), 1.77 (s, 3H, CH3), 0.88 (s, 9H, CH_3 TBDMS), 0.07 (s, 6H, CH_3 TBDMS)

^{13}C NMR ($CDCl_3$, 100 MHz, δ): 165.1, 152.8, 136.0, 112.2, 95.2, 89.9, 70.6, 61.5, 40.2, 31.0, 26.0, 11.8, -1.0

2.3.2. Synthesis of 3'-*O*-(4,4'-dimethoxytrityl)- 5'-*O*-*tert*-butylmethylsilyl-2'-deoxythymidine 7

5'-*O*-*tert*-Butylmethylsilyl-2'-deoxythymidine **6** (0.71 g, 2 mmol) was co-evaporated with 2 mL anhydrous pyridine and then dissolved in 5 mL of the same solvent. 4,4'-Dimethoxytrityl chloride (1.36 g, 4 mmol) was added and the reaction was stirred overnight under argon atmosphere at room temperature. After 18 h reaction was quenched by adding 2 mL of MeOH and stirring for 30 min. The mixture was evaporated to obtain a yellow oil. The oil was diluted with 20 mL of DCM and washed with saturated $NaHCO_3$ solution (4x 40 mL) until neutral pH, the organic layer was dried over anhydrous K_2CO_3 and filtered. The solvent was evaporated to dryness and lyophilized overnight.

HR-MS m/z: $[M+H]^+$ Calcd for $C_{37}H_{46}N_2O_7Si$: 659.3074, found 659.3078.

^1H NMR (DMSO, 400 MHz, δ): 11.10 (s, 1H, NH), 7.80-7.76 (m, 1H, C6), 7.35-6.87 (m, 13H, Ar DMT), 6.20-6.16 (t, 1H, H1'), 5.11-5.07 (m, 1H, H4'), 4.14 (m, 2H, H5', H5''), 3.73 (s, 6H, CH_3O DMT), 3.57-3.28 (m, 1H, H3'), 1.69 (s, 3H, CH_3), 1.58-1.54 (m, 2H, H2'), 0.76 (s, 9H, CH_3 TBDMS), -0.10 (s, 6H, CH_3 TBDMS)

^{13}C NMR (DMSO, 100 MHz, δ): 164.1, 158.3, 150.1, 144.2, 136.6, 135.9, 130.0, 129.3, 128.2, 127.7, 126.5, 115.0, 111.1, 95.5, 95.0, 91.1, 67.3, 63.1, 56.2, 39.0, 30.7, 25.8, 12.2, -1.8

2.3.3. Synthesis of 3'-*O*-(4,4'-dimethoxytrityl)-2'-deoxythymidine 8

3'-*O*-(4,4'-Dimethoxytrityl)-5'-*O*-*tert*-butylmethylsilyl-2'-deoxythymidine **7** (0.5g, 0.76 mmol) was dissolved in 5 mL of anhydrous tetrahydrofuran and triethylamine (TEA) (106 µL, 0.76

mmol) and triethylamine trihydrofluoride (TEAx3HF) (1.2 mL, 7.6 mmol) were added. The mixture was stirred under an argon atmosphere at room temperature for 8 h. The reaction was monitored by TLC (DCM-MeOH, 95:5). After the reaction was completed, the solvent was evaporated. The remaining yellowish oil was resuspended in ethyl acetate (10 mL) and work-up was carried out by washing with saturated $NaHCO_3$ (3x 20 mL) and brine (20 mL). The organic layer was collected and dried over anhydrous K_2CO_3. The solution was filtered and evaporated to dryness. The crude product was purified by column chromatography with DCM-MeOH gradient 0.5- 3% with 0.5% TEA.

HR-MS m/z: $[M+H]^+$ Calcd for $C_{31}H_{32}N_2O_7$: 545.2210, found 545.2198.

^{1}H NMR (DMSO, 400 MHz, δ): 11.26 (s, 1H, NH), 7.60 (s, 1H, C6), 7.42-6.90 (m, 13H, Ar DMT), 6.20-6.16 (t, 1H, H1'), 5.74 (s, 1H, OH), 4.94-4.92 (q, 2H, H4'), 4.23-4.22 (d, 1H, H3'), 3.72 (s, 6H, CH_3O DMT), 3.37-3.14 (m, 2H, H5', H5''), 1.70 (s, 3H, CH3), 1.50-1.47 (m, 2H, H2')

^{13}C NMR (DMSO, 100 MHz, δ): 164.0, 158.7, 150.9, 145.7, 136.5, 136.4, 136.2, 130.3, 130.3, 128.4, 128.3, 127.3, 113.8, 110.0, 87.0, 86.6, 84.2, 75.2, 61.8, 55.5, 38.8, 12.7

2.3.4. Synthesis of *N*^{6}-benzoyl-2'-deoxyadenosine **10**

2'-Deoxyadenosine (2 g, 7.5 mmol) was rendered anhydrous by evaporation with dry pyridine (20 mL) and lyophilization. The dried substrate was dissolved in 35 mL of dry pyridine, 4.75 mL (37.4 mmol) of trimethylsilyl chloride was added and the reaction mixture was stirred for 25 min at room temperature under argon. Next, 4.45 mL (37.4 mmol) of benzoyl chloride was added, and stirring continued for another 2 h. The mixture was cooled in an ice bath and the reaction was quenched with 5 mL of water and after 5 minutes 10 mL of aqueous ammonia (~30%) was added. The ice bath was removed and the mixture was stirred at room temperature for 30 min. Progress of reactions was monitored by TLC (DCM-MeOH, 95:5). After reaction completion, solvents were removed under reduced pressure. The remaining residue was dissolved in 60 mL of water and washed with ethyl acetate (2 x 40 mL). The aqueous phase was collected and soon after, the crystallization of the white solid started. The white powder was filtered and washed with 2 x 20 mL of ethyl acetate.

HR-MS m/z: $[M+H]^+$ Calcd for $C_{17}H_{17}N_5O_4$: 355.1281, found 355.1272.

^{1}H NMR ($CDCl_3$, 400 MHz, δ): 9.10 (br, 1H, NH), 8.71 (s, 1H, H8), 8.08 (s, 1H, H2), 8.03-7.32 (m, 5H, Ar Bz), 6.40-6.36 (t, 1H, H1'), 5.76-5.78 (br, 2H, 3'OH, 5'OH), 4.67-4.65 (m, 1H, H4'), 4.08-3.75 (m, 3H, H3', H5', H5''), 2.77-2.70 (m, 2H, H2')

^{13}C NMR ($CDCl_3$, 100 MHz, δ): 164.2, 152.5, 151.6, 150.0, 141.0, 134.4, 132.6, 129.0, 128.8, 127.5, 127.4, 123.4, 93.1, 89.9, 70.8, 61.7, 41.0

2.3.5. Synthesis of 5'-*O*-tert-butylmethylsilyl-*N*^{6}-benzoyl-2'-deoxyadenosine 11

N^6-Benzoyl-2'-deoxyadenosine (0.9 g, 2.5 mmol), *tert*-butylmethylsilyl chloride (TBDMSCl) (0.46 g, 3 mmol) and imidazole (0.41 g, 6 mmol) were dissolved in 20 mL of dry DMF and stirred at room temperature under argon atmosphere for 1 h. The reaction was monitored by TLC (DCM-MeOH, 95:5). After the reaction was completed, the remaining TBDMS-Cl was quenched with 1 mL of MeOH and stirred for 10 min. The mixture was evaporated to dryness and lyophilized overnight. Obtained crude oil was dissolved in 20 mL of DCM and washed with H_2O (3 x 40 mL). The organic layer was collected, dried over anhydrous Na_2SO_4, and then evaporated to dryness. The obtained white solid was recrystallized from boiling benzene (20 mL per each 1 g of crude material) by addition of *n*-hexane and mixture was immediately filtered. The white solid was dissolved in DCM, evaporated to dryness, and lyophilized overnight.

HR-MS m/z: $[M+H]^+$ Calcd for $C_{23}H_{31}N_5O_4Si$: 469.2145, found 469.2148.

^{1}H NMR ($CDCl_3$, 400 MHz, δ): 9.09 (br, 1H, NH), 8.48 (s, 1H, H8), 8.12 (s, 1H, H2), 8.05-7.41 (m, 5H, Ar Bz), 6.12-6.06 (t, 1H, H1'), 5.41 (br, 1H, 3'OH), 4.85-4.81 (m, 1H, H4'), 4.31-4.12 (m, 3H, H3', H5', H5''), 2.82-2.78 (m, 2H, H2'), 0.95 (s, 9H, CH_3 TBDMS), 0.16 (s, 6H, CH_3 TBDMS)

^{13}C NMR ($CDCl_3$, 100 MHz, δ): 164.8, 153.0, 152.2, 150.3, 141.1, 135.0, 132.5, 129.1, 128.2, 123.9, 94.1, 93.3 71.3, 68.2, 41.0, 31.3, 26.5, 26.4, -1.1

2.3.6. Synthesis of 3'-*O*-(4,4'-dimethoxytrityl)-5'-*O*-tert-butylmethylsilyl-*N*^{6}-benzoyl-2'-deoxyadenosine 12

5'-*O-tert*-Butylmethylsilyl-2'-deoxyadenosine (1.0 g, 2.1 mmol) was co-evaporated with 2 mL anhydrous pyridine and then dissolved in 5 mL of the same solvent. 4,4'-Dimethoxytrityl chloride (1.8 g, 5.3 mmol) was added and the reaction was stirred overnight under argon atmosphere at room temperature. After 16 h the reaction was quenched by adding 2 mL of

MeOH and stirring for 30 min. The mixture was evaporated to obtain a yellow paste. The residue was diluted with 20 mL of DCM and washed with saturated $NaHCO_3$ solution (3 x 40 mL, until neutral pH) and 1 x 10 mL with H_2O. The organic layer was collected and dried over anhydrous Na_2SO_4. The solvent was removed under vacuum and the resulting yellow oil was lyophilized.

HR-MS m/z: $[M+H]^+$ Calcd for $C_{44}H_{49}N_5O_6Si$: 771.3452, found 771.3438.

^1H NMR (DMSO, 400 MHz, δ): 9.11 (br, 1H, NH), 8.51 (s, 1H, H8), 8.09 (s, 1H, H2), 8.03-6.81 (m, 18H, Ar DMT, Bz), 6.10-6.07 (m, 1H, H1'), 3.73 (s, 6H, CH_3O DMT), 0.92 (s, 9H, CH_3 TBDMS), 0.18 (s, 6H, CH_3 TBDMS) [characteristic signals]

2.3.7. Synthesis of 3'-*O*-(4,4'-dimethoxytrityl)-N^6-benzoyl-2'-deoxyadenosine 13

3'-*O*-(4,4'-Dimethoxytrityl)-5'-*O*-*tert*-butylmethylsilyl-2'-deoxyadenosine (1.3 g, 1.7 mmol) was dissolved in 5 mL of anhydrous THF and triethylamine (TEA) (230 µL, 1.7 mmol) and triethylamine trihydrofluoride (TEA·3HF) (2.2 mL, 13.5 mmol) were added. The mixture was stirred under an argon atmosphere at room temperature for 8 h. The reaction was monitored by TLC (DCM-MeOH, 95:5). After the reaction was completed, the solvent evaporated. The remaining yellowish oil was resuspended in ethyl acetate (15 mL) and work-up was carried out by washing with saturated $NaHCO_3$ (3 x 30 mL) and brine (30 mL). The organic layer was collected, dried over anhydrous Na_2SO_4 and then the solvent was removed under vacuum. The product was purified using column chromatography with DCM-MeOH gradient 0.5-3% with 0.5% TEA.

HR-MS m/z: $[M+H]^+$ Calcd for $C_{38}H_{35}N_5O_6$: 657.2587, found 657.2601.

^1H NMR ($CDCl_3$, 400 MHz, δ): 9.10 (br, 1H, NH), 8.68 (s, 1H, H8), 8.06 (s, 1H, H2), 8.01-6.83 (m, 18H, Ar DMT, Bz), 6.37-6.33 (m, 1H, H1'), 5.66 (br, 1H, 5'OH), 4.64-4.62 (m, 1H, H4'), 4.06-3.72 (m, 3H, H3', H5', H5''), 3.79 (s, 6H, CH_3O DMT), 2.74-2.67 (m, 2H, H2')

^{13}C NMR ($CDCl_3$, 100 MHz, δ): 164.5, 158.8, 158.5, 152.0, 150.6, 150.1, 147.4, 145.1, 142.6, 139.4, 136.4, 136.2, 136.1, 133.4, 132.9, 130.2, 129.1, 128.9, 128.3, 128.1, 127.9, 127.1, 124.5, 113.4, 113.3, 113.1, 89.5, 88.8, 88.1, 87.4, 75.4, 63.3, 55.3, 39.8

2.3.8. Synthesis of N^6-benzoyl-2'-deoxy-2'-fluoroadenosine 18

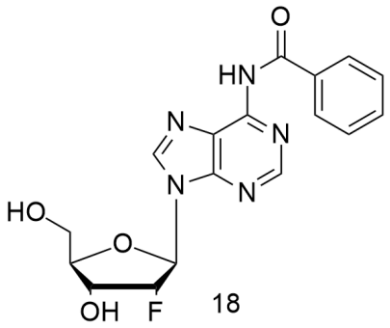

Figure 55. Structure of N^6-benzoyl-2'-deoxy-2'-fluoroadenosine 18.

2'-Deoxy-2'-fluoroadenosine (1.5 g, 5.57 mmol) was rendered anhydrous by evaporation with dry pyridine (20 mL) and lyophilization. The dried substrate was dissolved in 30 mL of dry pyridine, 3.5 mL (27.86 mmol) of trimethylsilyl chloride was added and the reaction mixture was stirred for 25 min at room temperature under argon. Next, 3.2 mL (27.86 mmol) of benzoyl chloride was added, and stirring continued for another 2 h. The reaction was cooled in an ice bath and the reaction was quenched with 5 mL of water and after 5 minutes 10 mL of aqueous ammonia (ca. 30%). The ice bath was removed and the mixture was stirred at room temperature for 30 min. The reaction progress was monitored using TLC with DCM-MeOH 95:5 as eluent. After reaction completion, solvents were removed under reduced pressure. The remaining residue was dissolved in 70 mL of water and washed with 50 mL of ethyl acetate. The aqueous phase was collected and concentrated under vacuum to ca. 10 mL (until the formation of the first crystals). The product was let to crystallize overnight. Finally, the white powder was filtered and washed with 2 x 20 mL of ethyl acetate.

HR-MS m/z: $[M+H]^+$ Calcd for $C_{17}H_{16}FN_5O_4$: 373.1186, found 373.1185.

^{1}H NMR (DMSO, 400 MHz, δ): 9.0 (s, 1H, NH), 8.76 (s, 1H, H8), 8.05 (s, 1H, H2), 7.90-7.32 (m, 5H, Ar Bz), 6.40-6.35 (m, 1H, H1'), 5.57-5.43 (m, 1H, H2'), 4.87 (br, 2H, OH), 4.60-4.52 (m, 1H, H3'), 4.03-4.01 (m, 1H, H4'), 3.81-3.61 (m, 2H, H5', H5'')

^{13}C NMR (DMSO, 100 MHz, δ): 169.2, 165.8, 151.7, 150.5, 142.7, 137.0, 133.4, 132.5, 130.2, 129.0, 128.5, 127.7, 125.7, 94.54, 92.7, 86.9, 85.9, 84.0, 68.2, 60.0

2.3.9. Synthesis of 5'-*O*-(4,4'-dimethoxytrityl)-N^6-benzoyl-2'-deoxy-2'-fluoroadenosine 19

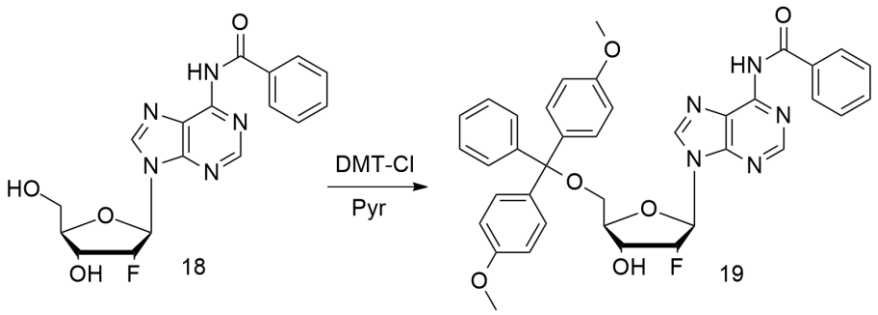

Figure 56. Synthesis of 5'-O-(4,4'-dimethoxytrityl)-N^6-benzoyl-2'-deoxy-2'fluoroadenosine 19.

N^6-Benzoyl-2'-deoxy-2'-fluoroadenosine **18** (0.57 g, 1.53 mmol) was rendered anhydrous by evaporation with dry pyridine (2 x 2 mL) and lyophilization prior to the synthesis. Then, it was dissolved in 4 mL of pyridine, 4,4'-dimethoxytrityl chloride (0.57 g, 1.68 mmol) was added and the reaction mixture was stirred for 1 h under argon at room temperature. Reaction completion was monitored by TLC (DCM-MeOH 95:5). After that time, the reaction was quenched by adding 1 mL of methanol and stirring for 5 min. Next, solvents were removed under reduced pressure and the residue was dissolved in dichloromethane (15 mL) and subsequently washed with saturated $NaHCO_3$ (2 x 20 mL). The organic layer was collected, dried over anhydrous Na_2SO_4 and then the solvent was removed by evaporation. The crude product **19** was purified with column chromatography using DCM-MeOH gradient 1- 5%.

HR-MS m/z: $[M+H]^+$ Calcd for $C_{38}H_{34}FN_5O_6$: 675.2493, found 675.2489.

^{1}H NMR (DMSO, 400 MHz, diagnostic signals δ): 9.82 (s, 1H, NH), 8.61 (s, 1H, H8), 8.22 (s, 1H, H2), 8.01-6.44 (m, 18H, Ar DMT, Bz), 6.21-6.20 (m, 1H, H1'), 5.68-5.50 (m, 1H, H2'), 5.01-4.95 (m, 1H, H3'), 4.26-4.22 (m, 1H, H4'), 3.78 (s, 6H, CH_3O DMT), 3.52-3.35 (m, 2H, H5', H5'')

^{13}C NMR (DMSO, 100 MHz, δ): 164.9, 158.0, 152.5, 151.9, 150.2, 144.3, 140.2, 136.3, 136.1, 134.3, 132.8, 132.5, 129.7, 129.0, 128.5, 128.4, 127.8, 127.7, 127.6, 127.5, 126.5, 124.0, 115.0, 96.9, 94.9, 92.1, 83.8, 69.1, 63.6, 55.7

2.4. SYNTHESIS OF 5'-*O*-(4,4'-DIMETHOXYTRITYL)-N^6-BENZOYL-2'-DEOXY-2'-FLUOROADENOSINE H-PHOSPHONATE TRIETHYLAMMONIUM SALT 20

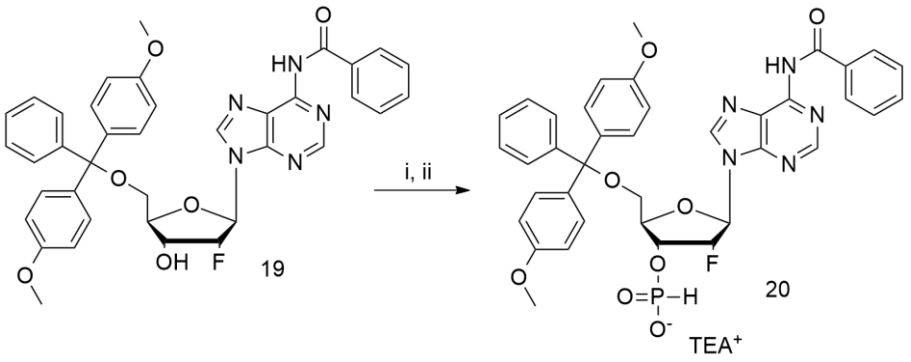

Figure 57. Pathway of 5'-O-(4,4'-dimethoxytrityl)-2'-deoxy-2'-fluoroadenosine H-phosphonate 20 synthesis. i) diphenyl phosphite, Pyr; ii) H_2O-TEA 1:1 v/v.

5'-*O*-(4,4'-Dimethoxytrityl)-N^6-benzoyl-2'-deoxy-2'-fluoroadenosine **19** (0.37 g, 0.55 mmol) was dissolved in 2 mL of dry pyridine and 350 µL of diphenyl phosphite (1.64 mmol) was added to the solution. The reaction mixture was stirred at room temperature for 20 min under argon. After that time, the reaction was quenched with 1 mL of water-triethylamine (1:1 v/v) and stirred for another 10 min yielding **20**. Next, solvents were removed under reduced pressure. The residue was dissolved in 15 mL of dichloromethane and washed with saturated $NaHCO_3$ (2 x 20 mL). The organic layer was collected and dried over anhydrous Na_2SO_4. The solvent was then evaporated and the crude product was subjected to purification via column chromatography using DCM-MeOH gradient 0-10% with 0.5% of TEA).

HR-MS m/z: $[M-H]^-$ Calcd for $C_{38}H_{34}FN_5O_8P^-$: 738.2135, found 738.2148.

^{1}H NMR ($CDCl_3$, 400 MHz, δ ppm): 9.07 (s, 1H, NH), 8.76 (s, 1H, H8), 8.27 (s, 1H, H2), 8.03-6.38 (m, 18H, Ar DMT, Bz), 6.17-6.16 (m, 1H, H1'), 5.75-5.60 (m, 1H, H2'), 5.29-5.07 (m, 1H, H3'), 4.44-4.43 (m, 1H, H4'), 3.76 (s, 6H, CH_3O DMT), 3.60-3.43 (m, 2H, H5', H5''), 2.83-2.77 (q, 6H, CH_2 TEA), 1.20-1.17 (t, 9H, CH_3 TEA)

^{13}C NMR ($CDCl_3$, 100 MHz, δ ppm): 164.5, 158.5, 152.7, 151.1, 149.5, 144.3, 141.1, 135.4, 133.7, 132.7, 130.0, 128.8, 128.1, 127.8, 126.9, 123.3, 113.2, 91.5, 87.3, 86.9, 86.6, 82.0, 70.3, 70.1, 61.7, 55.2, 53.4, 45.9, 9.9

^{31}P NMR ($CDCl_3$, 162 MHz, δ, J_{PH}= 628 Hz): 3.58

2.5. GENERAL PROCEDURE FOR DINUCLEOTIDE *H*-PHOSPHONATE SYNTHESIS **14**

3'-*O*-(4,4'-Dimethoxytrityl)-nucleoside (1.1 eq.) and 5'-*O*-(4,4'-dimethoxytrityl)-nucleoside *H*-phosphonate trimethylamine salt (1 eq) were mixed together and rendered anhydrous by evaporation with 1 mL of dry pyridine and lyophilization prior to the synthesis. The resulting solid was then dissolved in acetonitrile-pyridine 1:1 (2 mL) and 1-Adamantanecarbonyl chloride (3.3 eq.) was added and the mixture was stirred for 15 minutes under argon. Reaction progress was monitored using ^{31}P NMR. After completion, the reaction was quenched by adding 4-5 drops of water, and solvents were removed under reduced pressure. Next, the residue was dissolved in 10 mL of ethyl acetate and washed with brine (1x 25 mL). The organic layer was collected and dried over anhydrous Na_2SO_4. Finally, the solvent was evaporated under reduced pressure and the crude product was lyophilized overnight.

2.5.1. *O*-(5'-*O*-(4,4'-dimethoxytrityl)-2'-deoxythmidin-3'-yl)-*O*'-(3'-*O*-(4,4'-dimethoxytrityl)-2'-deoxythymidin-5'-yl) *H*-phosphonate **14a**

HR-MS m/z: $[M+H]^+$ Calcd for $C_{62}H_{63}N_4O_{15}P$: 1135.4028, found 1135.4076.

^{31}P NMR (ACN, 162 MHz, δ): 9.37, 8.13

2.5.2. *O*-(5'-*O*(-4,4'-dimethoxytrityl)-2'-deoxythmidin-3'-yl)-*O*'-(3'-*O*-(4,4'-dimethoxytrityl)-N^6-benzoyl-2'-deoxyadenosin-5'-yl) *H*-phosphonate **14b**

HR-MS m/z: $[M+H]^+$ Calcd for $C_{69}H_{66}N_7O_{14}P$: 1247.4405, found 1247.4398.

^{31}P NMR (ACN/Pyr, 162 MHz, δ): 9.36, 8.21

2.5.3. *O*-(5'-*O*-(4,4'-dimethoxytrityl)-N^4-benzoyl-2'-deoxy-2'-fluorocytidin-3'-yl)-*O*'-(3'-*O*-(4,4'-dimethoxytrityl)-2'-deoxythymidin-5'-yl) *H*-phosphonate **14c**

HR-MS m/z: $[M+H]^+$ Calcd for $C_{68}H_{65}FN_5O_{15}P$: 1241.4199, found 1241.4221.

^{31}P NMR (ACN/Pyr, 162 MHz, δ): 9.44, 8.51

2.6. GENERAL PROCEDURE FOR DINUCLEOTIDE PHOSPHORAMIDATES SYNTHESIS **15**

Dinucleotide *H*-phosphonate **14a-d** (1 eq.) was rendered anhydrous by evaporation with dry pyridine and lyophilization prior to the reaction. Next, the compound was dissolved in dry pyridine (1 mL) and carbon tetrachloride (100 µL), trimethylamine (15 µL) and cystamine (15 eq.) were added. The reaction mixture was stirred under argon for 1 h. Reaction progress was monitored by ^{31}P NMR. After completion, the solvent was removed under reduced pressure and the remaining residue was subjected to purification via column chromatography using DCM-MeOH gradient 10-20%.

2.6.1. *O*-(5'-*O*-(4,4'-dimethoxytrityl)-2'-deoxythmidin-3'-yl)-*O*'-(3'-*O*-(4,4'-dimethoxytrityl)-2'-deoxythymidin-5'-yl)-*N*-(2,2'-dithiobis(ethylamine)) phosphoramidate **15a**

HR-MS m/z: $[M+H]^+$ Calcd for $C_{66}H_{73}N_6O_{15}PS_2$: 1285.4313, found 1285.4389.

^{1}H NMR ($CDCl_3$, 400 MHz, δ ppm): 8.63 (s, 2H, NH), 7.71-6.38 (m, 34H, Ar DMT), 6.83-6.80 (br, 1H, PH), 6.23-6.19 (m, 2H, H1'), 5.09 (br, 2H, NH_2), 3.77-3.74 (m, 12H, CH_3O DMT) [characteristic signals]

^{13}C NMR ($CDCl_3$, 100 MHz, δ): 164.3, 164.1, 158.7, 158.7, 150.9, 150.4, 149.3, 144.7, 144.0, 136.3, 135.9, 135.8, 135.1, 135.0, 130.1, 130.0, 128.2, 128.1, 128.0, 127.1, 123.8, 113.3, 87.3, 87.2, 55.2, 38.9, 36.5, 28.0, 12.4, 11.6, 8.6

^{31}P NMR ($CDCl_3$, 162 MHz, δ): 8.52, 8.30

2.6.2. *O*-(5'-*O*-(4,4'-dimethoxytrityl)-2'-deoxythmidin-3'-yl)-*O*'-(3'-*O*-(4,4'-dimethoxytrityl)-N^6-benzoyl-2'-deoxyadenosin-5'-yl)-*N*-(2,2'-dithiobis(ethylamine)) phosphoramidate **15b**

HR-MS m/z: $[M+H]^+$ Calcd for $C_{73}H_{76}N_9O_{14}PS_2$: 1397.4691, found 1397.4693.

^{1}H NMR (CDCl3, 400 MHz, δ): 8.59 (s, 1H, NH), 7.87-6.25 (m, 34H, Ar DMT), 6.63 (br, 1H, PH), 5.86 (br, 2H, H1'), 5.09 (br, 2H, NH_2), 3.70-3.69 (m, 12H, CH_3O DMT) [characteristic signals]

^{13}C NMR ($CDCl_3$, 400 MHz, δ): 178.8, 168.0, 158.7, 158.5, 150.5, 149.5, 142.7, 136.1, 133.9, 128.4, 128.1, 128.0, 127.8, 127.3, 123.7, 113.4, 113.1, 110.6, 108.6, 87.3, 86.6, 86.5, 55.2, 55.1, 40.5, 39.2, 39.1, 37.2, 36.5, 36.3, 28.0, 12.5

^{31}P NMR ($CDCl_3$, 162 MHz, δ): 8.59, 8.25

2.6.3. *O*-(5'-*O*-(4,4'-dimethoxytrityl)-N^4-benzoyl-2'-deoxy-2'-fluorocytidin-3'-yl)-*O'*-(3'-*O*-(4,4'-dimethoxytrityl)-2'-deoxythymidin-5'-yl)-*N*-(2,2'-dithiobis(ethylamine)) phosphoramidate **15c**

HR-MS m/z: $[M+H]^+$ Calcd for $C_{72}H_{75}FN_7O_{15}PS_2$: 1391.4484, found 1391.4480

^{1}H NMR ($CDCl_3$, 400 MHz, δ): 7.82-6.24 (m, 34H, Ar DMT), 6.69 (br, 1H, PH), 5.86 (br, 2H, H1'), 5.79-5.77 (br, 1H, H2'), 3.80-3.76 (m, 12H, CH_3O DMT) [characteristic signals]

^{13}C NMR ($CDCl_3$, 400 MHz, δ): 168.7, 167.9, 164.8, 159.0, 158.8, 158.7, 154.8, 150.1, 143.7, 136.3, 133.2, 128.3, 128.1, 127.9, 127.7, 114.1, 113.9, 110.7, 109.0, 94.5, 88.1, 88.0 87.2, 87.1, 60.1, 57.3, 55.3, 55.2, 38.9, 27.9, 12.8

^{31}P NMR (ACN/Pyr, 162 MHz, δ): 8.8, 8.6

2.7. OLIGONUCLEOTIDE SYNTHESIS

Oligonucleotides were synthesized on K&A Laborgeraete H6 DNA/RNA/LNA Synthesizer in solid phase using commercial controlled pore glass (CPG) supports. Except for the modifications, oligonucleotide sequences were synthesized in a standard phosphoramidite approach using commercial substrates.

2.7.1. 0.2 µmol scale oligonucleotide synthesis

Step	Reagent	Time
Wash	Acetonitrile Argon	15 s
Detritylation	3% Dichloroacetic acid in dichloromethane	40 s
Wash	Acetonitrile Argon	30 s
Coupling	0.25 M BMT in acetonitrile 0.1 M phosphoramidite in acetonitrile	8 min

Wash	Acetonitrile Argon	20 s
Capping	Acetic anhydride/ 2,6-lutidine/ THF (1:1:8 v/v/v) 16% N-Methylimidazole in THF	2 min
Wash	Acetonitrile Argon	20 s
Oxidation	0.1 M Iodine in THF/ pyridine/ water (78:20:2 v/v/v)	1 min
Wash	Acetonitrile Argon	20 s

2.7.2. 1 µmol scale oligonucleotide synthesis

Step	Reagent	Time
Wash	Acetonitrile Argon	30 s
Detritylation	3% Dichloroacetic acid in dichloromethane	1 min
Wash	Acetonitrile Argon	30 s
Coupling	0.25 M BMT in acetonitrile 0.1 M phosphoramidite in acetonitrile	15 min
Wash	Acetonitrile Argon	30 s
Capping	Acetic anhydride/ 2,6-lutidine/ THF (1:1:8 v/v/v) 16% N-Methylimidazole in THF	2 min
Wash	Acetonitrile Argon	30 s
Oxidation	0.1 M Iodine in THF/ pyridine/ water (78:20:2 v/v/v)	2 min
Wash	Acetonitrile Argon	30 s

2.7.3. Disulfide linker-modified oligonucleotide synthesis

Solid support with partially synthesized oligonucleotide was manually washed with pulses of 3% DCA for controlled detritylation. After reaction completion, the support was flushed with ACN and dried with argon, removed from the synthesizer, and equipped with a 1 mL syringe

on one side. *H*-phosphonate of choice was dissolved in acetonitrile-pyridine and mixed with 1-Adamantanecarbonyl chloride immediately before use. The resulting mixture was drawn into another 1 mL syringe, which was connected to the other side of the column. The solid support was washed slowly with the solution for 5 minutes and after that time, the column was placed back on the synthesizer to be thoroughly flushed with acetonitrile. Next, the column was again removed from the synthesizer and the support was washed with a solution of cystamine and TEA in pyridine and CCl_4 in a manner similar to that described above in 5-minute intervals for 1 h. Later, the column was flushed with 10 mL of pyridine to remove the remains of the reaction mixture and then placed on the synthesizer to be washed with acetonitrile-argon cycles. Finally, an additional capping step with Ac_2O/2,6-lutidine/*N*-methylimidazole/THF was carried out for 3 minutes. Such prepared oligonucleotide was ready for further chain elongation via automated synthesis.

Table 10. Reagents used for P-cystamine modification of oligonucleotides

1 µmol scale			
***H*-phosphonate**	0.045 mmol	1 eq.	in 400 µL Py/ACN 1:1
Activator	0.135 mmol	3 eq.	
Cystamine	0.657 mmol	15 eq.	in 200 µL Py
Carbon tetrachloride	100 µL		
Triethylamine	10 µL		

2.7.4. Cleavage from the support and deprotection of oligonucleotides

Oligonucleotide type	Conditions
DNA/ P-cystamine DNA	Ammonium hydroxide 30% in H_2O for 2 h at 65°C or Ammonium hydroxide 30% in H_2O for 16 h at RT
RNA/ P-cystamine RNA	Ammonium hydroxide 30% in H_2O /Methylamine 40% in H_2O (1:1) for 20 min at RT and 10 min at 65°C or Ammonium hydroxide 30% in H_2O /Methylamine 40% in H_2O (1:1) for 2 h at RT

2.7.5. Deprotection of 2'-tert-butylmethylsilyl oligoribonucleotides

100 µL of N-methyl pyrrolidone was added to the vial with a lyophilized RNA sample and vigorously shaken until dissolved. When necessary, the sample was incubated for 3 min at 60°C for complete dissolution. Next, 50 µL of TEA and 67 µL of TEAx3HF were added to the vial, the mixture was briefly vortexed and instantly placed on a thermal shaker to be shaken for 1.5 h at 60°C. After completion, the reaction was quenched by precipitation of RNA with 950 µL of cold *n*-butanol. The sample was incubated at -17°C for at least 2 h and preferably overnight. Next, the vials were centrifuged for 15 min at 15000 rpm at 0°C, the supernatant was decanted and once the remaining *n*-butanol was removed, the RNA was reconstituted in autoclaved MiliQ water.

2.8. OLIGONUCLEOTIDE PURIFICATION AND CHARACTERIZATION

2.8.1. Polyacrylamide gel oligonucleotide purification

Oligonucleotides up to 12 nucleotides length and longer than 12 nucleotides were purified using denaturing 20% and 15% acrylamide/bis-acrylamide gel electrophoresis respectively. Electrophoresis was carried out over around 6 hours using 900 V at 120 mA.

Table 11. Polyacrylamide gel composition for oligonucleotide purification

Oligonucleotides <12 nt length	Oligonucleotides >12 nt length
20% w/v acrylamide/bis-acrylamide (29:1)	15% w/v acrylamide/bis-acrylamide (29:1)
1 x TBE buffer pH 8.3	1 x TBE buffer pH 8.3
7 M urea	7 M urea
0.3% w/v APS	0.3% w/v APS
0.03% TEMED	0.03% TEMED

The band containing the product oligonucleotide was cut out from the gel, placed in a tube, broken into smaller pieces, and immersed in autoclaved MiliQ water. The suspension was stored at -20°C for 4-12 h and subsequently the oligonucleotide was eluted by shaking the tube overnight at 4°C. Eluent containing oligonucleotide was separated from the gel and lyophilized before the product was subjected to desalting.

2.8.2. Analytical polyacrylamide gel electrophoresis

Oligonucleotide samples were analyzed using denaturing 15% acrylamide/bis-acrylamide gel electrophoresis. 10 x 10 cm gels were prepared using 15% w/v acrylamide/bis-acrylamide (29:1), 7 M urea in 1 X TBE buffer pH 8.3 solution with 0.3% w/v APS and 0.03% TEMED. 300-400 ng of lyophilized oligonucleotide sample was dissolved in 8 µL of 7 M urea, incubated for 10 minutes at 95°C, and briefly cooled down on ice. After loading the samples pre-electrophoresis was carried out for 10 minutes at 250 V and 10 mA to ensure proper diffusion into the gel and then the electrophoresis was conducted for 7 hours at 450 V and 40 mA. Oligonucleotides were dyed incubation with SYBRGold® in 1 X TBE buffer (1:10000) for 20 minutes and finally, gels were visualized using BioRad Gel Doc XR+.

2.8.3. Oligonucleotide desalting/buffer exchange

Oligonucleotides were desalted using Gel-Pak 1.0 or NAP-10 Sephadex desalting columns. In either case, columns were conditioned with 20 mL autoclaved MiliQ water. Oligonucleotides, reconstituted in 1 mL of water, were put on the resin and eluted with fractions of 1 mL. If the sample still contained significant traces of salt the desalting procedure was repeated.

The procedure for buffer exchange was carried out in an analogous manner, although in each step MiliQ water was replaced with a buffer of choice.

2.8.4. Reversed Phase High Pressure Liquid Chromatography (RP-HPLC) analysis

For analysis of the samples HPLC Shimadzu system was used, equipped with Shimadzu SPD-M20A photodiode array detector (DAD) using Phenomenex Clarity 3 µm Oligo-RP™ column (100 x 4.6 mm). Specific conditions for different analysis methods are presented in Table 12.

Table 12. Methods used for RP-HPLC analysis of oligonucleotides

Method	Details
Standard	T=40°C Linear gradient 0-40% buffer B (ACN) in buffer A (0.1 M TEAA pH 7.0 + 1% ACN), flow rate 1.0 ml/min over 30 min

Method	Details
80°C	T=80°C Linear gradient 0-40% buffer B (ACN) in buffer A (0.1 M TEAA pH 7.0 + 1% ACN), flow rate 1.0 ml/min over 30 min

2.8.5. Matrix Assisted Laser Desorption Ionisation Time Of Flight Mass Spectrometry (MALDI-TOF-MS) analysis

The solvent mixture used for sample and matrix preparation was acetonitrile/MiliQ water with 1% trifluoroacetic acid (50:50). Matrix (2′,4′,6′-Trihydroxyacetophenone monohydrate, THAP) stock solution was prepared by dissolving 50 mg of powder in 1 mL of the aforementioned solvent. A stock solution of ammonium citrate was prepared analogously (50 mg in 1 mL).

Prior to analysis, 0.1-0.2 OD of given oligonucleotide was prepared in a separate vial and lyophilized. The sample was then dissolved in 0.8-1.0 µL of ACN/H_2O/TFA solution. Matrix and ammonium citrate stock solutions were mixed together in a 9:1 ratio. Next, 0.5 µL of the sample was spotted on the AnchorChip 600 MALDI plate, and immediately after 0.5 µL of matrix-ammonium citrate solution was spotted on top of it and gently mixed with a pipette tip. Dried oligonucleotide samples analyzed on Autoflex MALDI-TOF-MS (Bruker Daltonics) equipped with nitrogen laser and operated in reflectron positive ions mode.

2.8.6. Optimized protocol for desalting of samples for MALDI-TOF-MS analysis using ZipTip$_{C18}$ pipette tips

To improve the quality of obtained MALDI-TOF-MS spectra, increase peak intensity, and decrease the amount of Na^+ peaks, some of the samples were desalted using ZipTip$_{C18}$ pipette tips (Merck), which allow for the exchange of metal cations with volatile TEA^+.

Table 13. Composition of solutions required for ZipTip desalting

Solution	Composition
Wetting solution	ACN/H_2O 50:50
Equilibration solution	1 M triethylammonium acetate (TEAA), pH 7.0
Wash solution 1	1 M triethylammonium acetate (TEAA), pH 7.0
Wash solution 2	H_2O
Elution buffer	ACN/H_2O 50:50

The sample was dissolved in 10 µL of the equilibration solution. 10 µL pipette was set to 10 µL and the ZipTip was pre-wetted with the wetting solution by pressing the pipette plunger to a dead stop, aspiring maximum volume and discarding it (twice). Equilibration of the tip was done by 3-times washing with 10 µL of equilibration solution. Binding of oligonucleotide was done by pressing the pipette plunger to a dead stop and 10 cycles of aspirating-dispensing of 10 µL of sample solution. This was done relatively slowly and carefully not to introduce air bubbles to increase the binding of the oligonucleotide to the bed. The bound sample was washed 3 times with wash solution 1 and 3 times with wash solution 2 (after each aspiration, the solution was discarded). In a new tube, 5-8 µL of the elution buffer was prepared, pipette with the tip on was set to the same volume. The eluent was carefully aspirated and dispensed 5 times without introducing air bubbles. The recovered oligonucleotide was shortly lyophilized and the sample for MALDI-TOF-MS analysis was prepared according to standard procedure.

2.8.7. Melting temperature measurements

The thermal stability of oligonucleotides was studied using a JASCO V-650 UV-VIS spectrophotometer with a heating-cooling system. Before the experiment, oligonucleotide concentration was calculated based on the extinction coefficient and absorbance measured at 80°C using the same instrument. Based on the concentration, a series of dilutions in the range 10^{-4} - 10^{-6} M were made in the melting buffer. Samples were placed in quartz cuvettes (30 µL, l=0.1 cm; 150 µL, 0.5 cm and 300 µL, 1 cm). The absorbance measurements were conducted at LAMBDA=260 nm. The temperature range was 20-90°C with a 1°C/min temperature ramp rate. Measurement was repeated 3 times for each dilution. Data obtained from an experiment were further analyzed with MeltWin 3.5 program.

2.9. MODIFIED OLIGONUCLEOTIDE CROSS-LINKING AND CONJUGATION

2.9.1. Reduction of disulfide linker- modified oligonucleotides

Lyophilized oligonucleotide bearing cystamine/homocystamine was resuspended in 100 mM dithiothreitol in 10 mM TBE buffer pH 8.3. The volume of DTT solution was proportional to the amount of the oligonucleotide and the ratio was 10 µL per 1 OD of oligonucleotide (e.g. 100 µL to 10 OD). The sample was incubated at room temperature for 1 h. Next, the sample mixture was washed with ethyl acetate three times with 3-times the reaction volume to remove most

of the DTT. Finally, the oligonucleotide was desalted with NAP-10 Sephadex column using autoclaved MiliQ water as eluent. Collected fractions were combined and lyophilized.

2.9.2. General protocol for oligonucleotide-oligonucleotide cross-linking

Oligonucleotides after reduction with DTT were reconstituted in 100 mM phosphate buffer pH 8.0 to final concentration 100 µM. In case two oligonucleotides were subjected to cross-linking, solutions were prepared to reach 100 µM final concentration after mixing. The reaction mixture was heated for 5 min at 90°C, let to gradually cool down to room temperature, and subsequently gently shaken for up to 72 hours. Finally, oligonucleotides were desalted with NAP-10 Sephadex column, eluted with autoclaved MiliQ water, and lyophilized.

2.9.3. Hairpin-forming oligonucleotide cross-linking

After reduction with DTT oligonucleotide was reconstituted in 100 mM phosphate buffer pH 8.0 to final concentration 100 µM. The oligonucleotide solution was heated for 10 min at 98°C. After that time, the vial with the reaction mixture was let to cool down to room temperature and incubated for 48 h, gently shaking. Finally, the product was desalted using NAP-10 Sephadex column, eluted with autoclaved MiliQ water, and lyophilized.

2.9.4. Oligonucleotide cross-linking via homobifunctional linkers

After reduction with DTT oligonucleotide was reconstituted in 1X PBS buffer pH 7.2 to final concentration 100 µM, incubated at 95°C for 5 minutes, and let to gradually cool down to room temperature. Fresh 20 mM stock solution of each maleimide linker was prepared directly before cross-linking by dissolving it in DMF. The oligonucleotide was then mixed with a 2-fold excess of cross-linker solution and incubated for 3 hours at room temperature. After that time, the sample was desalted with NAP-10 Sephadex column and lyophilized.

2.9.5. Oligonucleotide-RNase H1 cross-linking

Protein-oligonucleotide disulfide cross-linking was conducted in Structural Biology Center, Laboratory of Protein Structure at International Institute of Molecular and Cell Biology by members of dr hab. Marcin Nowotny laboratory. Detailed protocols for each step are described below.

2.9.6. Protein expression and purification

Fragments that corresponded to the catalytic domain of human hsRNase H1 (residues 136-286) and rat rnRNase H1 (residues 135-285) were subcloned into pET15b between NcoI/XhoI cloning sites. The mutations were introduced via commercially available gene synthesis (GenScript) or according to Stratagene's QuikChange protocol. To avoid nonspecific cross-linking, the endogenous Cys147 residue was substituted with Ser. Asn210 from the active site was substituted with Asp to inactivate enzymatic activity, and a Cys residue was introduced at different sites of the protein to allow site-specific cross-linking. All of the RNase H1 mutant variants are presented in Table 14.

Table 14. RNase H1 mutants used for cross-linking experiments

Name	Species	Mutations	Expression yield (μg/g bacterial pellet)
hsRH1 S149C	human	C147S S149C D210N	7.35
hsRH1 S150C	human	C147S S150C D210N	7.04
hsRH1 R278C	human	C147S D210N R278C	0.67
rnRH1 R277C	rat	C146S D209N R277C	54.08

The N-terminal His6-tag RNase H1 proteins were expressed in *Escherichia coli* BL21 Magic cells in LB medium. Cells were grown at 37°C until the optical density at 600 nm reached 0.7. The cultures were then cooled to 16°C, induced with 1 mM isopropyl β-D-1-thiogalactopyranoside (IPTG), and grown overnight. The cells were then harvested, resuspended in a lysis buffer, and disrupted by sonication. After centrifugation at 30,000 rpm at 4°C for 30 min, the cleared lysate was subjected to purification with affinity chromatography on HisTrap FF which was equilibrated with buffer 1. Next, the column was washed with an equilibration buffer, and proteins were eluted with the same buffer with the addition of 300 mM imidazole. The eluted fraction was subjected to thrombin digestion and dialyzed against buffer 2. The proteins were

further purified on a cation exchange column (Resource S) that was equilibrated with the same buffer. After elution in a linear gradient of 100-500 mM NaCl, fractions containing the protein were pooled, concentrated, and subjected to size-exclusion chromatography on a HiLoad 16/600 Superdex 75 pg column that was equilibrated with buffer 3. Selected fractions that contained purified RNase H1 were pooled and concentrated to 0.2 mg/mL in a cross-linking buffer.

2.9.7. Oligonucleotide-protein cross-linking

P-cystamine RNA oligonucleotides (10A and 10B) were annealed with GGAATmCAGGTGTmCGmCAmCT DNA (mC= 5-methylated cytidine) at 1:1 molar ratio by heating to 90°C for 5 min followed by cooling. Cross-linking reaction between formed RNA/DNA hybrid and RNase H1 was conducted at a 1.1:1 molar ratio (duplex:protein) in cross-linking buffer at 37°C for 2 h and next for an additional 14 h at 24°C. To verify the specificity of cross-linking, control reactions were treated with 5 mM DTT. All samples were analyzed on non-denaturing 15% SDS-PAGE gels.

2.9.8. Purification of cross-linked RNase H1-DNA/RNA complexes

In order to remove unbound oligonucleotide substrate, samples after cross-linking were purified on a HiLoad 16/600 Superdex 75 pg column that was equilibrated with buffer 2. Eluted fractions were pooled and loaded on a Heparin column that was equilibrated with the same buffer. Cross-linked complexes were collected in a flow-through fraction and concentrated. Non-cross-linked RNase H1 was eluted from the column with buffer 4.

Table 15. Composition of buffers used in protein purification

Buffer	Composition
Lysis buffer	20 mM HEPES pH 7.0, 1 M NaCl, 5% (v/v) glycerol, 2.8 mM β-mercaptoethanol, 10 mM imidazole, cOmplete EDTA-free protease inhibitor cocktail (Roche)
Buffer 1	20 mM HEPES pH 7.0, 1 M NaCl, 5% (v/v) glycerol, 2.8 mM β-mercaptoethanol, 60 mM imidazole
Buffer 2	20 mM HEPES pH 7.0, 100 mM NaCl, 5% (v/v) glycerol, 2 mM DTT, 0.5 mM EDTA

Buffer	Composition
Buffer 3	20 mM HEPES pH 7.0, 200 mM NaCl, 5% (v/v) glycerol, 2 mM DTT, 0.5 mM EDTA
Cross-linking buffer	50 mM Tris pH 7.4, 45 mM NaCl, 25 mM KCl, 30% (v/v) glycerol, 5 mM $MgCl_2$
Buffer 4	20 mM HEPES pH 7.0, 1 M NaCl, 5% (v/v) glycerol, 0.5 mM EDTA

VI. BIBLIOGRAPHY

1. Winkler, J. Oligonucleotide conjugates for therapeutic applications. *Ther. Deliv.* **4**, 791–809 (2013).
2. Corn, J. E. & Berger, J. M. FASTDXL: A Generalized Screen to Trap Disulfide-Stabilized Complexes for Use in Structural Studies. *Structure* **15**, 773–780 (2007).
3. Wang, L., Lee, S. & Verdine, G. L. Structural Basis for Avoidance of Promutagenic DNA Repair by MutY Adenine DNA Glycosylase. *J. Biol. Chem.* **290**, 17096–17105 (2015).
4. Stasińska, A. R., Putaj, P. & Chmielewski, M. K. Disulfide bridge as a linker in nucleic acids' bioconjugation. Part II: A summary of practical applications. *Bioorg. Chem.* **95**, 103518 (2020).
5. Tomasz, J. & Ludwig, J. Instability of the Phosphodiester-Amide Interribonucleotide Bond in Neutral Aqueous Solution. *Nucleosides and Nucleotides* **3**, 45–60 (1984).
6. Dahm, R. Friedrich Miescher and the discovery of DNA. *Dev. Biol.* **278**, 274–288 (2005).
7. Chargaff, E. Chemical specificity of nucleic acids and mechanism of their enzymatic degradation. *Experientia* **6**, 201–209 (1950).
8. Levene, P. A. The structure of yeast nucleic acid. IV. Ammonia hydrolysis. *J. Biol. Chem.* **40**, 415–424 (1919).
9. Avery, O. T., MacLeod, C. M. & McCarty, M. Studies on the chemical nature of the substance inducing transformation of pneumococcal types. *J. Exp. Med.* **79**, 137–158 (1944).
10. Watson, J.D., Crick, F. H. C. A structure for deoxyribose nucleic acid. *Nature* **4356**, 737 (1953).
11. Khorana, H. G., Razzell, W. E., Gilham, P. T., Tener, G. M. & Pol, E. H. SYNTHESES OF DIDEOXYRIBONUCLEOTIDES. *J. Am. Chem. Soc.* **79**, 1002–1003 (1957).
12. Gilham, P. T. & Khorana, H. G. Studies on Polynucleotides. I. A New and General Method for the Chemical Synthesis of the C 5 ″-C 3 ″ Internucleotidic Linkage. Syntheses of Deoxyribo-dinucleotides 1. *J. Am. Chem. Soc.* **80**, 6212–6222 (1958).
13. Khorana, H. G. *et al.* Polynucleotide Synthesis and the Genetic Code. *Cold Spring Harb. Symp. Quant. Biol.* **31**, 39–49 (1966).
14. Agarwal, K. L. *et al.* Total Synthesis of the Gene for an Alanine Transfer Ribonucleic Acid from Yeast. *Nature* **227**, 27–34 (1970).
15. Agarwal, K. L., Yamazaki, A., Cashion, P. J. & Khorana, H. G. Chemical Synthesis of Polynucleotides. *Angew. Chemie Int. Ed. English* **11**, 451–459 (1972).
16. Michelson, A. M. & Todd, A. R. Nucleotides part XXXII. Synthesis of a dithymidine dinucleotide containing a 3′: 5′-internucleotide linkage. *J. Chem. Soc.* **22**, 2632–2638 (1955).

17. Letsinger, R. L. & Mahadevan, V. Oligonucleotide Synthesis on a Polymer Support. *J. Am. Chem. Soc.* **87**, 3526–3527 (1965).

18. Eckstein, F. & Rizk, I. Oligonucleotide Syntheses by means of 2,2,2-Trichloroethyl Phosphorodichoridate. *Angew. Chemie Int. Ed. English* **6**, 949 (1967).

19. Eckstein, F. & Rizk, I. Synthesis of Oligonucleotides by Use of Phosphoric Triesters. *Angew. Chemie Int. Ed. English* **6**, 695–696 (1967).

20. Reese, C. B. & Saffhill, R. Oligonucleotide synthesis via phosphotriester intermediates: the phenyl-protecting group. *Chem. Commun.* 767 (1968). doi:10.1039/c19680000767

21. Letsinger, R. L., Ogilvie, K. K. & Miller, P. S. Nucleotide chemistry. XV. Developments in syntheses of oligodeoxyribonucleotides and their organic derivatives. *J. Am. Chem. Soc.* **91**, 3360–3365 (1969).

22. England, T. E. & Neilson, T. Oligoribonucleotide synthesis. IX. Synthesis of sequences corresponding to the dihydrouridine loop neck region common in several transfer RNA molecules. *Can. J. Chem.* **54**, 1714–1721 (1976).

23. van Boom, J. H., Burgers, P. M. J., van Deursen, P. H., Arentzen, R. & Reese, C. B. Internucleotide cleavage during unblocking in oligonucleotide synthesis by the phosphotriester approach. *Tetrahedron Lett.* **15**, 3785–3788 (1974).

24. Reese, C. B. A systematic approach to oligonucleotide synthesis. *Colloq. Int. CNRS* **182**, 319–328 (1970).

25. Catlin, J. C. & Cramer, F. Deoxy oligonucleotide synthesis via the triester method. *J. Org. Chem.* **38**, 245–250 (1973).

26. Katagiri, N., Itakura, K. & Narang, S. A. Use of arylsulfonyltriazoles for the synthesis of oligonucleotides by the triester approach. *J. Am. Chem. Soc.* **97**, 7332–7337 (1975).

27. Marugg, J. E. *et al.* Synthesis of DNA fragments by the hydroxybenzotriazole phosphotriester approach. *Tetrahedron* **40**, 73–78 (1984).

28. Jones, S. S., Rayner, B., Reese, C. B., Ubasawa, A. & Ubasawa, M. Synthesis of the 3'-terminal decaribonucleoside nonaphosphate of yeast alanine transfer ribonucleic acid. *Tetrahedron* **36**, 3075–3085 (1980).

29. Berlin, Y. A., Chakhmakhcheva, O. G., Efimov, V. A., Kolosov, M. N. & Korobko, V. G. Arenesulfonyl imidazolides, new reagents for polynucleotide synthesis. *Tetrahedron Lett.* **14**, 1353–1354 (1973).

30. Chattopadhyaya, J. B. & Reese, C. B. Chemical synthesis of a tridecanucleoside dodecaphosphate sequence of SV40 DNA. *Nucleic Acids Res.* **8**, 2039–2053 (1980).

31. Reese, C. B. & Pei-Zhuo, Z. Phosphotriester approach to the synthesis of oligonucleotides: a reappraisal. *J. Chem. Soc. Perkin Trans. 1* 2291 (1993). doi:10.1039/p19930002291

32. Crea, R., Kraszewski, A., Hirose, T. & Itakura, K. Chemical synthesis of genes for

human insulin. *Proc. Natl. Acad. Sci.* **75**, 5765–5769 (1978).

33. Wetzel, R. *et al.* Expression in escherichia coli of a chemically synthesized gene for a "mini-c" analog of human proinsulin. *Gene* **16**, 63–71 (1981).

34. Hall, R. H., Todd, A. & Webb, R. F. 644. Nucleotides. Part XLI. Mixed anhydrides as intermediates in the synthesis of dinucleoside phosphates. *J. Chem. Soc.* **868**, 3291 (1957).

35. Froehler, B. C. Deoxynucleoside H-Phosphonate diester intermediates in the synthesis of internucleotide phosphate analogues. *Tetrahedron Lett.* **27**, 5575–5578 (1986).

36. Garegg, P. J., Regberg, T., Stawinski, J. & Strömberg, R. Studies on the Oxidation of Nucleoside Hydrogenphosphonates. *Nucleosides and Nucleotides* **6**, 429–432 (1987).

37. Froehler, B. C., Ng, P. G. & Matteucci, M. D. Synthesis of DNA via deoxynudeoside H-phosphonate Intermediates. *Nucleic Acids Res.* **14**, 5399–5407 (1986).

38. Garegg, P. J. *et al.* Nucleoside H-phosphonates. III. Chemical synthesis of oligodeoxyribonucleotides by the hydrogenphosphonate approach. *Tetrahedron Lett.* **27**, 4051–4054 (1986).

39. Agrawal, S. & Tang, J.-Y. Efficient synthesis of oligoribonucleotide and its phosphorothioate analogue using H-phosphonate approach. *Tetrahedron Lett.* **31**, 7541–7544 (1990).

40. Dreef, C. E., Dreef-Tromp, C. M., van der Marel, G. A. & van Boom, J. H. A Convenient Approach Towards the Conversion of H-Phosphonate and H-Phosphonothioate Diesters into Phosphoro(di)thioate Derivatives. *Synlett* **1990**, 481–483 (1990).

41. Tram, K., Wang, X. & Yan, H. Facile Synthesis of Oligonucleotide Phosphoroselenoates. *Org. Lett.* **9**, 5103–5106 (2007).

42. Atherton, F. R., Openshaw, H. T. & Todd, A. R. Studies on phosphorylation. Part II. The reaction of dialkyl phosphites with polyhalogen compounds in presence of bases. A new method for the phosphorylation of amines. *J. Chem. Soc.* 660–663 (1945).

43. Atherton, F. R. & Todd, A. R. 129. Studies on phosphorylation. Part III. Further observations on the reaction of phosphites with polyhalogen compounds in presence of bases and its application to the phosphorylation of alcohols. *J. Chem. Soc.* 674 (1947). doi:10.1039/jr9470000674

44. Wang, Z. Atherton-Todd Reaction. in *Comprehensive Organic Name Reactions and Reagents* 114–118 (John Wiley & Sons, Inc., 2010). doi:10.1002/9780470638859.conrr027

45. Steinberg, G. M. Reactions of dialkyl chlorophosphates, tetraalkyl pyrophosphates, and mixed orthophosphate esters. *J. Org. Chem.* **15**, 637–647 (1950).

46. Le Corre, S. S., Berchel, M., Couthon-Gourvès, H., Haelters, J.-P. & Jaffrès, P.-A. Atherton–Todd reaction: mechanism, scope and applications. *Beilstein J. Org. Chem.*

10, 1166–1196 (2014).

47. Reiff, L. P. & Aaron, H. S. Stereospecific synthesis and reactions of optically active isopropyl methylphosphinate. *J. Am. Chem. Soc.* 92, 5275–5276 (1970).

48. Stec, W. & Mikołajczyk, M. Stereochemistry of organophosphorus cyclic compounds—II: : Stereospecific synthesis of cis- and trans 2-halogeno-2-oxo-4-methyl-1,3,2-dioxaphosphorinans and their chemical transformations. *Tetrahedron* 29, 539–546 (1973).

49. Xiong, B. *et al.* Systematic study for the stereochemistry of the Atherton-Todd reaction. *Tetrahedron* 69, 9373–9380 (2013).

50. Stawiński, J., Strömberg, R. & Zain, R. Stereospecific oxidation and oxidative coupling of H-phosphonate and H-phosphonothioate diesters. *Tetrahedron Lett.* 33, 3185–3188 (1992).

51. Nilsson, J. & Stawinski, J. Controlling stereochemistry during oxidative coupling. Preparation of Rp or Sp phosphoramidates from one P-chiral precursor. *Chem. Commun.* 10, 2566–2567 (2004).

52. Letsinger, R. L. & Lunsford, W. B. Synthesis of thymidine oligonucleotides by phosphite triester intermediates. *J. Am. Chem. Soc.* 98, 3655–3661 (1976).

53. Beaucage, S. L. & Caruthers, M. H. Deoxynucleoside phosphoramidites—A new class of key intermediates for deoxypolynucleotide synthesis. *Tetrahedron Lett.* 22, 1859–1862 (1981).

54. Matteucci, M. D. & Caruthers, M. H. Synthesis of deoxyoligonucleotides on a polymer support. *J. Am. Chem. Soc.* 103, 3185–3191 (1981).

55. McBride, L. J. & Caruthers, M. H. An investigation of several deoxynucleoside phosphoramidites useful for synthesizing deoxyoligonucleotides. *Tetrahedron Lett.* 24, 245–248 (1983).

56. Sinha, N. D., Biernat, J. & Köster, H. β-Cyanoethyl N,N-dialkylamino/N-morpholinomonochloro phosphoamidites, new phosphitylating agents facilitating ease of deprotection and work-up of synthesized oligonucleotides. *Tetrahedron Lett.* 24, 5843–5846 (1983).

57. Mullis, K. B. Nobel Lecture: The Polymerase Chain Reaction. (1993). Available at: https://www.nobelprize.org/prizes/chemistry/1993/mullis/lecture/.

58. Guainazzi, A. & Schärer, O. D. Using synthetic DNA interstrand crosslinks to elucidate repair pathways and identify new therapeutic targets for cancer chemotherapy. *Cell. Mol. Life Sci.* 67, 3683–3697 (2010).

59. Noll, David, M. Preparation of interstrand cross-linked DNA oligonucleotide duplexes. *Front. Biosci.* 9, 421 (2004).

60. Hostetter, A. A., Chapman, E. G. & DeRose, V. J. Rapid Cross-Linking of an RNA Internal Loop by the Anticancer Drug Cisplatin. *J. Am. Chem. Soc.* 131, 9250–9257 (2009).

61. Efimov, V. A., Fedyunin, S. V. & Chakhmakhcheva, O. G. Cross-linked nucleic acids: Formation, structure, and biological function. *Russ. J. Bioorganic Chem.* **36**, 49–72 (2010).

62. Axelrod, V. D., Feldman, M. Y., Chuguev, I. I. & Bayev, A. A. Transfer RNA cross-linked with formaldehyde. *Biochim. Biophys. Acta - Nucleic Acids Protein Synth.* **186**, 33–45 (1969).

63. Pieles, U., Sproat, B. S., Neuner, P. & Cramer, F. Preparation of a novel psoralen containing deoxyadenosine building block for the facile solid phase synthesis of psoralen-modified oligonucleotides for a sequence specific crosslink to a given target sequence. *Nucleic Acids Res.* **17**, 8967–8978 (1989).

64. Wellinger, R. E. & Sogo, J. M. In vivo mapping of nucleosomes using psoralen-DNA crosslinking and primer extension. *Nucleic Acids Res.* **26**, 1544–1545 (1998).

65. Skripkin, E., Isel, C., Marquet, R., Ehresmann, B. & Ehresmann, C. Psoralen Crosslinking between Human Immunodeficiency Virus Type 1 RNA and Primer tRNA3Lys. *Nucleic Acids Res.* **24**, 509–514 (1996).

66. Higuchi, M., Sakamoto, T., Kobori, A. & Murakami, A. Properties of novel antisense oligonucleotides containing 2′-O-modified adenosine with a photo-reactive group. *Nucleic Acids Symp. Ser.* **50**, 301–302 (2006).

67. Stewart, D. A., Thomas, S. D., Mayfield, C. A. & Miller, D. M. Psoralen-modified clamp-forming antisense oligonucleotides reduce cellular c-Myc protein expression and B16-F0 proliferation. *Nucleic Acids Res.* **29**, 4052–4061 (2001).

68. Kolb, H. C., Finn, M. G. & Sharpless, K. B. Click Chemistry: Diverse Chemical Function from a Few Good Reactions. *Angew. Chemie Int. Ed.* **40**, 2004–2021 (2001).

69. Kočalka, P., El-Sagheer, A. H. & Brown, T. Rapid and Efficient DNA Strand Cross-Linking by Click Chemistry. *ChemBioChem* **9**, 1280–1285 (2008).

70. Lietard, J., Meyer, A., Vasseur, J.-J. & Morvan, F. New Strategies for Cyclization and Bicyclization of Oligonucleotides by Click Chemistry Assisted by Microwaves. *J. Org. Chem.* **73**, 191–200 (2008).

71. Uszczyńska, B. *et al.* Application of click chemistry to the production of DNA microarrays. *Lab Chip* **12**, 1151 (2012).

72. Bouillon, C. *et al.* Microwave Assisted “Click” Chemistry for the Synthesis of Multiple Labeled-Carbohydrate Oligonucleotides on Solid Support. *J. Org. Chem.* **71**, 4700–4702 (2006).

73. Humenik, M., Huang, Y., Wang, Y. & Sprinzl, M. C-Terminal Incorporation of Bio-Orthogonal Azide Groups into a Protein and Preparation of Protein–Oligodeoxynucleotide Conjugates by CuI-Catalyzed Cycloaddition. *ChemBioChem* **8**, 1103–1106 (2007).

74. Harris, M. E. & Christian, E. L. RNA Crosslinking Methods. in *Methods in Enzymology* **468**, 127–146 (2009).

75. Verma, S. & Eckstein, F. MODIFIED OLIGONUCLEOTIDES: Synthesis and Strategy for

Users. *Annu. Rev. Biochem.* **67**, 99–134 (1998).

76. Favre, A. & Fourrey, J.-L. Structural Probing of Small Endonucleolytic Ribozymes in Solution Using Thio-Substituted Nucleobases as Intrinsic Photolabels. *Acc. Chem. Res.* **28**, 375–382 (1995).

77. Christian, E. L., McPheeters, D. S. & Harris, M. E. Identification of Individual Nucleotides in the Bacterial Ribonuclease P Ribozyme Adjacent to the Pre-tRNA Cleavage Site by Short-Range Photo-Cross-Linking. *Biochemistry* **37**, 17618–17628 (1998).

78. Nanda, K. & Wollenzien, P. Pattern of 4-Thiouridine-Induced Cross-Linking in 16S Ribosomal RNA in the Escherichia coli 30S Subunit †. *Biochemistry* **43**, 8923–8934 (2004).

79. Juzumiene, D., Shapkina, T., Kirillov, S. & Wollenzien, P. Short-Range RNA-RNA Crosslinking Methods to Determine rRNA Structure and Interactions. *Methods* **25**, 333–343 (2001).

80. Favre, A., Saintomé, C., Fourrey, J.-L., Clivio, P. & Laugâa, P. Thionucleobases as intrinsic photoaffinity probes of nucleic acid structure and nucleic acid-protein interactions. *J. Photochem. Photobiol. B Biol.* **42**, 109–124 (1998).

81. Wolfes, H., Fliess, A., Winkler, F. & Pingoud, A. Cross-linking of bromodeoxyuridine-substituted oligonucleotides to the EcoRI and EcoRV restriction endonucleases. *Eur. J. Biochem.* **159**, 267–273 (1986).

82. Nishimura, S. & Watanabe, K. The discovery of modified nucleosides from the early days to the present: A personal perspective. *J. Biosci.* **31**, 465–475 (2006).

83. Boccaletto, P. *et al.* MODOMICS: a database of RNA modification pathways. 2017 update. *Nucleic Acids Res.* **46**, D303–D307 (2018).

84. Stasińska, A. R., Putaj, P. & Chmielewski, M. K. Disulfide bridge as a linker in nucleic acids' bioconjugation. Part I: An overview of synthetic strategies. *Bioorg. Chem.* **92**, 103223 (2019).

85. Smith, C. I. E. & Zain, R. Therapeutic Oligonucleotides: State of the Art. *Annu. Rev. Pharmacol. Toxicol.* **59**, 605–630 (2019).

86. Bartold, K., Pietrzyk-Le, A., D'Souza, F. & Kutner, W. Oligonucleotide Analogs and Mimics for Sensing Macromolecular Biocompounds. *Trends Biotechnol.* **37**, 1051–1062 (2019).

87. Singh, S. K., Koshkin, A. a., Wengel, J. & Nielsen, P. LNA (locked nucleic acids): synthesis and high-affinity nucleic acid recognition. *Chem. Commun.* 455–456 (1998). doi:10.1039/a708608c

88. Nielsen, P., Egholm, M., Berg, R. & Buchardt, O. Sequence-selective recognition of DNA by strand displacement with a thymine-substituted polyamide. *Science (80-.).* **254**, 1497–1500 (1991).

89. Egholm, M. *et al.* PNA hybridizes to complementary oligonucleotides obeying the Watson-Crick hydrogen-bonding rules. *Nature* **365**, 566–568 (1993).

90. SUMMERTON, J. & WELLER, D. Morpholino Antisense Oligomers: Design, Preparation, and Properties. *Antisense Nucleic Acid Drug Dev.* **7**, 187–195 (1997).

91. Iversen, P. L. Phosphorodiamidate Morpholino Oligomers. in *Antisense Drug Technology* (ed. Crooke, S. T.) 375–389 (CRC Press, 2006). doi:10.1201/9781420002546.ch15

92. Manoharan, M., Johnson, L. K., Tivel, K. L., Springer, R. H. & Cook, P. D. Introduction of a lipophilic thioether tether in the minor groove of nucleic acids for antisense applications. *Bioorg. Med. Chem. Lett.* **3**, 2765–2770 (1993).

93. Goodwin, J. T., Osborne, S. E., Scholle, E. J. & Glick, G. D. Design, Synthesis, and Analysis of Yeast tRNA Phe Analogs Possessing Intra- and Interhelical Disulfide Cross-Links †. *J. Am. Chem. Soc.* **118**, 5207–5215 (1996).

94. Gundlach, C. W., Ryder, T. R. & Glick, G. D. Synthesis of guanosine analogs bearing pendant alkylthiol tethers. *Tetrahedron Lett.* **38**, 4039–4042 (1997).

95. Jin, S., Miduturu, C. V., McKinney, D. C. & Silverman, S. K. Synthesis of amine- and thiol-modified nucleoside phosphoramidites for site-specific introduction of biophysical probes into RNA. *J. Org. Chem.* **70**, 4284–4299 (2005).

96. Sigurdsson, S. T., Tuschl, T. & Eckstein, F. Probing RNA tertiary structure: interhelical crosslinking of the hammerhead ribozyme. *RNA* **1**, 575–83 (1995).

97. Cohen, S. B. & Cech, T. R. Dynamics of thermal motions within a large catalytic RNA investigated by cross-linking with thiol-disulfide interchange. *J. Am. Chem. Soc.* **119**, 6259–6268 (1997).

98. Hatano, A., Makita, S. & Kirihara, M. Synthesis and redox-active base-pairing properties of DNA incorporating mercapto C-nucleosides. *Tetrahedron* **61**, 1723–1730 (2005).

99. Shigdel, U. K. & He, C. A New 1′-Methylenedisulfide Deoxyribose that Forms an Efficient Cross-Link to DNA Cytosine-5 Methyltransferase (DNMT). *J. Am. Chem. Soc.* **130**, 17634–17635 (2008).

100. Glick, G. D. Synthesis of a Conformationally Restricted DNA Hairpin. *J. Org. Chem.* **56**, 6746–6747 (1991).

101. Goodwin, J. T. & Glick, G. D. Synthesis of a disulfide stabilized RNA hairpin. *Tetrahedron Lett.* **35**, 1647–1650 (1994).

102. Goodwin, J. T. & Glick, G. D. Incorporation of alkylthiol chains at C-5 of deoxyuridine. *Tetrahedron Lett.* **34**, 5549–5552 (1993).

103. Sun, S., Tang, X.-Q. & Merchant, A. Efficient Synthesis of 5-(Thioalkyl)uridines via Ring Opening of α-Ureidomethylene Thiolactones. *J. Org. Chem.* **61**, 5708–5709 (1996).

104. Chaudhuri, N. C. & Kool, E. T. Very High Affinity DNA Recognition by Bicyclic and Cross-Linked Oligonucleotides. *J. Am. Chem. Soc.* **117**, 10434–10442 (1995).

105. Prestinari, C. & Richert, C. Intrastrand locks increase duplex stability and base pairing selectivity. *Chem. Commun.* **47**, 10824–10826 (2011).

106. Hou, X., Wang, G., Gaffney, B. L. & Jones, R. A. Synthesis of guanosine and deoxyguanosine phosphoramidites with cross-linkable thioalkyl tethers for direct incorporation into RNA and DNA. *Nucleosides, Nucleotides and Nucleic Acids* **28**, 1076–1094 (2009).

107. Hou, X., Wang, G., Gaffney, B. L. & Jones, R. A. Preparation of DNA and RNA fragments containing guanine N 2-thioalky1 tethers. *Curr. Protoc. Nucleic Acid Chem.* 1–23 (2010). doi:10.1002/0471142700.nc0508s41

108. MacMillan, A. M. & Verdine, G. L. Synthesis of functionally tethered oligodeoxynucleotides by the convertible nucleoside approach. *J. Org. Chem.* **55**, 5931–5933 (1990).

109. Ferentz, A. E. & Verdine, G. L. Disulfide-crosslinked oligonucleotides. *J. Am. Chem. Soc.* **113**, 4000–4002 (1991).

110. Wolfe, S. A., Ferentz, A. E., Grantcharova, V., Churchill, M. E. A. & Verdine, G. L. Modifying the helical structure of DNA by design: recruitment of an architecture-specific protein to an enforced DNA bend. *Chem. Biol.* **2**, 213–221 (1995).

111. Allerson, C. R. & Verdine, G. I. Synthesis and biochemical evaluation of RNA containing an intrahelical disulfide crosslink. *Chem. Biol.* **2**, 667–675 (1995).

112. Allerson, C. R., Chen, S. L. & Verdine, G. L. A Chemical Method for Site-Specific Modification of RNA: The Convertible Nucleoside Approach. *J. Am. Chem. Soc.* **119**, 7423–7433 (1997).

113. Huxtable, R. J. Thiols, Disulfides, and Thioesters. in *The Biochemistry of Sulfur* 199–268 (Springer, Boston, MA, 1986). doi:https://doi.org/10.1007/978-1-4757-9438-0_5

114. Betz, S. F. Disulfide bonds and the stability of globular proteins. *Protein Sci.* **2**, 1551–1558 (1993).

115. Gilbert, H. F. Thiol/disulfide exchange equilibria and disulfide bond stability. *Methods Enzymol.* **251**, 8–28 (1995).

116. Čavužić, M. & Liu, Y. Biosynthesis of Sulfur-Containing tRNA Modifications: A Comparison of Bacterial, Archaeal, and Eukaryotic Pathways. *Biomolecules* **7**, 27 (2017).

117. Chen, S., Wang, L. & Deng, Z. Twenty years hunting for sulfur in DNA. *Protein Cell* **1**, 14–21 (2010).

118. Koval', I. V. The chemistry of disulfides. *Russ. Chem. Rev.* **63**, 735–750 (2007).

119. Greenwood, N. N. & Earnshaw, A. Sulfur. in *Chemistry of the Elements* **1**, 645–746 (Elsevier, 1997).

120. Singh, R. & Whitesides, G. M. Thiol-disulfide interchange. *Chem. Sulphur-Containing Funct. Groups* 633–658 (1993). doi:10.1002/9780470034408.ch13

121. Ferentz, A. E., Keating, T. A. & Verdine, G. L. Synthesis and Characterization of Disulfide Cross-Linked Oligonucleotides. *J. Am. Chem. Soc.* **115**, 9006–9014 (1993).

122. Milton, J., Connolly, B. a., Nikiforov, T. T. & Cosstick, R. Site-specific disulfide bridges in oligodeoxyribonucleotide duplexes containing 6-mercaptopurine and 4-thiothymine bases. *J. Chem. Soc. Chem. Commun.* 779 (1993). doi:10.1039/c39930000779

123. Coleman, R. S., McCary, J. L. & Perez, R. J. Thionucleoside disulfides as covalent constraints of DNA conformation. *Tetrahedron* **55**, 12009–12022 (1999).

124. Erlanson, D. A., Glover, J. N. M. & Verdine, G. L. Disulfide cross-linking as a mechanistic probe for the B to Z transition in DNA. *J. Am. Chem. Soc.* **119**, 6927–6928 (1997).

125. Wolfe, S. A. & Verdine, G. L. Ratcheting torsional stress in duplex DNA. *J. Am. Chem. Soc.* **115**, 12585–12586 (1993).

126. Fujita, M., Watanabe, S., Yoshizawa, M., Yamamoto, J. & Iwai, S. Analysis of structural flexibility of damaged DNA using thiol-tethered oligonucleotide duplexes. *PLoS One* **10**, 1–17 (2015).

127. Cain, R. J., Zuiderweg, E. R. P. & Glick, G. D. Solution structure of a DNA hairpin and its disulfide cross-linked analog. *Nucleic Acids Res.* **23**, 2153–2160 (1995).

128. Wang, H., Zuiderweg, E. R. P. & Glick, G. D. Solution Structure of a Disulfide Cross-Linked DNA Hairpin. *J. Am. Chem. Soc.* **117**, 2981–2991 (1995).

129. Gao, H., Yang, M. & Cook, A. F. Stabilization of double-stranded oligonucleotides using backbone-linked disulfide bridges. *Nucleic Acids Res.* **23**, 285–292 (1995).

130. Gao, H., Yang, M., Patel, R. & Cook, A. F. Circularization of oligonucleotides by disulfide bridge formation. *Nucleic Acids Res.* **23**, 2025–2029 (1995).

131. Osborne, S. E., Cain, R. J. & Glick, G. D. Structure and dynamics of disulfide cross-linked DNA triple helices. *J. Am. Chem. Soc.* **119**, 1171–1182 (1997).

132. Völker, J., Osborne, S. E., Glick, G. D. & Breslauer, K. J. Thermodynamic properties of a conformationally constrained intramolecular DNA triple helix. *Biochemistry* **36**, 756–767 (1997).

133. Azhayeva, E., Azhayev, A., Guzaev, A., Hovinen, J. & Lönnberg, H. Looped oligonucleotides form stable hybrid complexes with a single-stranded DNA. *Nucleic Acids Res.* **23**, 1170–1176 (1995).

134. De Stefano, M. & Vesterager Gothelf, K. Dynamic Chemistry of Disulfide Terminated Oligonucleotides in Duplexes and Double-Crossover Tiles. *ChemBioChem* **17**, 1122–1126 (2016).

135. Endo, M. & Majima, T. Control of A Double Helix DNA Assembly by Use of Cross-Linked Oligonucleotides. *J. Am. Chem. Soc.* **125**, 13654–13655 (2003).

136. Endo, M. & Majima, T. Structural arrangement of two DNA double helices using cross-linked oligonucleotide connectors. *Chem. Commun.* 1308–9 (2004). doi:10.1039/b402783c

137. Wolfrum, M., Schwarz, R. J., Schwarz, M., Kramer, M. & Richert, C. Stabilizing DNA

nanostructures through reversible disulfide crosslinking. *Nanoscale* **11**, 14921–14928 (2019).

138. Alefelder, S. & Sigurdsson, S. T. Interstrand disulfide cross-linking of internal sugar residues in duplex RNA. *Bioorganic Med. Chem.* **8**, 269–273 (2000).

139. Gauthier, F. *et al.* A 2′,2′-disulfide-bridged dinucleotide conformationally locks RNA hairpins. *Org. Biomol. Chem.* **16**, 3181–3188 (2018).

140. Maglott, E. J. & Glick, G. D. Probing structural elements in RNA using engineered disulfide cross-links. *Nucleic Acids Res.* **26**, 1301–1308 (1998).

141. Sigurdsson, S. T. Thiol-containing RNA for the study of structure and function of ribozymes. *Methods A Companion to Methods Enzymol.* **18**, 71–77 (1999).

142. Stage-Zimmermann, T. K. & Uhlenbeck, O. C. A covalent crosslink converts the hammerhead ribozyme from a ribonuclease to an RNA ligase. *Nat. Struct. Biol.* **8**, 863 (2001).

143. Gallo, M., Defaus, S. & Andreu, D. 1988–2018: Thirty years of drug smuggling at the nano scale. Challenges and opportunities of cell-penetrating peptides in biomedical research. *Arch. Biochem. Biophys.* **661**, 74–86 (2019).

144. Feener, E. P., Shen, W.-C. & Ryser, H. J.-P. Cleavage of Disulfide Bonds in Endocytosed Macromolecules. *J. Biol. Chem.* **265**, 18780–18785 (1990).

145. Yang, J., Chen, H., Vlahov, I. R., Cheng, J.-X. & Low, P. S. Evaluation of disulfide reduction during receptor-mediated endocytosis by using FRET imaging. *Proc. Natl. Acad. Sci.* **103**, 13872–13877 (2006).

146. Zhou, Z. *et al.* Reductive nanocomplex encapsulation of cRGD-siRNA conjugates for enhanced targeting to cancer cells. *Int. J. Nanomedicine* **Volume 12**, 7255–7272 (2017).

147. Bongartz, J. P., Aubertain, A. M., Milhaud, P. G. & Lebleu, B. Improved biological activity of antisense oligonucleotides conjugated to a fusogenic peptide. *Nucleic Acids Res.* **22**, 4681–4688 (1994).

148. Pooga, M. *et al.* Cell penetrating PNA constructs regulate galanin receptor levels and modify pain transmission in vivo. *Nat. Biotechnol.* **16**, 857–861 (1998).

149. Arar, K., Aubertin, A.-M., Roche, A.-C., Monsigny, M. & Mayer, R. Synthesis and Antiviral Activity of Peptide-Oligonucleotide Conjugates Prepared by Using N.alpha.-(Bromoacetyl)peptides. *Bioconjug. Chem.* **6**, 573–577 (1995).

150. Muratovska, A. & Eccles, M. R. Conjugate for efficient delivery of short interfering RNA (siRNA) into mammalian cells. *FEBS Lett.* **558**, 63–68 (2004).

151. El-Andaloussi, S., Johansson, H. J., Lundberg, P. & Langel, Ü. Induction of splice correction by cell-penetrating peptide nucleic acids. *J. Gene Med.* **8**, 1262–1273 (2006).

152. Ämmälä, C. *et al.* Targeted delivery of antisense oligonucleotides to pancreatic β-cells. *Sci. Adv.* **4**, 3386 (2018).

153. Astriab-Fisher, A., Sergueev, D., Fisher, M., Ramsay Shaw, B. & Juliano, R. L. Conjugates of antisense oligonucleotides with the Tat and Antennapedia cell-penetrating peptides: Effects on cellular uptake, binding to target sequences, and biologic actions. *Pharm. Res.* **19**, 744–754 (2002).

154. El-Andaloussi, S., Johansson, H. J., Holm, T. & Langel, Ü. A novel cell-penetrating peptide, M918, for efficient delivery of proteins and peptide nucleic acids. *Mol. Ther.* **15**, 1820–1826 (2007).

155. Dirin, M., Urban, E., Lachmann, B., Noe, C. R. & Winkler, J. Concise postsynthetic preparation of oligonucleotide–oligopeptide conjugates through facile disulfide bond formation. *Future Med. Chem.* **7**, 1657–1673 (2015).

156. Troy, C., Derossi, D., Prochiantz, A., Greene, L. & Shelanski, M. Downregulation of Cu/Zn superoxide dismutase leads to cell death via the nitric oxide-peroxynitrite pathway. *J. Neurosci.* **16**, 253–261 (1996).

157. Troy, C. M., Stefanis, L., Greene, L. A. & Shelanski, M. L. Nedd2 Is Required for Apoptosis after Trophic Factor Withdrawal, But Not Superoxide Dismutase (SOD1) Downregulation, in Sympathetic Neurons and PC12 Cells. *J. Neurosci.* **17**, 1911–1918 (1997).

158. Troy, C. M. *et al.* Caspase-2 Mediates Neuronal Cell Death Induced by β-Amyloid. *J. Neurosci.* **20**, 1386–1392 (2000).

159. Park, Y. S. *et al.* Specific down regulation of 3T3-L1 adipocyte differentiation by cell-permeable antisense HIF1α-oligonucleotide. *J. Control. Release* **144**, 82–90 (2010).

160. Park, Y. S. *et al.* In vivo delivery of cell-permeable antisense hypoxia-inducible factor 1α oligonucleotide to adipose tissue reduces adiposity in obese mice. *J. Control. Release* **161**, 1–9 (2012).

161. Astriab-Fisher, A., Sergueev, D. S., Fisher, M., Ramsay Shaw, B. & Juliano, R. L. Antisense inhibition of P-glycoprotein expression using peptide-oligonucleotide conjugates. *Biochem. Pharmacol.* **60**, 83–90 (2000).

162. Davidson, T. J. *et al.* Highly Efficient Small Interfering RNA Delivery to Primary Mammalian Neurons Induces MicroRNA-Like Effects before mRNA Degradation. *J. Neurosci.* **24**, 10040–10046 (2004).

163. Schratt, G. M. *et al.* A brain-specific microRNA regulates dendritic spine development. *Nature* **439**, 283–289 (2006).

164. Moulton, H. M., Nelson, M. H., Hatlevig, S. A., Reddy, M. T. & Iversen, P. L. Cellular Uptake of Antisense Morpholino Oligomers Conjugated to Arginine-Rich Peptides. *Bioconjug. Chem.* **15**, 290–299 (2004).

165. Cordier, C. *et al.* Delivery of antisense peptide nucleic acids to cells by conjugation with small arginine-rich cell-penetrating peptide (R/W)9. *PLoS One* **9**, (2014).

166. Chaubey, B. *et al.* A PNA-transportan conjugate targeted to the TAR region of the HIV-1 genome exhibits both antiviral and virucidal properties. *Virology* **331**, 418–428 (2005).

167. Pooga, M. *et al.* Cell penetrating PNA constructs regulate galanin receptor levels and modify pain transmission in vivo. *Nat. Biotechnol.* **16**, 857 (1998).

168. Abes, S. *et al.* Efficient splicing correction by PNA conjugation to an R6-Penetratin delivery peptide. *Nucleic Acids Res.* **35**, 4495–4502 (2007).

169. Kaushik, N., Basu, A., Palumbo, P., Myers, R. L. & Pandey, V. N. Anti-TAR Polyamide Nucleotide Analog Conjugated with a Membrane-Permeating Peptide Inhibits Human Immunodeficiency Virus Type 1 Production. *J. Virol.* **76**, 3881–3891 (2002).

170. Tripathi, S. *et al.* Anti-HIV-1 activity of anti-TAR polyamide nucleic acid conjugated with various membrane transducing peptides. *Nucleic Acids Res.* **33**, 4345–4356 (2005).

171. Turner, J. J. *et al.* Cell-penetrating peptide conjugates of peptide nucleic acids (PNA) as inhibitors of HIV-1 Tat-dependent trans-activation in cells. *Nucleic Acids Res.* **33**, 6837–6849 (2005).

172. Krummel, D. A. P., Kent, O., MacMillan, A. M. & Altman, S. Evidence for helical unwinding of an RNA substrate by the RNA enzyme RNase P: use of an interstrand disulfide crosslink in substrate. *J. Mol. Biol.* **295**, 1113–1118 (2000).

173. Peletskaya, E. N. *et al.* Cross-linking of the fingers subdomain of human immunodeficiency virus type 1 reverse transcriptase to template-primer. *J. Virol.* **75**, 9435–45 (2001).

174. Sarafianos, S. G. *et al.* Trapping HIV-1 reverse transcriptase before and after translocation on DNA. *J. Biol. Chem.* **278**, 16280–16288 (2003).

175. Huang, H. Structure of a Covalently Trapped Catalytic Complex of HIV-1 Reverse Transcriptase: Implications for Drug Resistance. *Science (80-.).* **282**, 1669–1675 (1998).

176. Huang, H., Harrison, S. C. & Verdine, G. L. Trapping of a catalytic HIV reverse transcriptase·template:primer complex through a disulfide bond. *Chem. Biol.* **7**, 355–364 (2000).

177. Banerjee, A., Santos, W. L. & Verdine, G. L. Structure of a DNA Glycosylase Searching for Lesions. *Science (80-.).* **311**, 1153–1157 (2006).

178. Banerjee, A., Yang, W., Karplus, M. & Verdine, G. L. Structure of a repair enzyme interrogating undamaged DNA elucidates recognition of damaged DNA. *Nature* **434**, 612–618 (2005).

179. Qi, Y. *et al.* Encounter and extrusion of an intrahelical lesion by a DNA repair enzyme. *Nature* **462**, 762–766 (2009).

180. Fromme, J. C., Banerjee, A., Huang, S. J. & Verdine, G. L. Structural basis for removal of adenine mispaired with 8-oxoguanine by MutY adenine DNA glycosylase. *Nature* **427**, 652–656 (2004).

181. Paalman, S. R., Noll, D. M. & Clarke, N. D. Formation of a covalent complex between methylguanine methyltransferase and DNA via disulfide bond formation between the active site cysteine and a thiol-containing analog of guanine. *Nucleic Acids Res.*

25, 1795–1801 (1997).

182. He, C. & Verdine, G. L. Trapping distinct structural states of a protein/DNA interaction through disulfide crosslinking. *Chem. Biol.* 9, 1297–1303 (2002).

183. Duguid, E. M., Mishina, Y. & He, C. How Do DNA Repair Proteins Locate Potential Base Lesions? A Chemical Crosslinking Method to Investigate O6-Alkylguanine-DNA Alkyltransferases. *Chem. Biol.* 10, 827–835 (2003).

184. Mishina, Y. & He, C. Probing the Structure and Function of the Escherichia coli DNA Alkylation Repair AlkB Protein through Chemical Cross-Linking. *J. Am. Chem. Soc.* 125, 8730–8731 (2003).

185. Erlanson, D. A., Chen, L. & Verdine, G. L. DNA Methylation through a Locally Unpaired Intermediate. *J. Am. Chem. Soc.* 115, 12583–12584 (1993).

186. Metelev, V. G., Kubareva, E. A., Vorob'eva, O. V., Romanenkov, A. S. & Oretskaya, T. S. Specific conjugation of DNA binding proteins to DNA templates through thiol-disulfide exchange. *FEBS Lett.* 538, 48–52 (2003).

187. Yang, Q., Faucher, F., Coseno, M., Heckman, J. & Doublié, S. Purification, crystallization and preliminary X-ray diffraction of a disulfide cross-linked complex between bovine poly(A) polymerase and a chemically modified 15-mer oligo(A) RNA. *Acta Crystallogr. Sect. F Struct. Biol. Cryst. Commun.* 67, 241–244 (2011).

188. Ho, W. C., Fitzgerald, M. X. & Marmorstein, R. Structure of the p53 core domain dimer bound to DNA. *J. Biol. Chem.* 281, 20494–20502 (2006).

189. Corey, D. & Schultz, P. Generation of a hybrid sequence-specific single-stranded deoxyribonuclease. *Science (80-.).* 238, 1401–1403 (1987).

190. Chu, T. C. *et al.* Aptamer:toxin conjugates that specifically target prostate tumor cells. *Cancer Res.* 66, 5989–5992 (2006).

191. Kelly, L., Kratschmer, C., Maier, K. E., Yan, A. C. & Levy, M. Improved Synthesis and *In Vitro* Evaluation of an Aptamer Ribosomal Toxin Conjugate. *Nucleic Acid Ther.* 26, 156–165 (2016).

192. Bonfils, E., Mendes, C., Roche, A. C., Monsigny, M. & Midoux, P. Uptake by macrophages of a biotinylated oligo-.alpha.-deoxythymidylate by using mannosylated streptavidin. *Bioconjug. Chem.* 3, 277–284 (1992).

193. Bonfils, E. *et al.* Drug targeting: Synthesis and endocytosis of oligonucleotide-neoglycoprotein conjugates. *Nucleic Acids Res.* 20, 4621–4629 (1992).

194. Rajur, S. B., Roth, C. M., Morgan, J. R. & Yarmush, M. L. Covalent protein-oligonucleotide conjugates for efficient delivery of antisense molecules. *Bioconjug. Chem.* 8, 935–940 (1997).

195. Uckun, F. M., Qazi, S., Dibirdik, I. & Myers, D. E. Rational design of an immunoconjugate for selective knock-down of leukemia-specific E2A-PBX1 fusion gene expression in human Pre-B leukemia. *Integr. Biol.* 5, 122–132 (2013).

196. Fidanza, J. A. & McLaughlin, L. W. Use of a Thiol Tether for the Site-Specific

Attachment of Reporter Groups to DNA. *J. Org. Chem.* **57**, 2340–2346 (1992).

197. Voet, D. & Voet, J. G. *Biochemistry*. (John Wiley & Sons, 2011).

198. Oivanen, M., Kuusela, S. & Lönnberg, H. Kinetics and mechanisms for the cleavage and isomerization of the phosphodiester bonds of RNA by bronsted acids and bases. *Chem. Rev.* **98**, 961–990 (1998).

199. Saenger, W. Principles of nucleic acid structure. in *Principles of nucleic acid structure* (Springer-Verlag, 1984).

200. Niedle, S. *Principles of Nucleic Acid Structure*. (2008).

201. Patani, G. A. & LaVoie, E. J. Bioisosterism: A rational approach in drug design. *Chem. Rev.* **96**, 3147–3176 (1996).

202. Meanwell, N. A. Fluorine and Fluorinated Motifs in the Design and Application of Bioisosteres for Drug Design. *J. Med. Chem.* **61**, 5822–5880 (2018).

203. Pallan, P. S. *et al.* Unexpected origins of the enhanced pairing affinity of 2'-fluoro-modified RNA. *Nucleic Acids Res.* **39**, 3482–3495 (2011).

204. Andrus, A., Efcavitch, J. W., McBride, L. J. & Giusti, B. Novel activating and capping reagents for improved hydrogen-phosphonate DNA synthesis. *Tetrahedron Lett.* **29**, 861–864 (1988).

205. Sinha, N. D. & Cook, R. M. The preparation and application of functionalised synthetic oligonucleotides: III. Use of H-phosphonate derivatives of protected amino-hexanol and mercapto-propanol or-hexanol. *Nucleic Acids Res.* **16**, 2659–2670 (1988).

206. Stawinski, J. & Strömberg, R. Di- and Oligonucleotide Synthesis Using <I>H</I>-Phosphonate Chemistry. in *Oligonucleotide Synthesis* **288**, 081–100 (Humana Press, 2004).

207. Garegg, P., Regberg, T., Stawinski, J. & Strömberg, R. Nucleoside H-Phosphonates. V. The Mechanism of Hydrogenphosphonate Diester Formation Using Acyl Chlorides as Coupling Agents in Oligonucleotide Synthesis by the Hydrogenphosphonate Approach. *Nucleosides, Nucleotides and Nucleic Acids* **6**, 655–662 (1987).

208. Ti, G. S., Gaffney, B. L. & Jones, R. A. Transient protection: efficient one-flask syntheses of protected deoxynucleosides. *J. Am. Chem. Soc.* **104**, 1316–1319 (1982).

209. Nilsson, J. Studies on Oxidative Couplings in H-Phosphonate Chemistry. *Stockholm University* (2004).

210. Gołębiewska, J., Rachwalak, M., Jakubowski, T., Romanowska, J. & Stawinski, J. Reaction of Boranephosphonate Diesters with Amines in the Presence of Iodine: The Case for the Intermediacy of H-Phosphonate Derivatives. *J. Org. Chem.* **83**, 5496–5505 (2018).

211. Almer, H., Stawinski, J., Stroemberg, R. & Thelin, M. Synthesis of diribonucleoside phosphorothioates via stereospecific sulfuration of H-phosphonate diesters. *J. Org. Chem.* **57**, 6163–6169 (1992).

212. Powles, N., Atherton, J. & Page, M. I. Reactive intermediates in the H-phosphonate synthesis of oligonucleotides. *Org. Biomol. Chem.* **10**, 5940 (2012).

213. Chen, L. *et al.* Theoretical Study on the Relationship between Rp-Phosphorothioation and Base-Step in S-DNA: Based on Energetic and Structural Analysis. *J. Phys. Chem. B* **119**, 474–481 (2015).

214. Turner, J. J., Williams, D., Owen, D. & Gait, M. J. Disulfide conjugation of peptides to oligonucleotides and their analogs. *Curr. Protoc. Nucleic Acid Chem.* **Chapter 4**, Unit 4.28 (2006).

215. Vivès, E. & Lebleu, B. Selective coupling of a highly basic peptide to an oligonucleotide. *Tetrahedron Lett.* **38**, 1183–1186 (1997).

216. Stevens, R., Stevens, L. & Price, N. The stabilities of various thiol compounds used in protein purifications. *Biochem. Educ.* **11**, 70 (1983).

217. Whitesides, G. M., Lilburn, J. E. & Szajewski, R. P. Rates of thiol-disulfide interchange reactions between mono- and dithiols and Ellman's reagent. *J. Org. Chem.* **42**, 332–338 (1977).

218. Ferentz, A. E., Wiorkiewicz-Kuczera, J., Karplus, M. & Verdine, G. L. Molecular Dynamics Simulations of Disulfide Cross-Linked DNA Decamers. *J. Am. Chem. Soc.* **115**, 7569–7583 (1993).

219. Bloomfield, V. A., Crothers, D. M. & Tinoco, I. J. *Nucleic Acids: Structures, Properties and Functions*. *University Science Books* (2000).

220. Smyth, D., Blumenfeld, O. & Konigsberg, W. Reactions of N-ethylmaleimide with peptides and amino acids. *Biochem. J.* **91**, 589–595 (1964).

221. Svoboda, P. & Cara, A. D. Hairpin RNA: a secondary structure of primary importance. *Cell. Mol. Life Sci.* **63**, 901–908 (2006).

222. Cheong, C. & Cheong, H.-K. RNA Structure: Tetraloops. *Encycl. Life Sci.* (2010). doi:10.1002/9780470015902.a0003135.pub2

223. Germer, K., Leonard, M. & Zhang, X. RNA aptamers and their therapeutic and diagnostic applications. *Int. J. Biochem. Mol. Biol.* **4**, 27–40 (2013).

224. Pfeiffer, F. & Mayer, G. Selection and Biosensor Application of Aptamers for Small Molecules. *Front. Chem.* **4**, 1–21 (2016).

225. Kiliszek, A., Błaszczyk, L., Kierzek, R. & Rypniewski, W. Stabilization of RNA hairpins using non-nucleotide linkers and circularization. *Nucleic Acids Res.* **45**, 4–12 (2017).

226. Woese, C. R., Winker, S. & Gutell, R. R. Architecture of ribosomal RNA: constraints on the sequence of 'tetra-loops'. *Proc. Natl. Acad. Sci.* **87**, 8467–8471 (1990).

227. Cerritelli, S. M. & Crouch, R. J. Ribonuclease H: the enzymes in eukaryotes. *FEBS J.* **276**, 1494–1505 (2009).

228. Akman, G. *et al.* Pathological ribonuclease H1 causes R-loop depletion and aberrant DNA segregation in mitochondria. *Proc. Natl. Acad. Sci.* **113**, E4276–E4285 (2016).

229. Liang, X.-H., Sun, H., Nichols, J. G. & Crooke, S. T. RNase H1-Dependent Antisense Oligonucleotides Are Robustly Active in Directing RNA Cleavage in Both the Cytoplasm and the Nucleus. *Mol. Ther.* **25**, 2075–2092 (2017).

230. Nowotny, M., Gaidamakov, S. A., Crouch, R. J. & Yang, W. Crystal structures of RNase H bound to an RNA/DNA hybrid: Substrate specificity and metal-dependent catalysis. *Cell* **121**, 1005–1016 (2005).